

# Optimization of the Impregnation Process of Cellulose Materials in High Voltage Power Transformers

Susceptibility of high-density materials to partial discharge  
activity

Nadira Irahhauten

Supervisor: Dr. Ir. P. H. F. Morshuis

Daily supervisor: Dr. L. Chmura

A thesis presented for the degree of  
M.Sc of Electrical Engineering

Electrical Sustainable Energy Department  
DC Systems and Storage Group  
Technical University of Delft  
The Netherlands

## Thesis Committee:

*Dr. Ir. P.H.F. Morshuis*

*Dr. ir. D. Djairam*

*Ir. C. J. G. Spoorenberg*

*Ing. P. van Nes*

*Dr. L. Chmura*

Delft University of Technology  
Faculty of Electrical Engineering, Mathematics and Computer Science  
Electrical Sustainable Energy Department  
DC Systems and Storage Group  
The Netherlands

## ABSTRACT

The manufacturing process of high voltage power transformers consists of several phases such as design, assembly, drying and impregnation process which are time consuming. Before electrical testing, a transformer needs an extra standing time for further impregnation of cellulose material in particular those of high density. It should be noted that the duration of the standing time depends on the ratings of the transformer. The main reason for considering this standing time is to reduce the probability of failure during electrical testing. This means that the reduction of such standing time is a crucial issue. Therefore, the main goal of this thesis is to optimize the post impregnation process of high density cellulosic material.

One of the requirements for shortening the post impregnation standing time is that during the electrical tests of the transformer the PD level should not exceed the PD acceptance given by IEC standard level. In this thesis, it is investigated if the standing time is related to the occurrence of partial discharges in high density materials. This is done by performing a number of partial discharge measurement on different samples. Further on,  $\tan\delta$  measurements were performed on different samples in the course of impregnation process to investigate whether the losses decrease in the course of time.

In this research, the impregnation processes of two different cellulosic materials, namely transformerboard (PSP) and laminated wood (KP) are studied. Based on that, an empirical model that predicts the time needed to fully impregnate a cellulosic sample is developed. This model relates the impregnation time with sample material, dimensions, shapes, impregnation and temperature. The proposed model shows a good agreement with the measurements.

# Contents

- Abstract.....ii
- 1. Introduction.....1
  - 1.1. General: Role of a transformer .....1
  - 1.2. The role of oil impregnated cellulosic material .....3
  - 1.3. The transformer manufacturing process.....3
  - 1.4. Thesis objectives.....5
  - 1.5. Thesis overview.....5
- 2. Background theory .....7
  - 2.1. The construction of a transformer .....7
    - 2.1.1. Core.....7
    - 2.1.2. Winding.....8
    - 2.1.3. Insulation.....8
  - 2.2. Oil impregnated insulations .....9
    - 2.2.1. Mineral oil .....9
    - 2.2.2. Cellulose materials ..... 11
  - 2.3. Impregnation process and capillary effect..... 15
    - 2.3.1. The impregnation process..... 15
    - 2.3.2. Flow Dynamics ..... 16
    - 2.3.3. Capillary action ..... 17
    - 2.3.4. Factors affecting the impregnation process..... 18
  - 2.4. Stresses in the transformer ..... 18
  - 2.5. Partial discharges in oil-filled transformer..... 19
    - 2.5.1. Partial discharge physics ..... 19
    - 2.5.2. Behavior of partial discharges..... 22
    - 2.5.3. Partial discharges occurrence in partially oil-impregnated transformerboard (Paschen curve)..... 23
- 3. Impregnation process monitoring and measurement setups ..... 26
  - 3.1. Purpose of tests ..... 26
  - 3.2. Sample preparation ..... 27
    - 3.2.1. Samples sizes, shapes and materials..... 27
    - 3.2.2. Drying process..... 30
    - 3.2.3. Impregnation process ..... 31
  - 3.3. Measurements methods..... 32
    - 3.3.1. Weight measurements ..... 32

3.3.2.	PD measurement method .....	34
3.3.3.	$\tan\delta$ measurement methods.....	35
3.4.	Measurement setups : Weight, PD and $\tan\delta$ .....	39
3.4.1.	test setup for weight measurements .....	39
3.4.2.	test setup for $\tan\delta$ : Impregnation at HV laboratory .....	39
3.4.3.	test setup for PD : Impregnation at HV laboratory .....	41
3.4.4.	Experimental test setup for PD and dielectric loss: Impregnation at SMIT.....	42
4.	The results of PD and $\tan\delta$ measurements.....	44
4.1.	Samples impregnated at High voltage Laboratory in Delft.....	44
4.2.	Measurements using Smit testing tank.....	48
4.2.1.	Samples description.....	48
4.2.2.	$\tan\delta$ measurements results .....	49
4.2.3.	PD measurements results.....	50
4.3.	Testing the Tank.....	51
4.3.1.	Test circuit and description.....	51
4.3.2.	Results and discussion.....	52
5.	Analysis and Modelling of Impregnation Time .....	54
5.1.	Impregnation process modelling .....	54
5.1.1	Proposed model for impregnation process.....	54
5.1.2	estimation of saturation time.....	57
5.2.	Data analysis of PSP material .....	57
5.2.1	Effect of side surface on the post impregnation time of PSP material.....	57
5.2.2	Effect of shapes (traveling distance) on the post impregnation time .....	58
5.2.3	Effect of temperature on the post impregnation time .....	60
5.2.4.	Effect of drilled hole in transformerboard sample.....	63
5.2.5	Summary: Data collection for PSP material .....	65
5.3.	Data Analysis of KP material.....	67
5.3.1	Effect of surface.....	67
5.3.2	Effect of shape .....	68
5.3.3	Effect of temperature.....	69
5.3.4	Summary: Data collection for KP material .....	69
5.4	Modelling of the impregnation time .....	70
5.4.1	Data modeling of rise time constant .....	71
5.4.2.	Model paramters for cylindrical shape.....	73
5.4.3.	Model paramters for cuboidal shape.....	77

5.4.4	Model validation.....	80
5.5.	Discussion.....	84
6.	Conclusions and recommendations.....	86
6.1	Summary and Conclusions.....	86
6.2.	Recommendations for future work.....	87
Appendix A: Mineral oil Nynas Viscosity versus temperature.....		89
Appendix B: a schematic for samples used for PD/tan $\delta$ measurements using Smit Tank.....		90
Appendix C: PD test results using smit tank.....		93
Appendix D: tan $\delta$ results using testing smit tank.....		98
Acknowledgments .....		100
7.	Bibliography .....	101

# 1. INTRODUCTION

Nowadays the thermally upgraded paper, pressboard and pressed wood are mainly used as insulants in the oil-filled transformers due to their mechanical and thermal stability and high electrical strength [1]. However, the impregnation of the pressboard and pressed wood are complicated because of their high density especially when using oils with high viscosity such as natural esters [2].

According to the manufacturer, the impregnation process during the production of high-voltage oil-filled transformers requires time of at least 48 hours. Later on, a standing time of 10 to 14 days takes place before electrical testing. This standing time is recommended to reduce the probability of failure to a minimum [3].

The reduction of such post-impregnation standing time becomes a crucial issue in order to optimize the whole manufacturing process. For instance, when the cellulosic material is not sufficiently impregnated with oil, the remaining gases inside the cavities might cause partial discharges. This may lead to a decrease of the life of the insulation [4]. Therefore, it is necessary to investigate the correlation between this standing time and partial discharge occurrence in high density material and optimize the impregnation process for such materials.

## 1.1. GENERAL: ROLE OF A TRANSFORMER

The transformer is one of the most important components in the electrical network. The cost of such a device varies between €500,000 for a unit of 40 MVA and €2,500,000 for a 500 MVA unit [5]. As illustrated in Figure 1, transformers can be installed in different parts of the grid. The transmission and distribution systems are highly dependent on the transformer. At generation level, the voltages typically range from 10 to 25 kV. The transformers are used to step up the voltage supplied by the generators to a high voltage necessary for transmission. The main reason for transmission at high voltages is to minimize the transmission losses that scale quadratically with current e.g. higher voltage imply lower load current. Moreover, this reduction in load current makes the voltage drops more controllable along the line. And it can be transmitted in a cable of practical size and weight with a high efficiency.

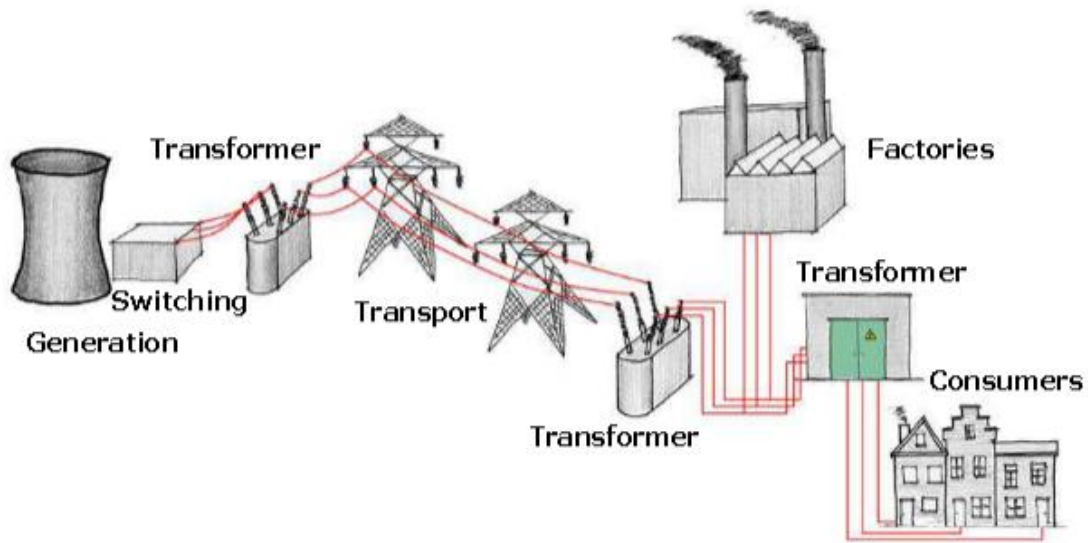


Figure 1: A schematic of the electricity grid [5]

A transformer is a complex device and different failure modes can occur. One of the most common failure causes is an insulation failure as it is clearly shown in Figure 2 where the winding failure is the major contributor [7]. In addition, the lifetime of the transformer winding depends strongly on the quality of the insulation.

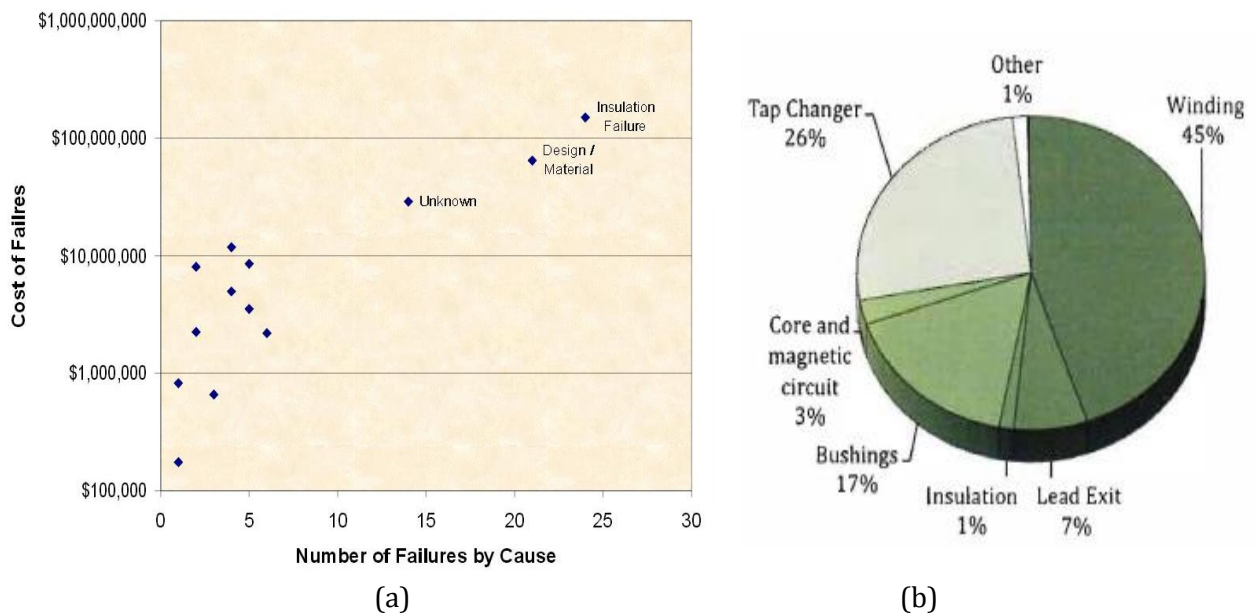


Figure 2: (a) Frequency of failure of transformers by cause versus severity [7] (b) Failure location of substation transformers(>100kV) based on 365 failures [8]

Nowadays utilities are most concerned with investigating on the one hand the aging and deterioration of the insulating material. On the other hand, the transformer manufacturers tend to improve their product in order to increase the reliability in long-term performance. When for example a tap changer reaches the end of its life while the condition of the cellulose insulation is still acceptable and still has 50% of its life left, the life of the transformer can be extended by at

least 10-50% by repairing the tap changer (costing €70,000- €150,00) instead of buying a new transformer (costing between €500.000 for a 40 MVA unit and €2.500.000 for a 500 MVA) [5].

## 1.2. THE ROLE OF OIL IMPREGNATED CELLULOSIC MATERIAL

In high-voltage oil-filled transformers both liquid and solid insulation are used. This insulation is composed of e.g., mineral oil and cellulosic material such as paper, pressboard and wood. The cellulosic material is first dried under vacuum at high temperature and then saturated with an impregnating medium. This impregnation is done to replace the free spaces inside the cellulosic material by oil and hence avoid partial discharge activity [2]. The cellulosic materials are used to provide a mechanical structure for the windings in the transformer. When impregnated with oil, the materials insulate parts of winding with different potentials.

In principle, paper is used to insulate the wires of the windings and the pressboard can be used between the co-axial cylindrical windings of a high voltage transformer where the electrical stresses are very high. Wood is used for lead support frames and cleats. Furthermore it can provide an alternative to pressboard for winding end support slabs [9].

The oil impregnated insulation is designed to withstand the different stresses that the transformer may suffer from. These stresses are of electrical, thermal and mechanical nature and beside normal operation they might origin from transients such as lightning impulses, switching impulses and short circuits.

## 1.3. THE TRANSFORMER MANUFACTURING PROCESS

In Figure 3, a general overview of a transformer manufacturing process is presented. After constructing the core from laminated sheets, the high voltage (HV) and low voltage (LV) windings, these are assembled together. The next step is to dry the completed core and windings using vapor phase ovens. After the final tightening, the construction is put in a tank and then the impregnation process starts. The tank is filled with oil under vacuum, at different speeds. When the tank is totally filled with oil the vacuum is released and the so-called standing time starts.

Before testing, each transformer has a standing time of several days varying between 10 and 14 days depending on the voltage level of the transformer. This standing time is necessary to reduce the probability of failure during tests. For instance, the full impregnation of cellulosic material, especially those of high density is time consuming, therefore electrical testing before a complete impregnation may endanger the transformer life. In addition to that, the moisture at interfacial locations; between the cellulosic material and the oil; needs time to reach the equilibrium [3]. For these reasons, a standing time between oil filling and electrical testing is required.

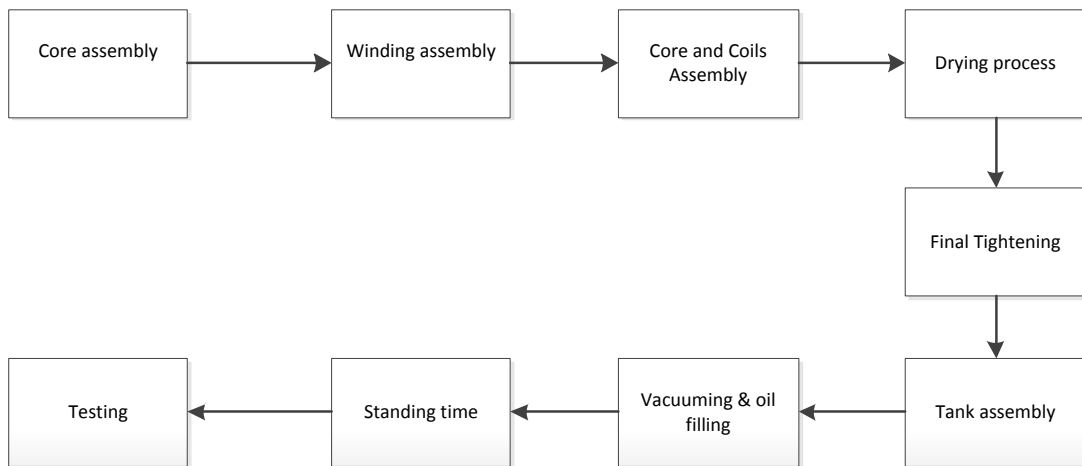


**Figure 3: Exemplary flow chart depicting a transformer manufacturing process**

Before transportation of the transformer to the client, several test types have to be performed to verify that the transformer will perform well in service .

The tests are performed according to the IEC standard ,i.e. lightning impulse (LI), switching impulse (SI) and the A.C. voltage.

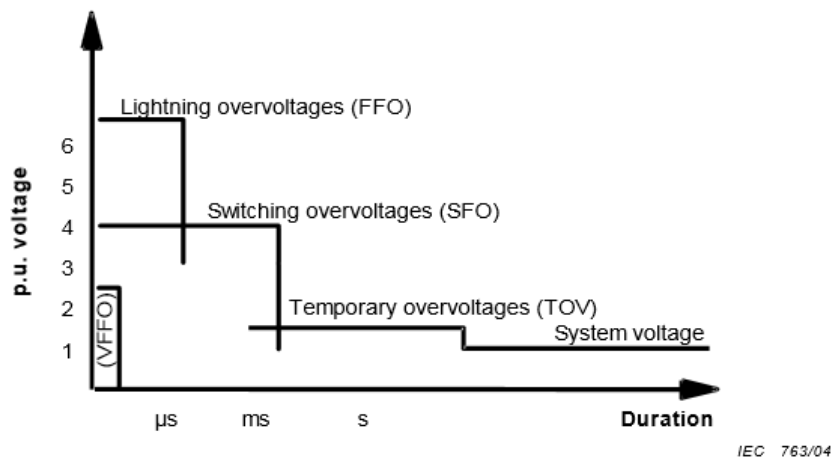


**Figure 4: Types of dielectric stresses [10]**

Table 1 summarizes the classes and shapes of the overvoltage and standard withstand tests.

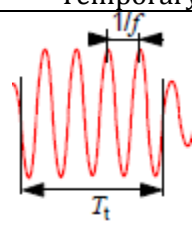
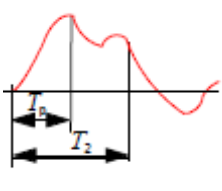
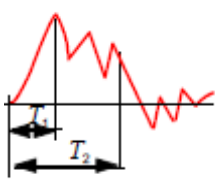
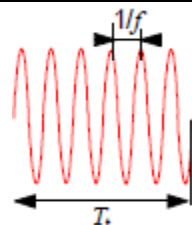
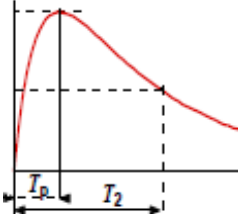
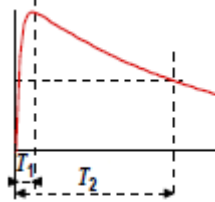
Class	Low frequency	Transient	
	Temporary	Slow front	Fast front
Overvoltage shapes			
Range of overvoltage shapes	10 Hz <math>f</math> <math>500</math> Hz 0.03 μs <math>T_t</math> <math>3600</math> μs	20 μs <math>T_p</math> <math>5000</math> μs <math&gt;t_2 20&lt;="" \leq="" math&gt;="" ms<="" td=""> <td>0.1 μs &lt;math&gt;T_1 \leq 20&lt;/math&gt; μs <math&gt;t_2 20&lt;="" \leq="" math&gt;="" td="" μs<=""> </math&gt;t_2></td></math&gt;t_2>	0.1 μs <math>T_1 \leq 20</math> μs <math&gt;t_2 20&lt;="" \leq="" math&gt;="" td="" μs<=""> </math&gt;t_2>
Standard Voltage shapes			
Standard withstand test	Short duration power frequency test	Switching impulse test	Lightning impulse test

Table 1: Shapes and ranges of overvoltage and standard withstand tests

#### 1.4. THESIS OBJECTIVES

From the point of view of the manufacturer, it is interesting to shorten the post-impregnation period. That would help to optimize the production process of the transformers.

The main goal of this research was to investigate the impregnation processes and to optimize the impregnation times of cellulosic material in particular those of high-density materials. This was done by building an empirical model of the impregnation process. The model relates sample shapes and dimensions, impregnation temperature and time needed to complete the impregnation. Moreover, a number of experiments was performed on different samples to investigate the correlation between the standing time and partial discharges occurrence in high density material and the improvement of dielectrics losses in the course of impregnation process as well.

#### 1.5. THESIS OVERVIEW

Chapter 2 introduces the relevant theoretical background of transformer construction and the stresses affecting its insulation. The chapter will include also a description of the impregnation

process of the insulation, the influencing parameters and partial discharge mechanisms of oil-filled insulation.

Chapter 3 describes the samples used for laboratory investigations and the preparation procedure. Further on, the experimental test setups and the experimental methods for measuring partial discharges (PD), dielectrics losses ( $\tan\delta$ ) and weight increase during the post-impregnation standing time as well as the investigated materials and sample types are presented.

The results of the tests and the analysis of the obtained data will be presented in chapter 4. Moreover, a theoretical model of the time of the impregnation process speed is presented in chapter 5. Chapter 6 presents the conclusions and recommendations for future work.

## 2. BACKGROUND THEORY

### 2.1. THE CONSTRUCTION OF A TRANSFORMER

In general a power transformer consists of high voltage winding, low voltage winding, a magnetic core and insulating parts of different type. A schematic showing overview of a high voltage power transformer arrangement is depicted in Figure 5.

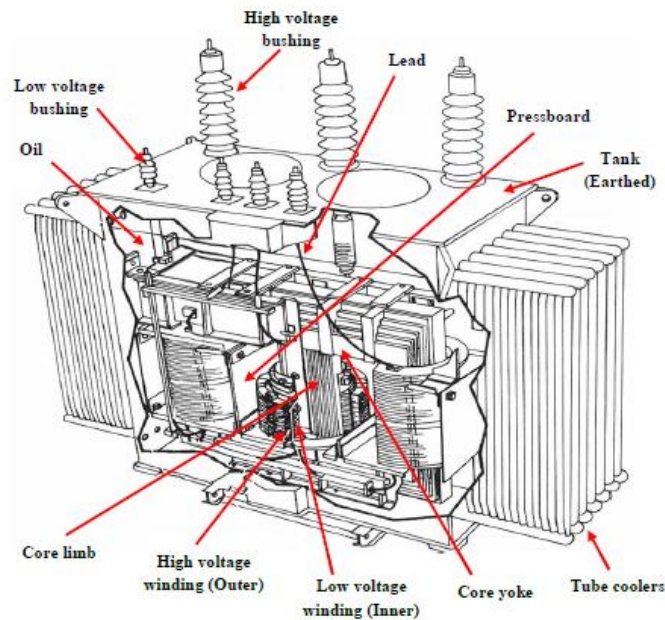


Figure 5: Oil-filled transformer arrangement [11]

#### 2.1.1. CORE

The core provides a low-reluctance path for the magnetic flux to link the primary and secondary windings. Due to changes in magnetic flux the eddy currents can be induced in the core what leads to heat generation and energy losses. To limit these currents, the core is made from many thin steel sheets which are insulated from each other with varnish and then formed into a core. The laminations are build up in a way to have as near as possible a circular cross-section (Figure 6)

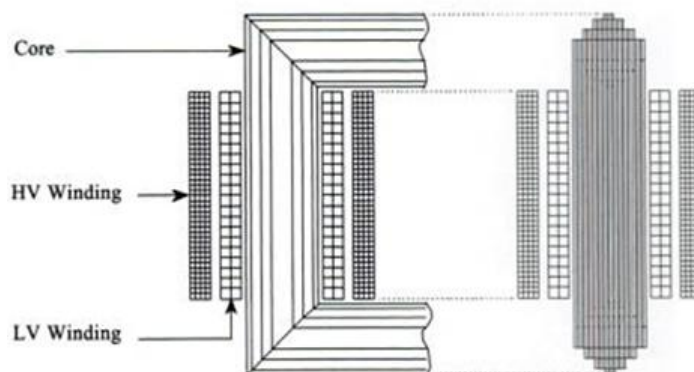


Figure 6: Cross section of a transformer with primary and secondary windings on a common circular core leg[12].

Moreover, for an efficient power transfer the hysteresis losses that are present in the core has to be reduced. This losses are function of maximum flux density and a constant of material. These magnetic losses are reduced by adding small amount of silicon or aluminum. Besides, by adding silicon to the iron the permeability and resistivity increases which reduces also the eddy current losses [9].

### 2.1.2. WINDING

Because of the high conductivity, mechanical proprieties and low costs, copper is used to make the transformer windings. The winding conductors used are usually flat with rectangular cross-section instead of conductors with circular cross section. This is for its good space factor and high mechanical stability. For instance higher axial and radial short circuit withstand [9][13]. To reduce the eddy current that occur in the conductors, the total cross-sectional area of the winding conductor has to be reduced or the winding conductor has to be made by a large number of thin stripes insulated from each other. These stripes are usually continuously transposed. This transposition provides that the overall leakage flux is approximately the same. Figure 7 shows flat conductors that are insulated with enamel and transposed continuously

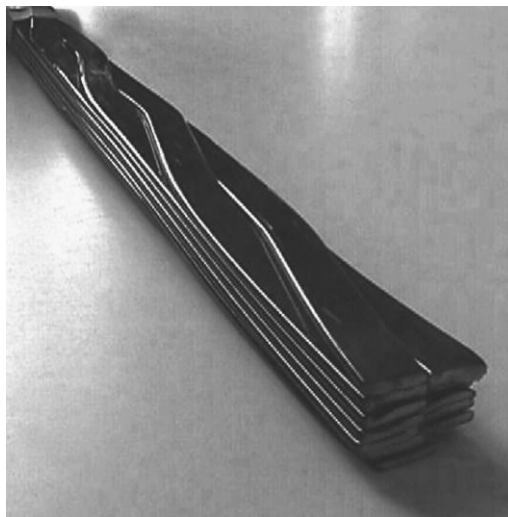


Figure 7: Continuously transposed cable (CTC) [14]

Each individual strand is insulated from the other by wrapping with paper strips. The winding surrounds the leg of the core as shown in Figure 6. The core encloses the winding to provide link between the windings and a return flux path

### 2.1.3. INSULATION

In high voltage oil-filled power transformers, the insulation is the most important part as the reliability of the transformer is highly dependent on the insulation [15]. The insulation system in power transformers is grouped into two categories. The first is minor insulation, this refers to the insulation within the windings which is used to separate one layer of turns from the next layer. The second is major insulation, which consists of insulation between the windings, between the winding and windings and the core limb/yoke and between leads and ground [11][16].

Different insulating materials, both solid and liquid are used as insulation in a transformer. These include mineral oil as well cellulose-based solid material such as paper, transformerboard and laminated wood.

The conductors are wrapped with paper. The transformerboard of different thicknesses and forms is used in, used for making barriers (winding to winding, winding to ground, lead to lead), blocks, spacers. The laminated transformer board or laminated wood is used for making support blocks and pressure ring [17].

## 2.2.OIL IMPREGNATED INSULATIONS

### 2.2.1. MINERAL OIL

Mineral oil is widely used as an insulating material for electrical equipment such as transformers. In oil-filled power transformers, mineral oil has a dual contributions. It is used for cooling as well as insulating purposes [9]:

**As a coolant:** Due to losses generated inside a transformer, the temperature of the system (core frames, winding, tank) rises. The mineral oil helps to cool down the transformer by transferring the heat due to conduction and convection. The natural convection occurs due to the difference between the density of the hot and cool oil.

**As an insulator:** Mineral oil contributes to the insulation of different parts within the transformer and it also improves the electrical strength of the solid insulation by filling the voids between the layers and fibers of the cellulosic material.

Mineral oils are obtained from crude petroleum. Crude petroleum composition and quality depends on its origin of extraction. It has a complex mixture of carbon hydrogen and small proportion of nitrogen and sulphur.

There are three main structures of mineral oil molecules: paraffin's, naphthenic and aromatics. Figure 8 illustrates the different molecular structure of three types of hydrocarbon.

The paraffinic molecules( $C_{2n}H_{2n+2}$ ) are composed from straight and benched chain of carbons and hydrogen. While the naphthenic structures ( $C_{2n}H_{2n}$ ) is saturated ring-like, contrary to the aromatic structure ( $C_nH_n$ ) which is unsaturated.

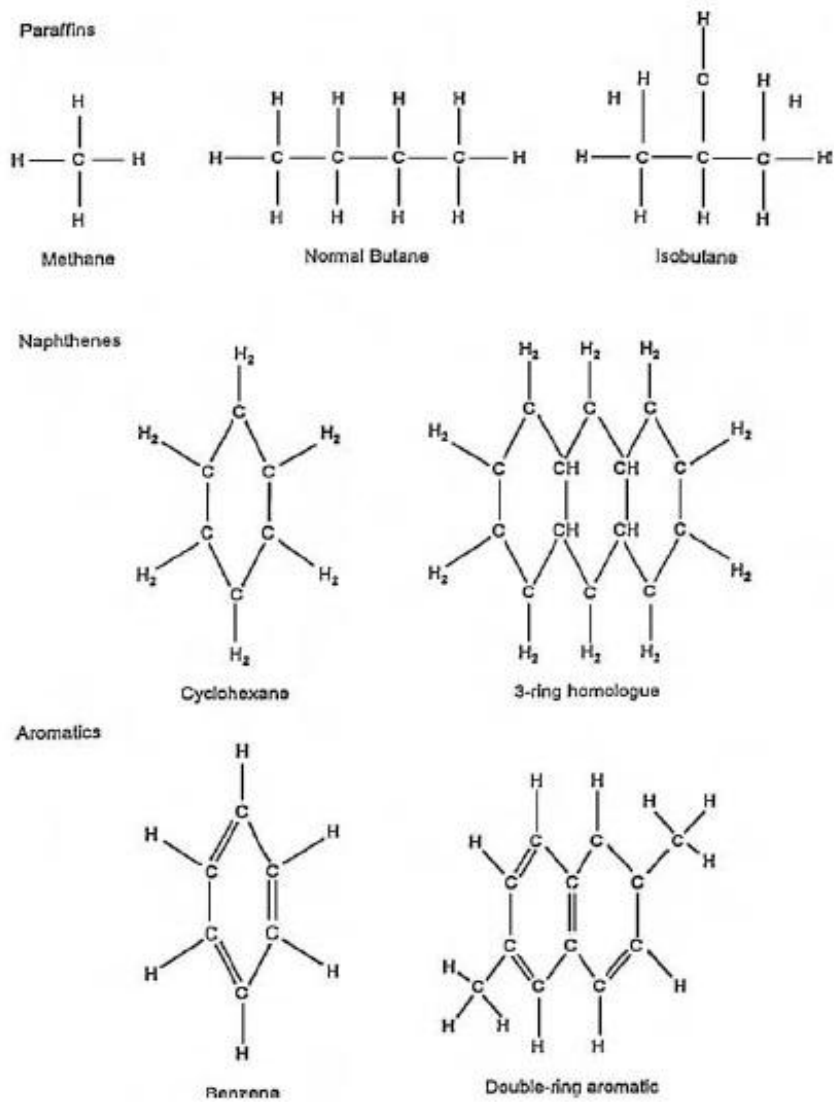
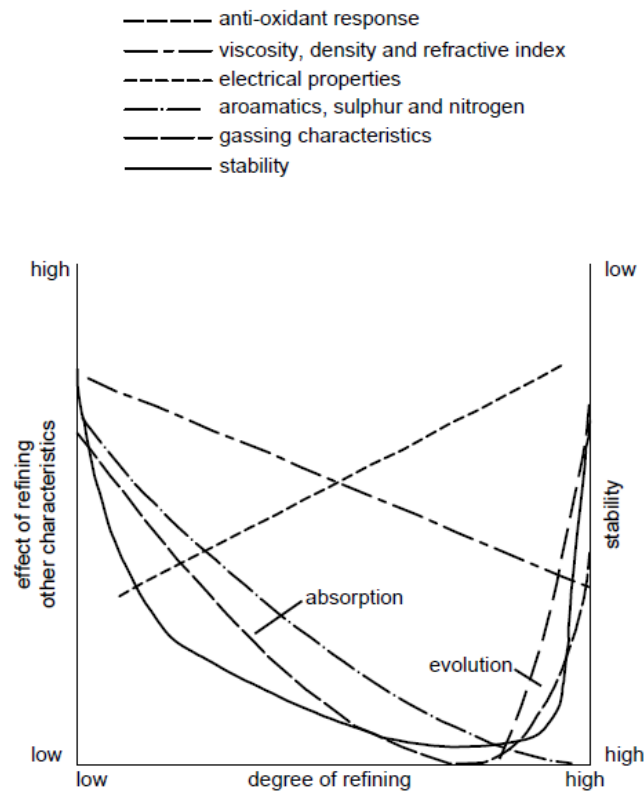


Figure 8: Molecular structures of hydrocarbons [9]

Both chemical and physical properties of the oil are highly dependent on its composition and its refining treatment. As illustrated in Figure 9, the refining treatment of crude oil has a noticeable influence on the properties of insulating oil.



**Figure 9: Effect of refining on the oil properties [9]**

Mineral oil used in the transformers is required to have the following characteristics [9]:

- High breakdown strength therefore the water and impurities contents are required to be as low as possible.
- low viscosity is not only important for a fast impregnation but also to ensure a fast natural convection and hence an efficient heat transfer from core and windings.
- Low pour point, to allow the use of oil in very cold climate.
- High flash point (lowest temperature at which the oil can vaporize and produce a flammable mixture in air). A high flash point is required as it minimize the chances of a fire hazard in the transformer.
- Excellent chemical stability.
- No decomposition (giving off gas) under influence of electrical discharges.

### 2.2.2. CELLULOSE MATERIALS

Inside the transformer different solid insulating materials are used. Paper, pressboard and laminated wood can be found. These material are made based on cellulose material. In general the cellulose material is a long polymer carbohydrate chain, which is composed of glucose units. Figure 10 shows the molecular structure of the cellulose.

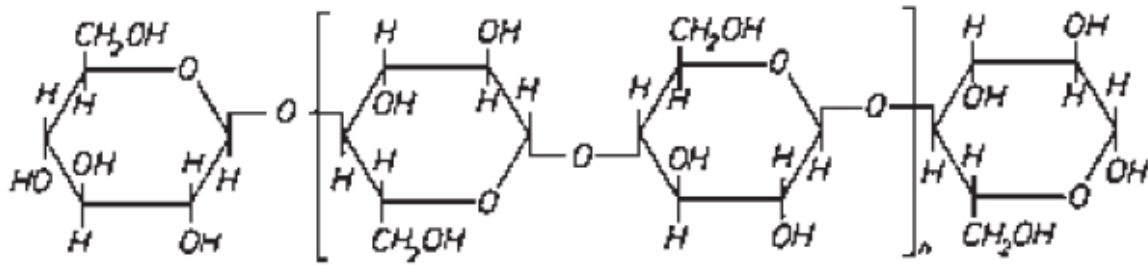


Figure 10: Structure of Cellulose Molecule [18]

The cellulose macromolecule is composed in the form of chain of glucose units and can be described by  $(C_6H_{10}O_5)_n$

For insulating paper manufacturing, the Alpha cellulose is required. This material is a polymer carbohydrate chain consisting of glucose units with a polymerization level of approximately 2000 [19] [20].

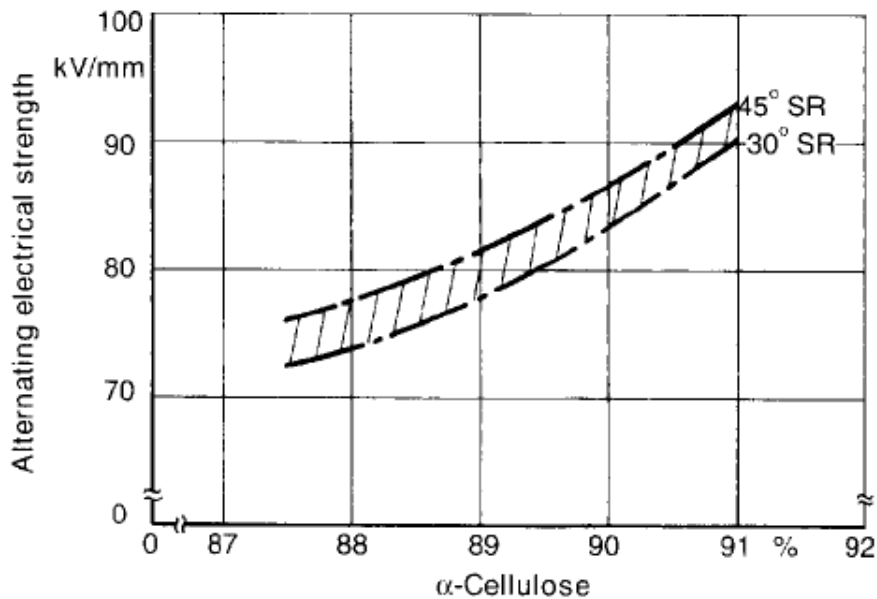


Figure 11: Influence of  $\alpha$ -cellulose on electrical strength, prepared at different beating SR, 1 mm nominal thickness, vacuum-dried and oil impregnated [19]

The electrical strength increases with increasing  $\alpha$  portion. Figure 11 illustrates how the electrical strength increases with increasing alpha portion at different beating<sup>1</sup> degrees (Schopper-Riegler °SR).

<sup>1</sup> Beating of cellulosic pulp is a mechanical treatment in water which produces a heavy changes in the fibers structure [20]

Cellulosic materials are obtained not only from wood but also from as unbleached soft wood sulphate pulp combined with cotton fibers, synthetic fibers, etc. [18]

Wood contains not only the cellulose fibers (approx. 40-60%) but also other substances such as lignin, lignin catabolic products, waxes and resins. Therefore a separation of these substances is required to obtain paper and transformerboard with an acceptable electrical and mechanical strength.

By several cleaning processes, the pure sulphate cellulose is dissolved in water, decomposed into single fibers and beaten in order to suspend the fibers. The fiber mats with loose cellulose fiber bundles are sieve-sorted and pressed together into cellulose fiber. The schematic overview of the manufacturing process of cellulose based transformer board is depicted in Figure 12. The first stages are the same as for paper production; the pure and virgin sulphate cellulose sheets are dispersed in water and stocked in chests. The individual fibers are crushed and refined. The paper and pressboard strength is primary determined by bonding forces between fibers. The fibers are stressed far below the breaking point. These bonding forces are influenced by the type and degree of refining [18].

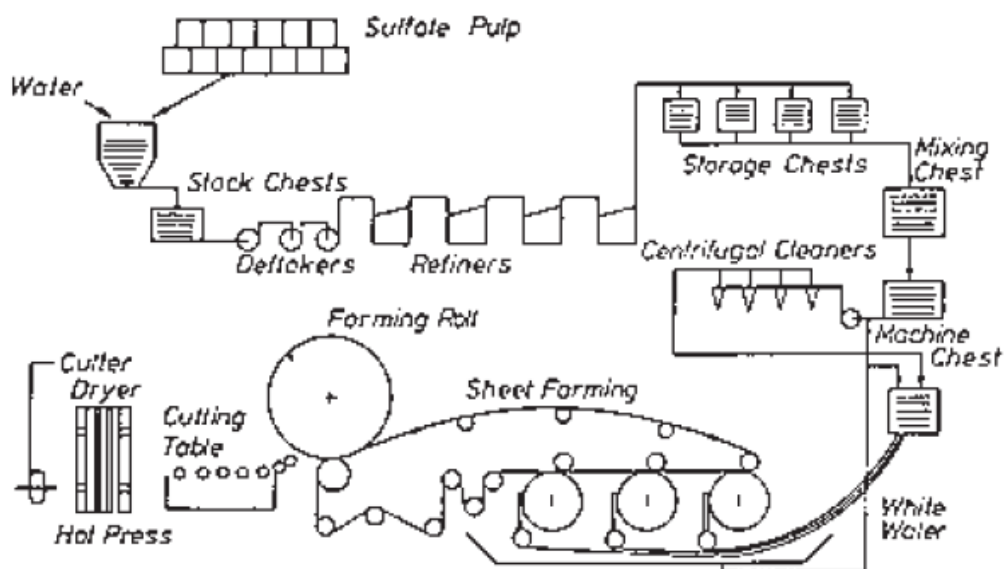


Figure 12: Manufacturing Process of Cellulosic paper [18]

The microscopic view of cellulose material shows the fibrous and non-homogenous character of the material. Figure 13 illustrates the structure of the cellulose fibers.

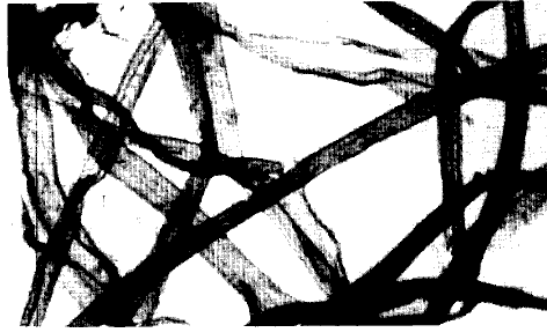


Figure 13: Microscopic view of cellulose fibers (enlargements 120:1) [19]

### Laminated wood (KP material)

Laminated wood is material of wood-like nature. Comparing to pressboard, this material has a higher mechanical strength. Laminated wood is usually used for making different parts in the transformer such as pressure plate, pressure ring, spacing elements, support block (Figure 14).

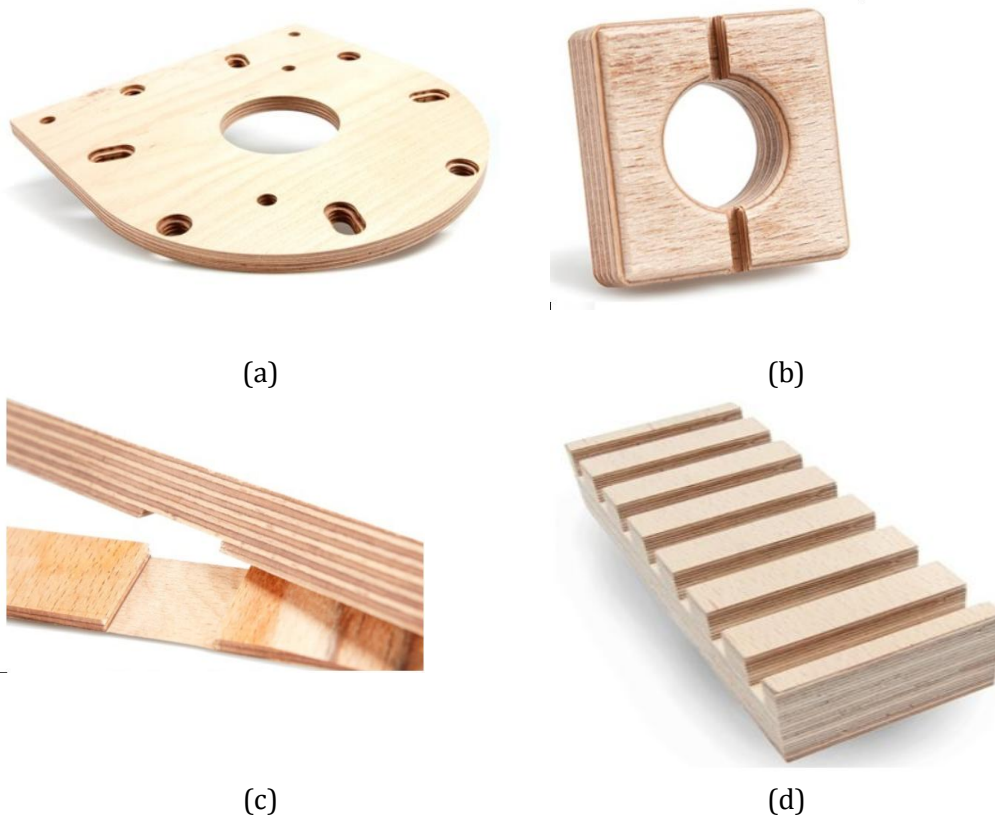


Figure 14: Different parts that are used in a transformer made of KP material (laminated wood) (a) Pressure plate (b) Pressure ring (c) spacing element (d) Support Blocks [21]

### 2.3. IMPREGNATION PROCESS AND CAPILLARY EFFECT

The oil-impregnation of insulation based on cellulosic material (paper, pressboard) is necessary to improve its dielectric strength as well as protect the material from degradation.

Oil impregnation is a process in which the oil is used to fill the pores existing in a material. For cellulosic material, the oil impregnation can happen in the cavities between the fibers or in the voids within the fiber itself. For instance when a cellulosic material is impregnated with water, the fibers expand and the volume increases. However the impregnation of transformer board results in negligible difference in dimensions of the sample, therefore the oil impregnation of transformer board is considered to be just in the cavities between the fibers [22].

The impregnation process is governed by two mechanisms:

1. The capillary action, the oil can flow in the narrow spaces within pressboard without the help of any external forces such as gravity. This mechanism is only a consequence of the intermolecular forces between liquid and solid surfaces
2. The force applied by the oil on the wall of the samples (gravitational forces or pressure of the oil in the walls of the pressboard)

#### 2.3.1. THE IMPREGNATION PROCESS

After assembly, a transformer is vacuumed and then filled with oil. The air remaining in the cellulosic material is evacuated during vacuum phase. During filling, the oil penetrates the pores in the material by capillary action. Once the vacuum is released, the voids inside the materials acts as a vacuum chamber and then begin to suck the oil into a capillary. The air exerts a positive pressure and therefore contributes together with capillary action in filling the voids with oil. A simple illustration of how the process works is depicted in Figure 15.

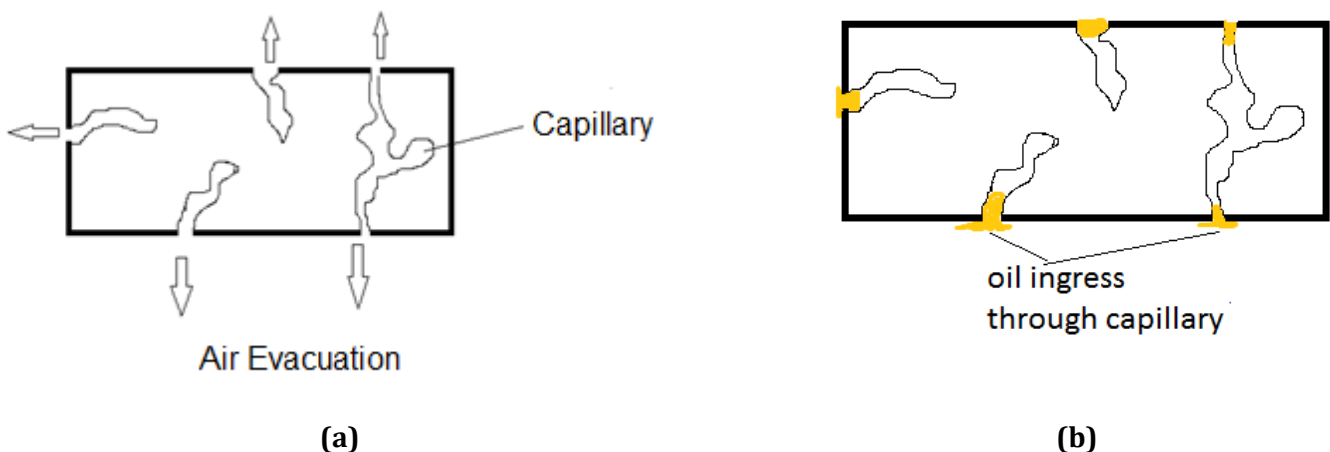
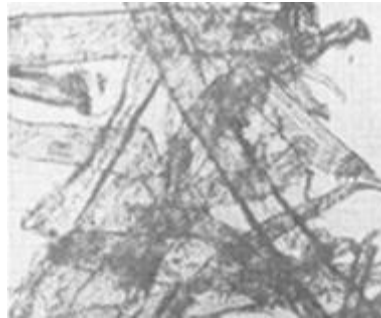


Figure 15: Illustrations of impregnation process steps: (a) Cellulosic material under vacuum (b) Impregnation under vacuum (capillary action)

### 2.3.2. FLOW DYNAMICS

In the literature sources, the pressboard is assumed as a porous body that behaves as an assemblage of cylindrical capillaries with very small radius, which obeys the same law as the rise of the liquid in capillary tubes of circular cross section [23]. However, in real situation the structure of transformer pressboard is much more complicated (see Figure 16) in comparison to the structure of a wood sample ( see Figure 17)



**Figure 16: Fiber structure of a layer of transformer pressboard. Thickness of pressboard is perpendicular to the page [22]**

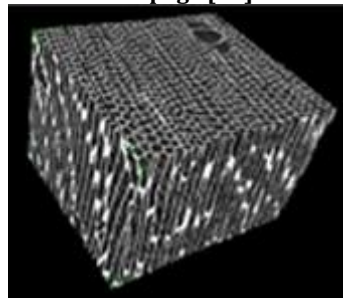


**Figure 17: Wood Sample Analyzed at 2.5 microns resolution (Sample size 1mm) [24]**

Theoretically, in porous media like wood different liquid flows might occur. However, the most dominant flows are viscous and linear laminar flow, while the turbulent flow is unlikely to occur in wood capillaries [25].

When cellulosic material is impregnated with oil, the cell wall absorbs slightly the oil. Therefore, it is generally accepted to consider the impregnation as the movement of free liquid (oil) only. In this case the flow of the oil follows the well-known laws governing the flow of the liquid through small tubes [26].

In general, by assuming pure viscous flow of liquids through a porous media; the flow of liquids can be described by different fundamental laws:

The Darcy law: This law is often used to characterize the flow of a liquid (oil) through wood [27][28]. The Darcy law is described as:

$$Q = \frac{kA}{\eta L} \Delta P \quad (1)$$

Where :

Q: is the conductivity ( $m^3/s$ ) or the volumetric flow rate of liquid

k: is the substrate permeability ( $m^2$ )

$\eta$ : is the dynamic viscosity of the liquid (N s/m<sup>2</sup>)

A: is the area of cross-section through which there is a flow (m<sup>2</sup>)

$\Delta P$ : is the pressure differential giving rise to flow (N/m<sup>2</sup>)

L: is the length of flow path (m)

Based on Poiseuille 's law [23] : The quantity of oil per unit time flowing into the capillaries inside cellulose materials is:

$$Q = \frac{dV}{dt} = \frac{\pi}{8\eta} \cdot \frac{r^4}{L} \Delta P \quad (2)$$

Where

V: is the volume of oil inside the capillary this equals to  $\pi r^2 L$  (m<sup>3</sup>)

r: is the average equivalent capillary radius (m)

$\eta$ : is the dynamic viscosity of the liquid (N s/m<sup>2</sup>)

According to equation (1) and equation (2) the forced penetration of liquid into the capillaries of the cellulose material is possible due to the pressure gradient. The pressure difference can be considered as the difference between the sum of external, hydrostatic and capillary pressures [25] (see equation3)

$$\Delta P = (P_{external} + P_{hydrostatic} + P_{capillary}) - P_{internal} \quad (3)$$

The internal pressure is the total pressure of the gaseous mixture remaining within the voids consisting mainly of air and water-vapour. The external pressure is the sum of the ambient pressure and the over-pressure in this case the pressure of oil on the sides of the material.

When the oil starts to penetrate the cellulose based material, the remaining gas inside the void becomes compressed. The ingress of the oil will be then slowed down due to the increase of back pressure. When the pressures are at equilibrium, a further ingress of the oil will take place only if the pressure of residual gases decrease or when the external pressure increases.

### 2.3.3. CAPILLARY ACTION

The effect of the capillary forces can be approximately described by Jurin's law which gives the capillary rise as a function of the radius of the capillary and liquid properties such as surface tension and the dynamic viscosity of the liquid

$$h^2 = \frac{r\sigma t}{2\eta} \quad (4)$$

Where : h: capillary rise (m)

$\sigma$ : surface tension at interface (pa)

t: time (s)

$\eta$ : is the dynamic viscosity of the liquid (N s/m<sup>2</sup>)

To summarize, the complexity of cellulosic materials structure and the different phenomena's that occur during the impregnation complicate the theoretical flow mechanism analysis of the oil in transformerboard. Moreover the estimation of the internal pressure is very complicated. This pressure builds up with time because of the compression of the residual air inside the cavities. Another factor that contributes to this, is the remaining bubble presence in oil that might penetrate the voids.

#### *2.3.4. FACTORS AFFECTING THE IMPREGNATION PROCESS*

The factors that influence the ingress of oil into cellulosic-based material can be categorized in two groups. The first group consists of factors related to the cellulosic material such as structure of the material, air and moisture content and sample dimensions. The second category includes factors related to the oil such as viscosity, surface tension and air solubility.

#### **Factors related to Cellulosic material**

The most important factor that influences the ingress of oil is the capillary structure, the geometry of the capillaries and their accessibility. These are different in laminated wood, paper, pressboard and laminated transformerboard. The dimensions of the pieces of the material influence the ingress of oil especially for laminated transformer board where the impermeable glue is used between the layers and hence the flow of oil can only in a direction parallel to the layers.

The residual air in cellulosic materials affects strongly its permeability. It slows down the speed of oil penetration. When the oil penetrates a capillary, the residual air inside becomes compressed by the capillary forces and hence the internal pressure builds up. For this reason, in order to reach a faster ingress of oil it is very important to have less air inside. The efficiency of removal of trapped air is dependent on the vacuum level used.

#### **Factors related to the impregnating oil**

The most critical characteristics that affect the capillary rise and the flow rate in cellulosic material are viscosity of the oil and surface tension at the oil-gas interface. According to equation (2), the volume of the oil that entered inside the capillary is inversely proportional to the viscosity. However the viscosity of the oil decreases when the temperature increases.

### **2.4. STRESSES IN THE TRANSFORMER**

#### **Thermal stresses**

During operation, the insulating materials in the oil-filled transformers are exposed not only to electrical stresses but also mechanical and thermal ones. The thermal stresses are caused by the rise of temperature due to the losses in copper (resistive), iron (hysteresis), and dielectric materials.

#### **Mechanical stresses**

One of the major reason for faults inside the transformers is attrition of the winding and conductor insulation as a result of vibrations due to electromechanical forces. The highest forces usually occur under short circuit conditions. Therefore a short circuit test is the worst case regards to maximum forces [29].

The mechanical stresses can occur due to vibration or possible short-circuit. Another cause for these stresses might be the thermal expansion of the winding.

### **Electrical stresses**

Moreover, the electric stresses that might occur during operation of the transformers are originating from:

- Power frequency voltage
- Temporary overvoltage
- Switching impulses
- Lightning impulse

The electrical stresses lead to degradation of oil performance as to decrease the dielectric strength and its negative influence on the cooling action [30] .

### **2.5.PARTIAL DISCHARGES IN OIL-FILLED TRANSFORMER**

As defined in IEC standard, a partial discharge is localized electrical discharge within any insulation system under high voltage field stress. This discharge or electrical pulse does not completely bridge the electrodes between which the voltage is applied unlike breakdown [31].

There are three types of PD [32]:

- The internal discharges : occur in cavities or void in a solid dielectric usually filled with gas (air).
- Surface discharges: it occur along the dielectric interfaces.
- Corona discharges: occur at sharp metallic points in an electric field, in gaseous dielectrics in the presence of inhomogeneous field.

#### *2.5.1. PARTIAL DISCHARGE PHYSICS*

The insulating systems inside a power transformer consists mainly of a liquid dielectric (e.g. mineral oil) and a solid dielectric in the form of oil-impregnated cellulosic materials. An improper impregnation of these materials can lead to remaining gas cavities (vapour, air) inside. This gas contains electrons, if an electric field is applied, the electrons are accelerated in the direction of the electric field. These accelerated free electrons are very critical for initiating a partial discharges. The electron will collide with the gas molecules and loose the energy. Further on, the electron gains energy again due to electric field.

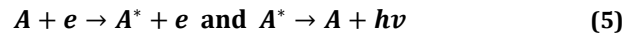
There are three necessary conditions to initiate a partial discharge mechanism:

1. Creation of start electron.
2. Multiplication of electrons leading to avalanche.
3. Feedback process to create secondary electrons.

- **Starting electron**

The first condition of PD occurrence is a presence of a starting electron to start the process. This electron is released from the gas (or electrode). The electric field accelerates the electrons and three reactions may occur:

1. Elastic collision where the electron loses only a small fraction of its energy.
2. Inelastic collision where the atom in the gas is excited into a higher energy state and after a short time falls back into its ground state and a photon is emitted.



3. Ionization, here the atom is excited at higher energy level and the collision liberates an electron.



Three types of ionization can be distinguish:

**Thermal ionization:** at very high temperature ( $T > 1000K$ ), the molecules of the gas might be disassociated into atoms. Higher temperature means more kinetic energy for the atoms and more chaotic movements and the atoms start to collide. Two processes occur. The first is ionization of the atoms; namely when the kinetic transferred during collision is higher than ionization energy  $eV_i$ . The second is excitation of the atom; when the kinetic energy due to collision is not high enough, the atoms goes back to the ground state and a photon is released. Hence the photo- ionization of other atoms might occur.

**The photo-ionization:** Ionization occurs when the photon energy  $h\nu$  is larger than the ionization  $eV_i$  energy of the gas. These photons occur due to the radiation emitted when gas atoms fall back to their ground state or external radiation.

**The collision ionization,** in the case that an electron with sufficient kinetic energy collides with a gas a molecule.

As a result of ionization process, free electrons will experience electric field. The ionizations by electron can be described by the next ionization factor:

$$\alpha = \frac{\text{number of electrons}}{\text{cm in the field direction}} \quad (7)$$

$\alpha$  is proportional to the number of collisions and thus to the gas pressure  $p$

However the kinetic energy of the accelerated electron is proportional to the gas pressure and  $\alpha$  increases with kinetic energy of the colliding electrons:

$$W = eE\lambda \propto \frac{eE}{p} \quad \text{and} \quad \alpha \propto f\left(\frac{E}{p}\right) \quad (8)$$

By combining the two equations we get

$$\alpha \propto pf\left(\frac{E}{p}\right) \quad (9)$$

For many gases type the ionization factor is :

$$\alpha = Ap \cdot \exp\left(-\frac{Bp}{E}\right) \quad (10)$$

The maximum ionization takes place at certain pressure. Figure 18 shows how the ionization factor in function of pressure. At low pressure where the mean free paths are very large which results in very few collisions with gas molecules en thus a drop in ionization factor. At high pressure, the mean free paths are very small leading to insufficient energy for ionization.

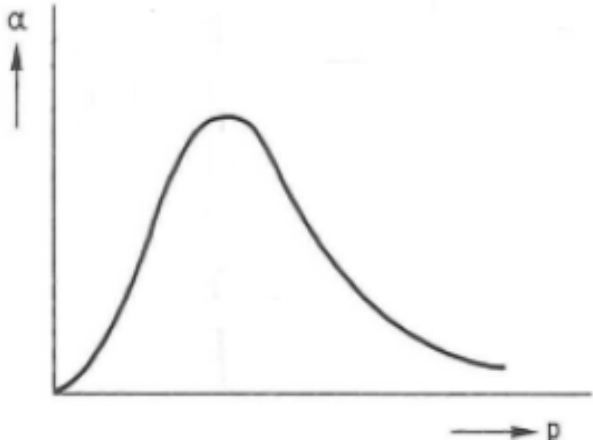


Figure 18: Ionization factor as a function of pressure p [32]

- **Electron avalanches**

The repeated ionization process leads to a multiplication of number of electrons. At a distance of x along the electric field, the initial free electrons  $N_x$  create a  $dN_x$  free electrons by ionization. which are according to the definition  $\alpha$ :

$$dN_x = N_x \alpha dx \tag{11}$$

In uniform field , the total of free electrons at distance x from starting point along the electric field is:

$$N_x = N_0 \exp(\alpha x) \tag{12}$$

The number of electrons increases exponentially. One or few starting electrons are sufficient to create an electron avalanche. As the electrons are somewhat in a sideward direction, the avalanche increases in thickness. The ionization of atoms creates not only fast electrons but also positive gas ions which are much slower.

- **Feedback process**

Electron avalanches in themselves causes only a leakage current in the insulating medium, they do not cause breakdown. For a breakdown, a feedback process is needed to ensure the release of new starting electrons called secondary electrons. In gases of low pressure this feedback process is formed by a  $\gamma$  process. Figure 19 illustrates the ionization and the feedback process.

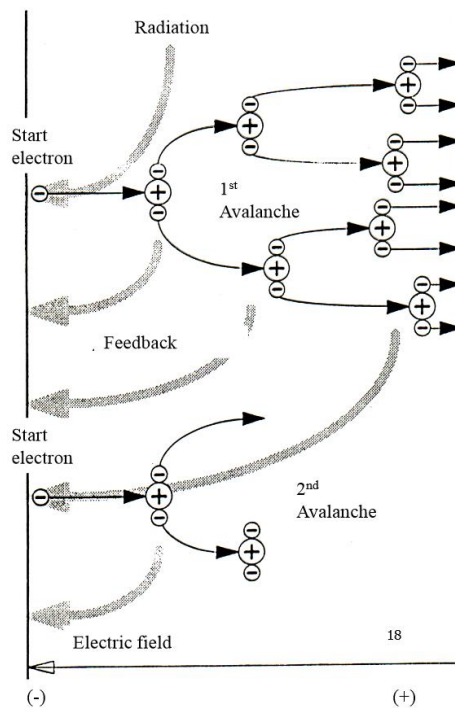


Figure 19: Ionization /feedback mechanism [33]

### 2.5.2. BEHAVIOR OF PARTIAL DISCHARGES

To understand the behavior of the voltages and currents in a sample with an internal discharges, a simple equivalent circuit can be used. This circuit is depicted in Figure 20.

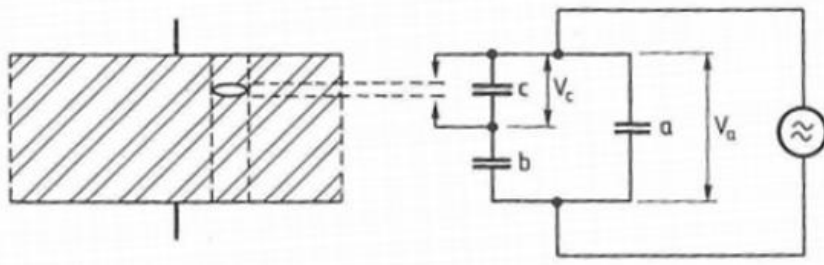


Figure 20: the abc equivalent circuit with sample a, dielectric b in series with the cavity c [32]

The capacitance  $c$  represents the capacitance of the cavity in series with capacitance  $b$  which is the capacitance between the edges of the cavity and the electrodes. The healthy part of the sample is represented by capacitance  $a$ . Where normally  $b < c \ll a$

When a A.C. voltage  $U_a$  is applied over the sample, a synchronous voltage  $U_c$  is generated at the cavity. Without discharges, this voltage is :

$$U_c = \frac{b}{b+c} U_a \quad (13)$$

When the voltage  $U_c$  becomes greater than the breakdown voltage  $U^+$ , discharges will occur.  $U^+$  is dependent on the geometry of the cavity and the Paschen curve of the gas within the cavity. A schematic of the voltage across the cavity with discharge is shown in Figure 21.

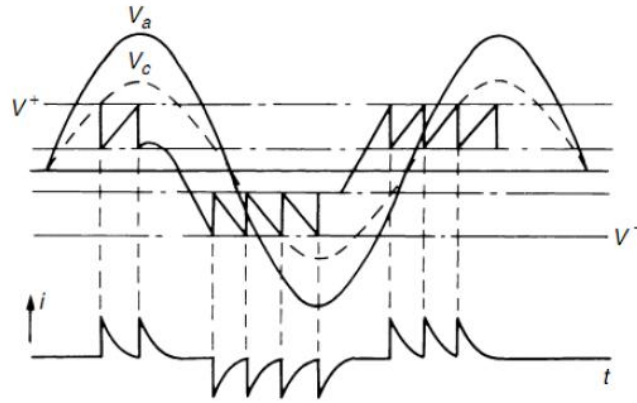


Figure 21: Voltage behavior at the cavity when A.C. voltage is applied [32]

In a gas filled cavities within a solid insulation, the partial discharges occur in both half cycles (see Figure 21). The partial discharges at both polarities are equal.

### 2.5.3. PARTIAL DISCHARGES OCCURRENCE IN PARTIALLY OIL-IMPREGNATED TRANSFORMERBOARD (PASCHEN CURVE)

Cellulosic based insulating material has a porous structure therefore it should be properly impregnated to fill the cavities with oil. Any un-impregnated void can lead to a local field enhancements. When this electric field exceeds the breakdown strength, partial discharges might occur. In this section, a theoretical investigation of the possibility of partial discharges occurrence will be discussed.

#### Oil-impregnated Transformerboard: pores sizes

Using X-rays, a sample of PSP transformerboard is scanned. Figure 22b and 22c shows a results of the scanning. At resolution of 20  $\mu\text{m}$  no pores could be visible. For our further calculation, we assume that the pores has a maximum size of 20  $\mu\text{m}$ .

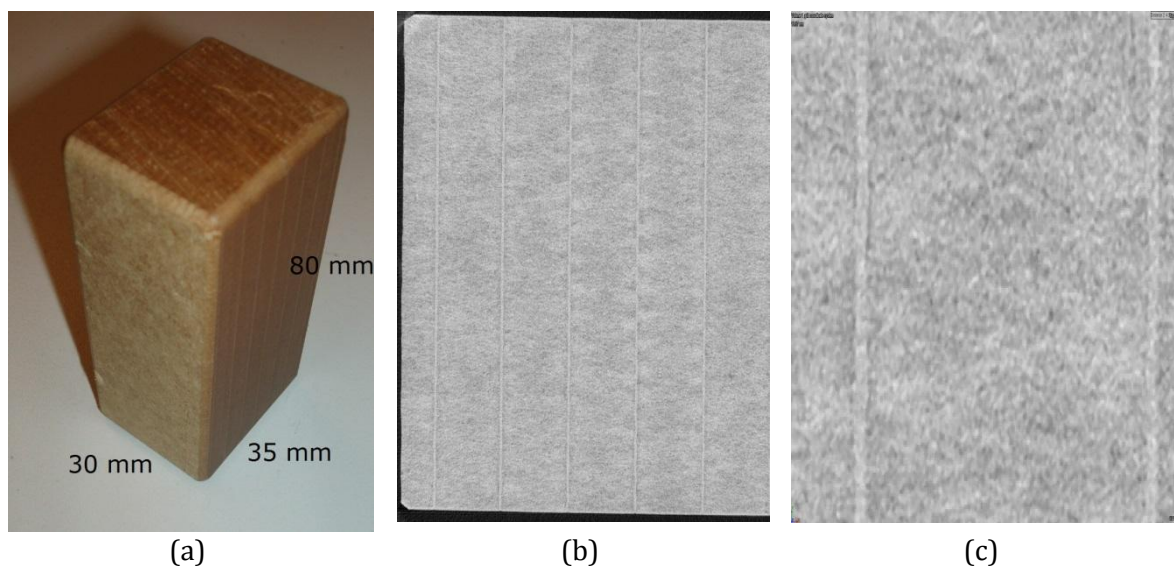


Figure 22 : (a) Sample of PSP (b) (c) X-ray scans of PSP sample

## Calculation of the electric field in the cavities

Because of the complexity and non-homogeneity of the structure of the material, we assume some simple shapes of air cavities inside the transformerboard. These air cavities can be spherical voids, parallel or perpendicular fissures to the electrodes. These are shown in Figure 23.

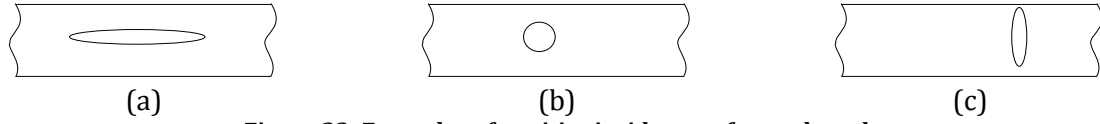


Figure 23: Examples of cavities inside transformerboard

The field strength in the fissure (cavities perpendicular to the field) is about  $\varepsilon E_d$  even if the strength of electrical field in the dielectric  $E_d$  is low, it will be enhanced inside the cavity by a factor of  $\varepsilon$  which is the permittivity of the material and may cause discharges. When the cavity is in the direction of the field, the field strength, in this case, equals  $E_d$ . In the case of spherical cavity the field will be enhanced by  $\frac{3\varepsilon}{1+2\varepsilon} E_d$  [32].

According to the manufacturer, the maximum stress level that can affect the material is 4kV/mm. Further on, between these two electrodes several layers of oil and Cellulosic material can be found. This implies that the electrical stress in the transformerboard is much lower than 4kV/mm (RMS). Assuming that only one layer of transformerboard is between the electrodes, the electric field strength in the transformerboard will be lowered by a factor of  $\varepsilon_{oil}/\varepsilon_{cellulose}$ .

### Permittivity of impregnated transformerboard

In an impregnated cellulosic material, the combination of the cellulose and oil is relatively complex. Therefore the resultant permittivity of the mixed dielectrics (cellulose, oil) can be calculated using formula 14 [34]

$$\varepsilon_{rk}^{\alpha} = v_z * \varepsilon_{rz}^{\alpha} + v_i * \varepsilon_{ri}^{\alpha} \quad (14)$$

Where

$\varepsilon_{rk}$  = resultant permittivity of mixed dielectric

$\varepsilon_{rz}$  = permittivity of cellulose;  $\varepsilon_{rz} = 4$

$\varepsilon_{ri}$  = permittivity of impregnation medium;  $\varepsilon_{ri} = 2.2$  for mineral oil

$v_z$  = volumetric proportion of cellulose;  $v_z = 0.5 - 0.7$

$v_i$  = volumic proportion of impregnating medium;  $v_i = 0.3 - 0.5$

$\alpha$  = mixed form exponent;  $-1 < \alpha < 1$ ; a parameter that determine the type of mixing rule ( -1 for serial mixing and 1 for parallel mixing).

The values of the volumetric proportion of cellulose and impregnating medium given by literature [34] seems to be not valid for the PSP material. According to the specification of the transformerboard, the oil absorption is approximately 13%. The volumetric proportion of oil equals:

Volume of the oil/ volume of the cellulose=13%\*density of cellulose/density of oil

This implies that the volumetric proportions of the transformerboard and impregnation medium are 17.81% and 82.19% respectively. Taking  $\alpha=1$  (as this gives the upper limits of the effective dielectric constant [35] by assuming that the mixing of oil and cellulose in PSP material is parallel) and substituting in equation 14 obtain the permittivity of impregnated transformerboard is 3.68.

### Electric field in air cavity

Assuming a parallel flat air cavity inside the transformerboard, the field strength in this cavity is:

$$E_{cavity} = \epsilon E_b = \epsilon \frac{U_b}{d} \quad (15)$$

Where  $\epsilon$  is the relative permittivity of the insulation equals 3.68 and  $E_b$  is the electric field strength of the insulation is 2.38 kV/mm(RMS) in case of one layer of transformerboard between electrodes. The electric field strength inside the air cavity can be calculated from equation (15):  $E_{cavity}= 3.68*2.38=8.758$  kV/mm (RMS)

### Probability of PD occurrence by means of paschen curve

Because we are interested in partial discharges insides air cavities within impregnated transformerboard, we need to check if there is a possibility of getting internal discharges at given conditions. Therefore the modified Paschen curve depicted in Figure 24 can be used. This modified curve is based on Paschen's law of air  $E_i = f(p, d)$  where the breakdown strength is a function of pressure in the cavity and size of cavity.

Knowing that the maximal field strength inside the cavity is 12.5kV/mm (crest) and assuming that the maximal void in transformer board is 20  $\mu$ m, by using modified Paschen curve depicted in Figure 24; for the given conditions; the point lays under the dashed curve which means that the internal partial discharge inside the voids in the transformerboard is unlikely to occur.

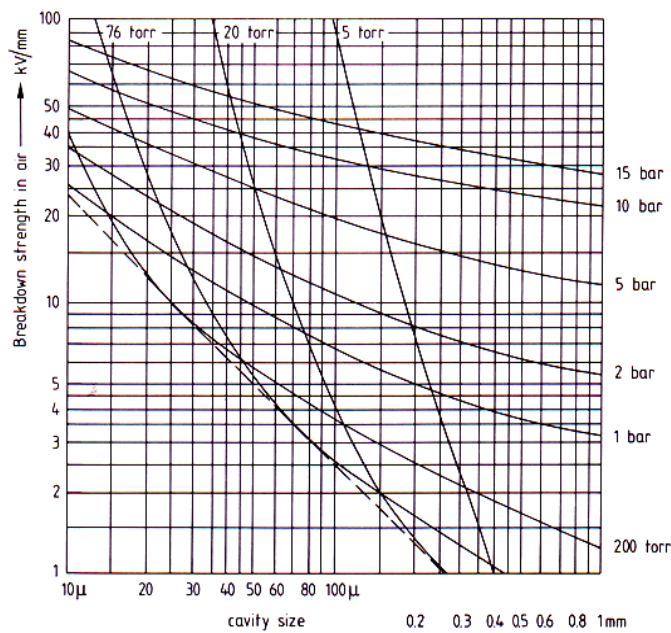


Figure 24: Modified Paschen curve - Breakdown strength in function of cavity size and pressure [32]

### 3. IMPREGNATION PROCESS MONITORING AND MEASUREMENT SETUPS

This chapter describes the measuring techniques and test setups used in our study. These include PD,  $\tan\delta$  and weight measurements.

Section 3.1 describes the purposes of the tests performed during this research. Further on, a description of the samples preparation process, measurements methods and test setups are given in section 3.2, 3.2, and 3.4 respectively.

#### 3.1. PURPOSE OF TESTS

In order to optimize the standing time needed before testing an oil-filled transformer, it is necessary to understand the process of oil ingress into the cellulose material. The PD activity that might occur within a transformer would endanger the transformer's insulation life-time. Therefore the following hypothesis can be stated:

*Extra post-impregnation standing time is needed to complete the impregnation of high-density cellulosic materials within a transformers. In particular to get the required insulation properties. An incomplete impregnation of such material leads to remaining air cavities inside the material which might lead to a Partial discharges (PDs).*

To solve the problem, the approach is to build a mathematical model that relates the time needed for complete impregnation with the sample shape and dimensions and oil temperature. This will be done by monitoring the impregnation process of several sample types by means of:

- Measuring the weight increase during the post impregnation period until the saturation level.
- PDs measurements versus time. This intends to reveal possible changes of partial discharge inception voltage (PDIV) and partial discharge (PD) level over the post-impregnation standing period.
- $\tan\delta$  measurements to monitor the oil ingress into the samples during the post-impregnation period.

As Explained in the previous chapter, the impregnation time depends highly on the type of the material used. A cellulose material with lower density would be impregnated faster. Lower density of the material implies larger size of pores and according to Poisseuille's Law (see equation 2) the amount of oil that is seeped per unit time is a function of capillaries dimensions (radius of the capillary  $r$  and its length  $L$ ), i.e. for larger  $r$  the amount of oil per time unit becomes larger and hence the impregnation process is faster.

Another factor that influences the impregnation is the size and the shape of an object to be impregnated. For instance, the distance that the oil has to travel towards the center of the object and the side surface through which the oil ingresses influence the impregnation speed [2][23]. The impregnation speed highly depends on the viscosity of the oil; using oil with lower viscosity, the cellulose material would be impregnated faster [2]. The oil viscosity depends highly on the temperature (see Appendix A1).

## 3.2. SAMPLE PREPARATION

In this research thesis, the impregnation process of two materials different cellulosic materials namely the Transformerboard (PSP) and laminated wood (KP) will be studied. The focus will be on the influence of sample shape and dimensions on the time necessary to complete the impregnation.

In this section, a description of the studied samples will be presented and the preparation procedure of the sample will be explained. This includes the drying and impregnation processes.

### 3.2.1. SAMPLES SIZES, SHAPES AND MATERIALS

#### Material

In the oil-filled transformers different cellulosic materials are used as insulants. Some examples of those materials are:

- Paper: which is used for windings insulation
- Transformerboard (PSP): these are of a form of sheets used as cylinders to create barriers.
- Transformerboard laminated - casein (PSP): Layers of material that are assembled with glue to create solid blocks. Each layer is about 5 mm thick.
- Laminated wood (KP) used as support beams, planks, blocks, uprights, pressure ring etc.

The density of the laminated wood is lower than the transformer board [39][40]. The resin glue used between the layers in the laminated transformerboard is not permeable. Therefore, the oil penetrates the sample only from the sides. Only the top and the bottom layer of the sample are impregnated through one additional side.

In this study we will focus only on two materials: laminated transformerboard (PSP) and laminated wood (KP).

#### Chosen sizes and shapes:

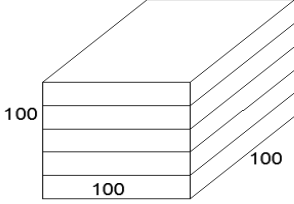
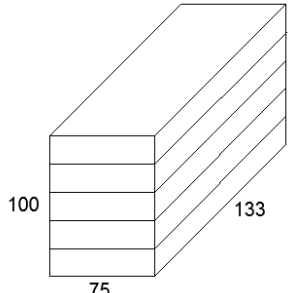
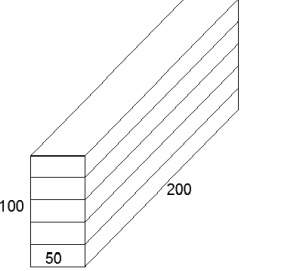
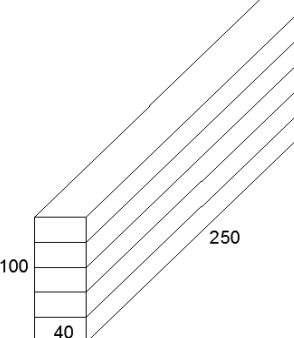
The impregnation time depends highly on the dimensions of the sample. Therefore it is necessary to investigate how the side surface of a sample will influence the impregnation time. For this reason, samples with constant volume and different side surface are studied.

Moreover the distance which the oil has to travel to entirely impregnate the sample is of importance. Therefore samples with same side surfaces and different shapes and hence different distance from edges of the sample to the centre are investigated.

- Samples used to investigate the influence of the side surface on the speed of impregnation:

To investigate this dependencies, we consider a cuboidal samples with the same volume ( $V=1000\text{cm}^3$ ) and different side surfaces. Only 4 options are taken in consideration due to restriction concerning the size of the available vacuum oven. An overview of the sample dimensions is given in Table 2. Characteristics of the samples are given in the table. Note that the sample dimensions are not scaled with respect to the picture.

**Table 2: Cuboidal samples with fixed volume and different side surfaces**

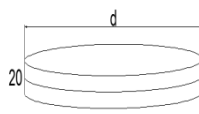
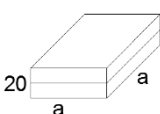
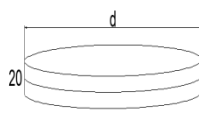
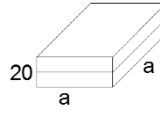
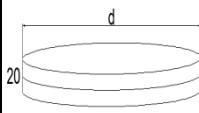
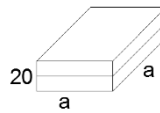
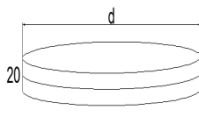
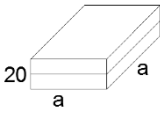
Sample dimension	Side surface[mm <sup>2</sup> ]	Volume[mm <sup>3</sup> ]
 <p>Type R1</p>	40.000	1.000.000
 <p>Type R2</p>	41.600	1.000.000
 <p>Type R3</p>	50.000	1.000.000
 <p>Type R4</p>	58.000	1.000.000

- Samples used to investigate the Influence of the distance to the center:

In this investigation, we change the shape of the samples while keeping the side surface fixed. Because of the fact that the transformerboard (PSP) can be impregnated only through the side area, we keep the height constant  $h=20\text{mm}$  and change only the diameter of the cylinders.

Table 3 summarizes the chosen samples including the shapes and dimension.

**Table 3: Samples with different shapes and same side surface**

	Cylindrical	Square
$S=4.000\text{mm}^2$	Sample type C1  $d=63.5\text{mm}$	Sample type S1  $a=50\text{mm}$
$S=4.160\text{mm}^2$	Sample type C2  $d=66\text{mm}$	Sample type S2  $a=52\text{mm}$
$S=5000\text{mm}^2$	Sample type C3  $d=80\text{mm}$	Sample type S3  $a=62.5\text{mm}$
$S=5800\text{mm}^2$	Sample type C4  $d=93\text{mm}$	Sample type S4  $a=72.5\text{mm}$

### 3.2.2. DRYING PROCESS

One of the most important stages in transformer manufacturing is the cellulosic insulation drying process. This is to remove the moisture from the insulating materials. Separately oil is dried and degassed as well. The most effective method used by the transformer manufacturers is the vapour-phase techniques, where the active parts of the transformer are dried under vacuum and by using a solvent. Under vacuum, the boiling point of water is reduced; therefore, the evaporation of water can be achieved at low temperature.

#### Drying of the sample

According to Weidman Datasheets [39], the PSP material absorbs approximately 7% of moisture per weight. Before impregnation, the samples are dried using a vacuum oven (see Figure 25(a)). This is done under vacuum of approximately 7.5mBar at 125 °C for 24 hours. Because of the space restriction in the oven and the use of the oven for impregnation purposes, To speed up and optimize the operation, first the samples pre-dried in an oven (Figure 25 (b)) at 85 °C for several days. The samples lose from 5 to 6 % of their weights and then are dried under vacuum to complete the drying process.

#### Drying of the oil

The oil used for impregnation is the Nynas oil. This oil is dried at a temperature of 90-100 °C under vacuum of approximately 10 mBar (Figure 25 (c)). To speed up the drying process several cycles (heating up – cooling down) are made. After several cycles, the residual moisture content in the oil is between 5 and 6 ppm.

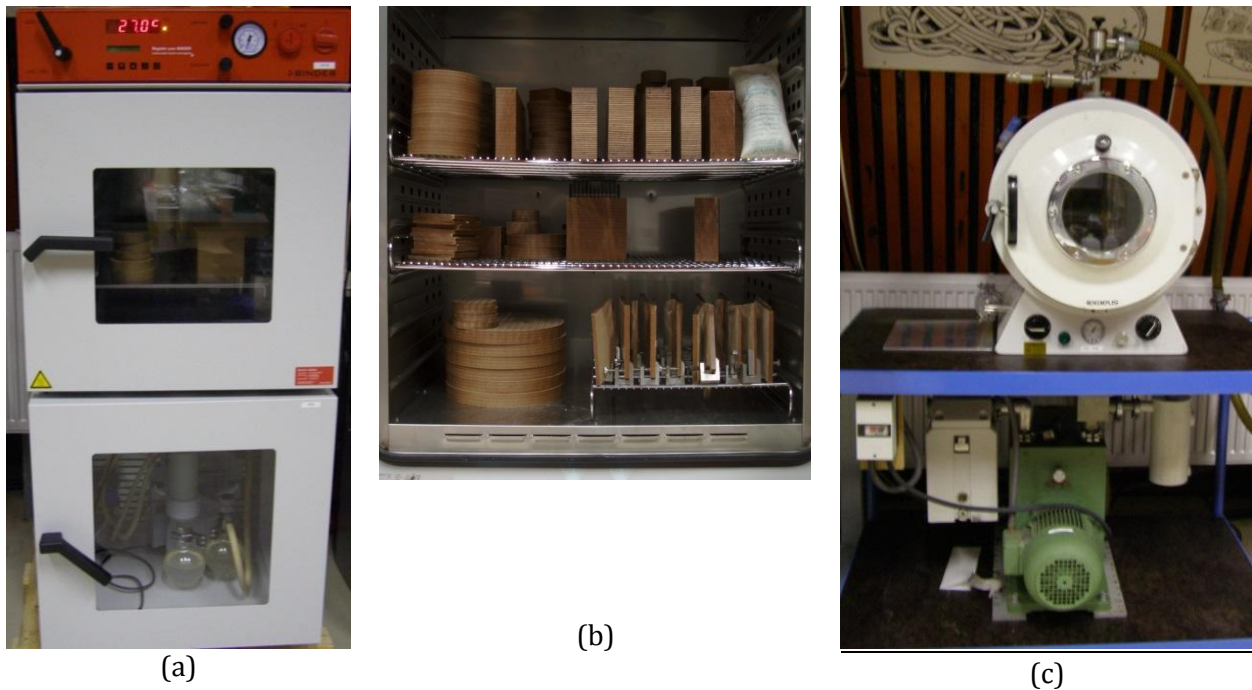


Figure 25: (a) Vacuum oven used for sample drying (b) ordinary oven with samples (c) vacuum oven used for oil drying

### 3.2.3. IMPREGNATION PROCESS

The impregnation process is done under vacuum of approximately 7 mBar. Figure 26 shows the oven used for impregnation. To facilitate the impregnation, an inlet for the oil has been installed in the oven. Such arrangement allows the oil flow from the external container into the oven chamber while vacuum is still maintained. The container with a sample to be impregnated is under vacuum and via a pipe is filled slowly with oil. When the container is filled, the vacuum is released and then the post impregnation time starts. First, the impregnation was done at ambient temperature ( $\sim 22^{\circ}\text{C}$ ), and then all the procedures are repeated at  $50^{\circ}\text{C}$  and  $70^{\circ}\text{C}$ .



**Figure 26: Vacuum oven used for Impregnation**

### 3.3. MEASUREMENTS METHODS

This section describes the methods used for monitoring the impregnation process; the weight, PD and  $\tan\delta$  measuring method.

#### 3.3.1. WEIGHT MEASUREMENTS

One of the ways to monitor the oil ingress in the sample is to measure its weight increase over time. The weight of the sample will increase until the capillaries and pores are filled with oil and the sample is saturated (saturation time).

Different methods are proposed to measure the weight with an acceptable accuracy. These are described in the following section:

#### Continuously weighting method

In this approach, the sample will be hang on the scale and the weight will be measured The scale would send the measurement results to the PC (see Figure 34(b)).

A schematic of the measuring setup is shown in Figure 27.

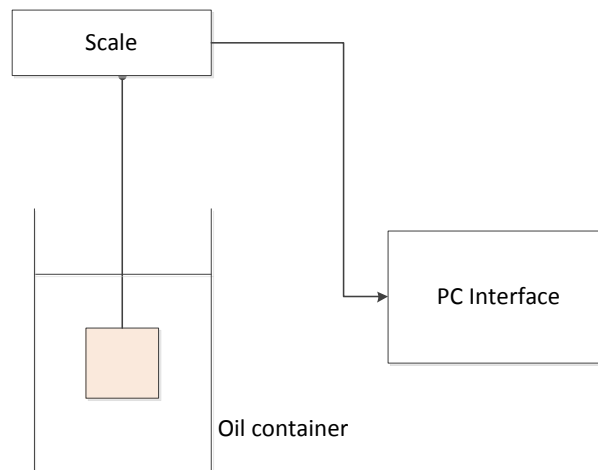


**Figure 27: scheme of continuously weighting approach**

The force measured by the scale is the difference between the force applied by the weight of the sample and Archimedes force

$$F = mg - V \cdot \rho \cdot g \quad (16)$$

Where:

F : is the net force measured by the scale

m: is the real mass of the sample

g: is the gravitational force

V: is the volume of the sample

$\rho$ : is the oil density

The apparent mass measured by the scale is then

$$M_{apparent} = m - V \cdot \rho \quad (17)$$

This approach seems to be appropriate, however there are several factors that affect the accuracy of the measurements. At a certain moment, the scale shows a value of 0. This can be explained by an equilibrium between the Archimedes forces and the weight of the sample. During impregnation not only the mass is increasing but also the volume is slightly increasing. Moreover during experiment some unexplained jumps occurred in the plotted curve representing the obtained data. This might be because of the sensitivity of the device itself. Therefore, this method turned out not to be suitable.

**Periodical weighting method**

Periodical weighting is the second approach to monitor the impregnation progress. Here a sample is taken out of the oil and oil residuals are wiped out of the sample surface. Since in the beginning the increase in weight is higher, the measurement is performed approximately each 30 min after impregnation and later on each hour.

To investigate the effect of taking the samples out of the oil on the impregnation process, identical samples (type S4) are prepared and impregnated at the same conditions. The weight of one sample is measured every 30 min, for the the second one every 1 hour and for the third one every 2 hours. As shown in Figure 28, the difference between the results obtained is negligible. All samples saturate at the same time.

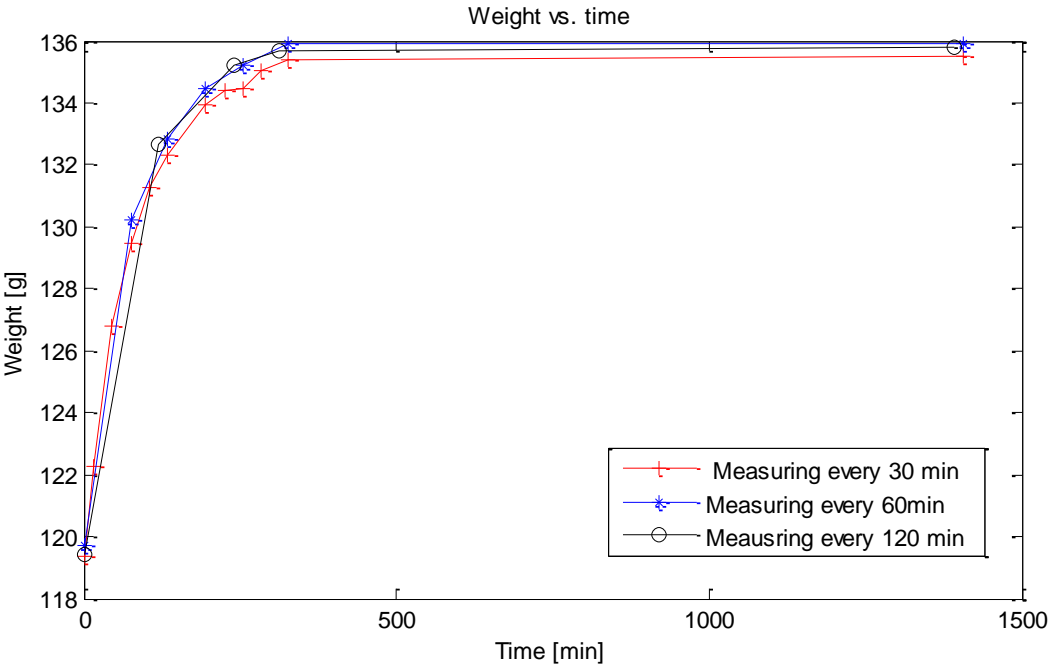


Figure 28: Weight in function of time identical samples when measuring every 30min, 60min, 90 min.

In this research, the followed methods in measuring the weight of the samples is the periodical weighting.

### 3.3.2. PD MEASUREMENT METHOD

The purpose of the test is to investigate if directly after impregnation a PD activity occurs and what will be the PD and PD inception voltage (PDIV). In addition, the PDIV variation in function of standing time.

#### Measuring method: Straight detection circuit

The electrical detection of partial discharge is based on measuring the electrical pulse created by the current generated in the void. The duration of these pulses are in the range of nanoseconds to microseconds and have measurable frequency components.

In the straight detection circuit different components are used. These are the test object  $C_a$ , coupling capacitor  $C_k$ , Coupling device CD and a noise filter Z. The filter is introduced at high voltage to reduce background noise from the power supply. The coupling capacitor  $C_k$  is connected in parallel a the test object in order to provide a closed circuit for the discharge.

In general, there are two coupling modes [31] depending on how the coupling device is connected. A common used mode is when the coupling device is connected in series coupling capacitor (see Figure 29). This configuration is usually used during testing in the High voltage laboratory to avoid damaging the testing equipment due to test object breakdown or a flashover.

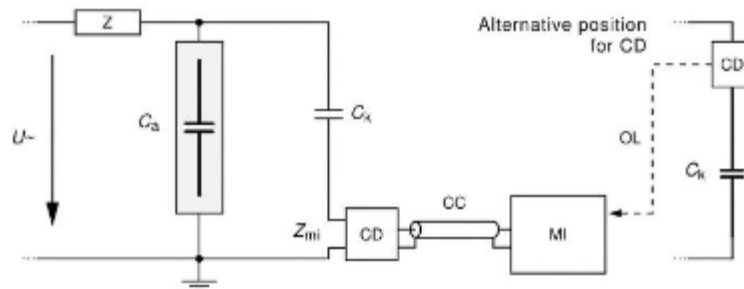


Figure 29: Coupling device in series with coupling capacitor [31]

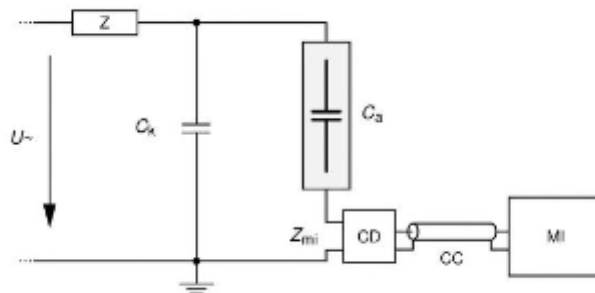


Figure 30: Coupling device in series with test object [31]

The second coupling mode is when the CD is connected in series with test object (see Figure 30). Using this arrangement, higher sensitivity can be obtained [31].

### 3.3.3. TANδ MEASUREMENT METHODS

Dielectric properties of an insulant are dependent on many factors such as frequency, time, temperature, chemical composition, and the structure of the whole insulation system composed of different dielectrics [36].

One of the most common diagnostic tools used to assess a HV voltage equipment, is the dissipation factor ( $\tan\delta$ ) and capacitance measurements. A change in  $\tan\delta$  provides useful information about the insulation quality. However this technique is a global method where only global changes of the insulation can be identified but not localized defects [36].

In this research, the measurement of  $\tan\delta$  are carried out to see how it will change over in the course of the standing time. The expectation of this experiments is that the value of  $\tan\delta$  will decrease over the time; i.e., when the oil ingresses into the cellulose material.

Two different methods of measuring  $\tan\delta$  are used. The first method is based on the Schering Bridge arrangement and the second is based on the frequency domain spectroscopy measured with IDAX™.

#### Dielectric losses definition

An insulation material such as pressboard and pressed wood are not ideal insulators. When a test object is subjected to an A.C. voltage, losses appears in the material. The material can be represented using the parallel equivalent circuit of the lossy capacitor depicted in Figure 31(a).

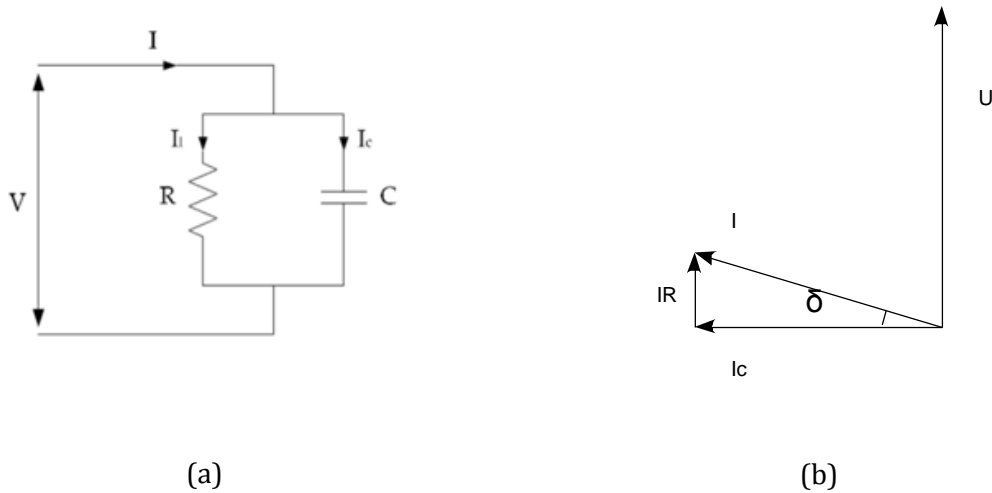


Figure 31: (a) Parallel equivalent circuit for a lossy capacitor (b) loss angle  $\delta$

The definition given in the International Standard of the IEC (International Electro-technical Commission) [37] related to dielectric dissipation factor is:

Dielectric dissipation factor of an insulating material is the tangent of the loss angle. The loss angle is the angle by which the phase difference between applied voltage and the resulting current deviates from  $\pi/2$  rad as shown in Figure 31(b).

$$\tan\delta = \frac{I_R}{I_C} = \frac{1}{\omega RC} \quad (18)$$

The dielectric losses (amount of energy) caused by a small loss component  $I_R$  are:

$$W = U \cdot I_R = U \cdot I_C \cdot \tan\delta = U^2 \cdot \omega C \cdot \tan\delta \quad (19)$$

the losses that appears in the impregnated paper, pressboard and pressed wood may have several physical origins. To get a complete analysis of the dielectric losses, it is necessary to investigate the effect of several variables such as frequency, voltage, temperature [38].

**The conductive losses:** When the insulation resistance R of the dielectric decreases, the leakage current is increased and adds to the dielectric losses. The  $\tan\delta$  decreases if the frequency is increased. This can be clearly seen from equation 18.

**Polarization losses:** At low frequencies, the friction between the rotating electric dipoles and the insulation material is low what results in a low  $\tan\delta$ . When the frequency increases the  $\tan\delta$  increases. At a certain high frequency the  $\tan\delta$  reaches its maximum. At very high frequencies, the losses decrease again because the dipoles are immobile.

**Discharge losses:** When the partial discharges occur in a dielectric,  $\tan\delta$  increases due to additional losses. The increase of  $\tan\delta$  is larger if the number and the magnitude of the discharge is larger. Below the inception voltage the  $\tan\delta$  equals to that of the discharge free material.

### Measuring methods using Schering bridge

One of the most used methods for measuring the  $\tan\delta$  with high accuracy is the high voltage Schering bridge (Figure 32).

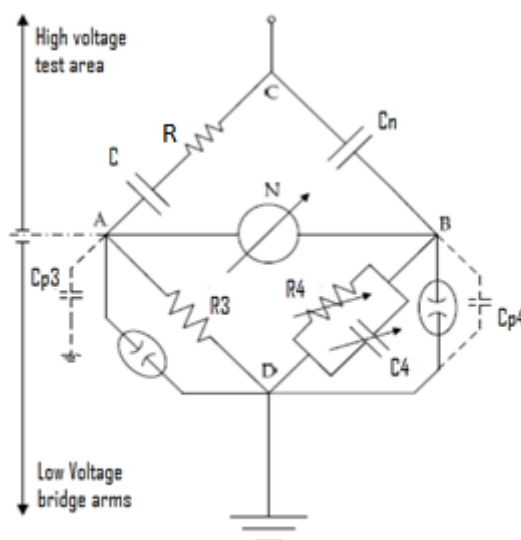


Figure 32: Schering bridge [38]

This bridge measures the capacitance  $C_x$  and the  $\tan\delta$  of a capacitor or a dielectric. The gas-filled standard capacitor  $C_n$  has a very low loss which can be neglected over a wide frequency range. The other HV arm of the bridge consist of the unknown samples  $C_x$  of which the dielectric loss is to be measured. The calibrated impedances  $R_4$  and  $C_4$  are necessary to balance the bridge. The balance conditions are obtained when the null detector shows zero deflection, then:

$$Z_{CA} = \frac{Z_{CB}}{Z_{BD}} Z_{AD} \quad (20)$$

Where:

$$Z_{CA} = R - j\frac{1}{\omega C}, Z_{CB} = -j\frac{1}{\omega C_N}, Z_{BD} = \frac{R_4[-j(\frac{1}{\omega C_4})]}{R_4 - j(\frac{1}{\omega C_4})} \text{ and } Z_{AD} = R_3$$

From which we get by separation of real and imaginary parts:

$$C = \frac{R_4}{R_3} C_N \quad (21)$$

And

$$R = R_3 \frac{C_4}{C_N} \quad (22)$$

by substituting equations (21) and (22) in equation (18)  $\tan\delta$  can be obtained:

$$\tan\delta = \omega R_4 C_4 \quad (23)$$

### Dielectric Spectroscopy using IDAX

The dielectric spectroscopy or the dielectric frequency response is used to measure the dielectric properties of the material as a function of the frequency. Usually, the dielectric dissipation is determined at power frequency. However, in some cases it is not enough to qualify the changes in the insulation system [36]. Measuring losses over a wide range especially at low frequencies provides more information about the status of the insulation.

Therefore, in this research, another measuring system based on spectroscopy named IDAX manufactured by Megger is used.

#### Measurement technique of IDAX

IDAX operational principle is based on measuring the impedance of the sample at one specific frequency. And from the measured impedance, different parameters can be calculated such as  $\tan\delta$  and power factor.

When the sample is subjected to a sinusoidal voltage with desired frequency, a current flowing through the sample is generated. IDAX contains two internal voltage sources of maximum peak output  $10V_{\text{peak}}$  and  $200 V_{\text{peak}}$ . The current is measured using electrometer which behaves as a current to voltage converter. By measuring the voltage and the current, The impedance can be determined by:  $Z = \frac{U}{I}$ . And then  $\tan\delta$  can be calculated from  $Z$ . The same procedure can be repeated at different frequencies and voltage levels to get more information on the sample. A schematic overview of the measurement of the electrical impedance is depicted in Figure 33.

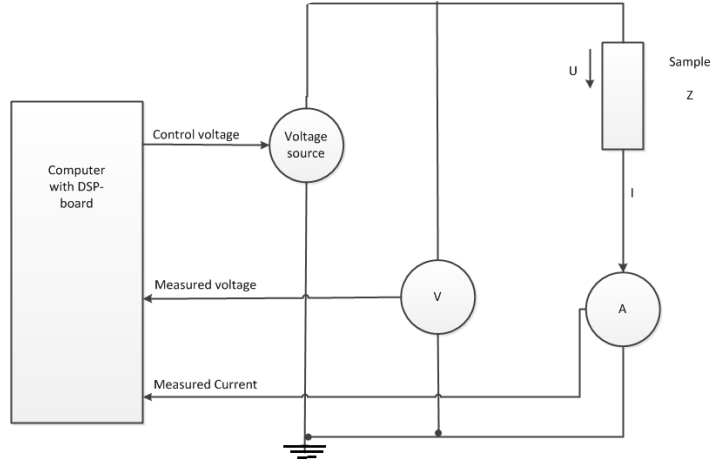


**Figure 33: IDAX - Measurement of Electrical Impedance**

**Calculation of  $\tan\delta$  by IDAX** Considering the parallel model of the dielectric depicted in Figure 31(a), the impedance of the dielectric is as follows:

$$Z = \frac{R_p}{1 + j\omega R_p C_p} \quad (24)$$

Moreover the impedance as a complex number can be represented in the rectangular form as:

$$Z = \text{Re}\{Z\} + j \text{Im}\{Z\} \quad (25)$$

From equation (24) and (25):

$$R_p = \frac{1}{\text{Re}\left\{\frac{1}{Z}\right\}} \quad \text{and} \quad C_p = \text{Re}\left\{\frac{1}{j\omega Z}\right\} \quad (26)$$

From equation (18),  $\tan\delta$  is :

$$\tan\delta = -\frac{\text{Re}\{Z\}}{\text{Im}\{Z\}} \quad (27)$$

### 3.4. MEASUREMENT SETUPS : WEIGHT, PD AND TAN $\Delta$

This section describes the measurements setups used in this research. These are: the setup for weight monitoring, PD and tan $\delta$  measurements.

#### 3.4.1. TEST SETUP FOR WEIGHT MEASUREMENTS

To monitor the weight increase of the samples during the post-impregnation standing period, the Kern scale with a sensitivity of 0.01g is used (see Figure 34(a)).

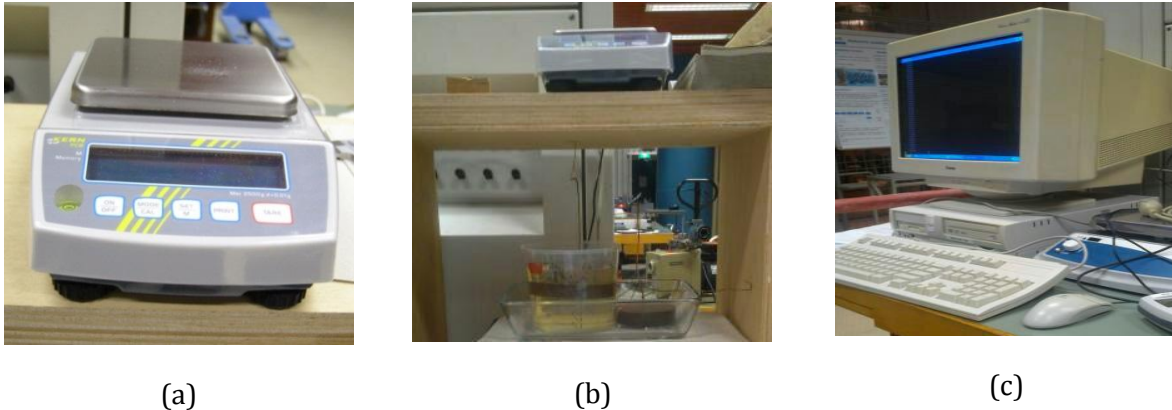


Figure 34: (a) Scale used for weight measurement (b)+(c) continuous weighing

#### 3.4.2. TEST SETUP FOR TAN $\Delta$ : IMPREGNATION AT HV LABORATORY

The sample is dried according to the procedure mentioned in section 3.2 and placed between the electrodes in a container. After vacuuming the sample, the impregnation process starts. The container is filled with dried oil under vacuum at a given temperature till the moment the upper electrodes is covered with oil (see Figure 35). After impregnation, the vacuum is released and the leads of the electrodes are connected to the measuring equipment immediately. The post-impregnation standing time starts at the moment the vacuum is released from the oven and the monitoring process starts.



Figure 35: Sample to be tested placed between the electrodes for tan $\delta$  measurements.

The LV electrode for measuring tan $\delta$  is made with guarding. The idea behind guarding is to minimize the influence of surface leakage currents on the measurements.

The tan $\delta$  is measuring first using TETTEX as described in the circuit diagram depicted Figure 36. Tettex measures tan $\delta$  based on the balance conditions of the Schering bridge.

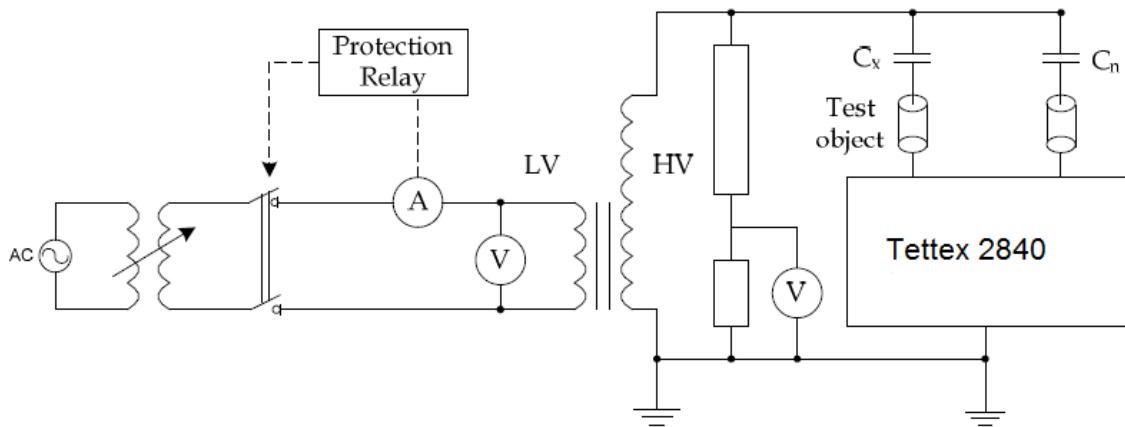


Figure 36: The circuit diagram for  $\tan\delta$  measurements

The sample is connected in parallel to the standard capacitor  $C_n$  which has a nominal capacity of 100pF. Figure 37 shows how the sample is connected and Figure 38 Shows the LV side TETTEX and IDAX.

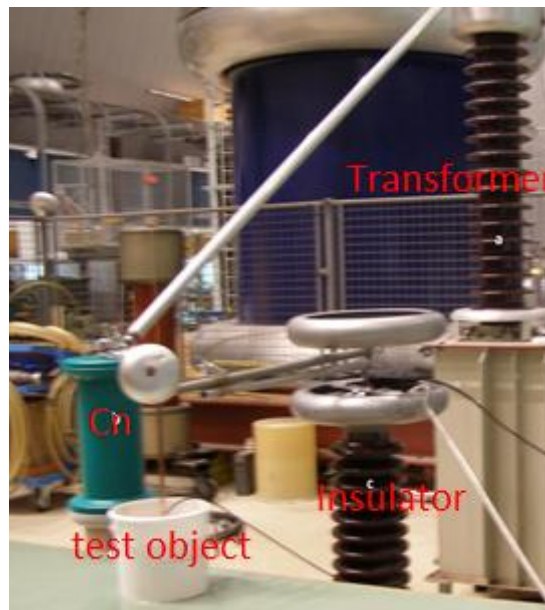


Figure 37: HV connection for measuring  $\tan\delta$  using Tettex



Figure 38: LV side; TETTEX and IDAX for measuring  $\tan\delta$

Tanδ is measured also using IDAX. The IDAX is equipped with an internal voltage source that is connected directly to HV electrode, the LV electrode is connected to the measuring system and the guard electrode is earthed.

**3.4.3. TEST SETUP FOR PD : IMPREGNATION AT HV LABORATORY**

Partial discharges are detected using the DDX 9101 (PD detector made by Heafely) in an arrangement shown in Figure 39. The test object is connected in parallel with a coupling capacitor of nominal value 1nF.

As shown in the circuit diagram of PD detection in Figure 39, the test setup consists of test object  $C_x$  which is connected in parallel with a standard capacitor  $C_n$  of nominal value of 1nF. A filter is introduced to reduce the noise from HV source. The measuring impedance  $Z_m$  is connected to DDX (PD detector). The circuit is calibrated with a step generator in series with a small capacitor  $b$ . In this way a discharge of  $q_{calibration}=b.\Delta V$  is injected in the sample.

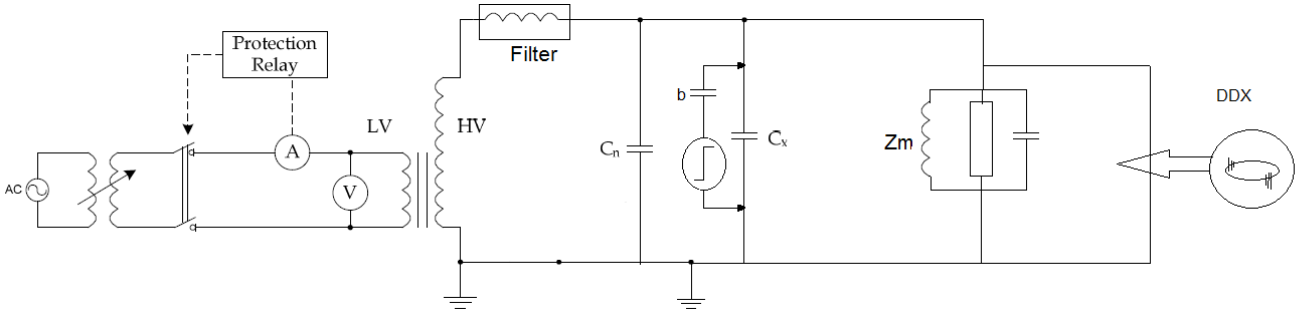


**Figure 39: Circuit diagram for partial discharge detection**

The test object consists of a sample of cellulosic material (KP or PSP) placed between the HV and LV steel electrodes (see Figure 40) . The edges of HV and LV electrodes rounded ensure a uniform electric field distribution across the sample and avoid corona discharges



**Figure 40: Prepared container for PD measurement: Impregnated sample on the top of LV electrode**

### 3.4.4. EXPERIMENTAL TEST SETUP FOR PD AND DIELECTRIC LOSS: IMPREGNATION AT SMIT

In order to reproduce impregnation condition as exist in the factory, Royal Smit Transformers has built a special test tank. The details of the construction are presented in Figure 41 and Figure 42 respectively.

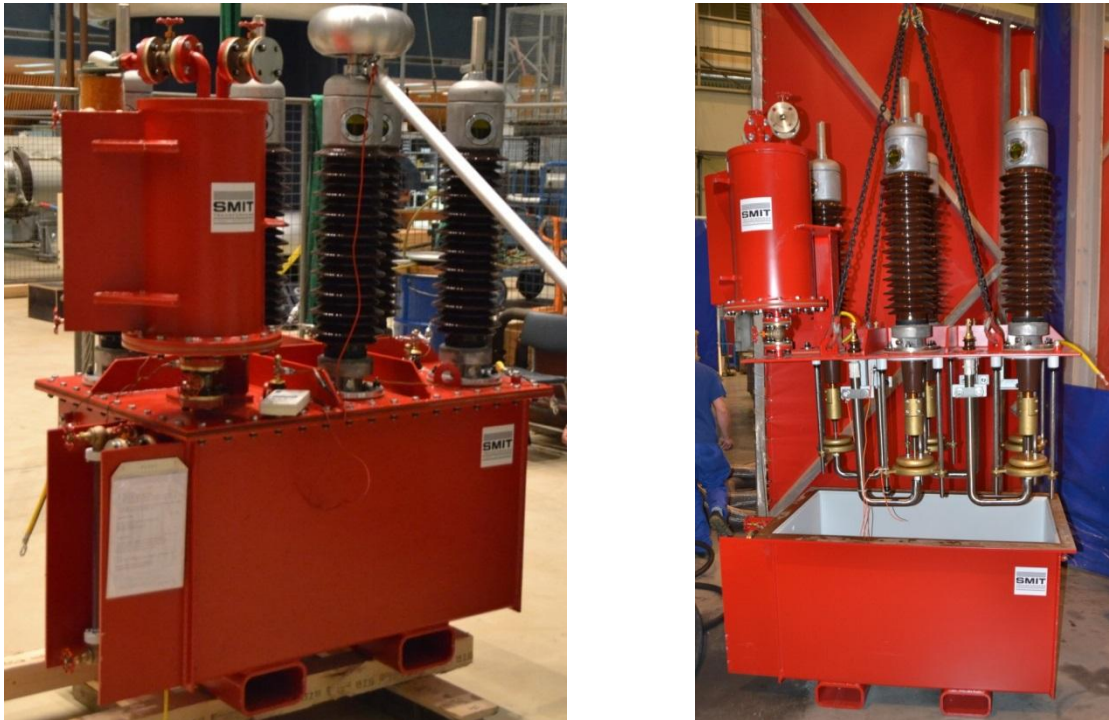
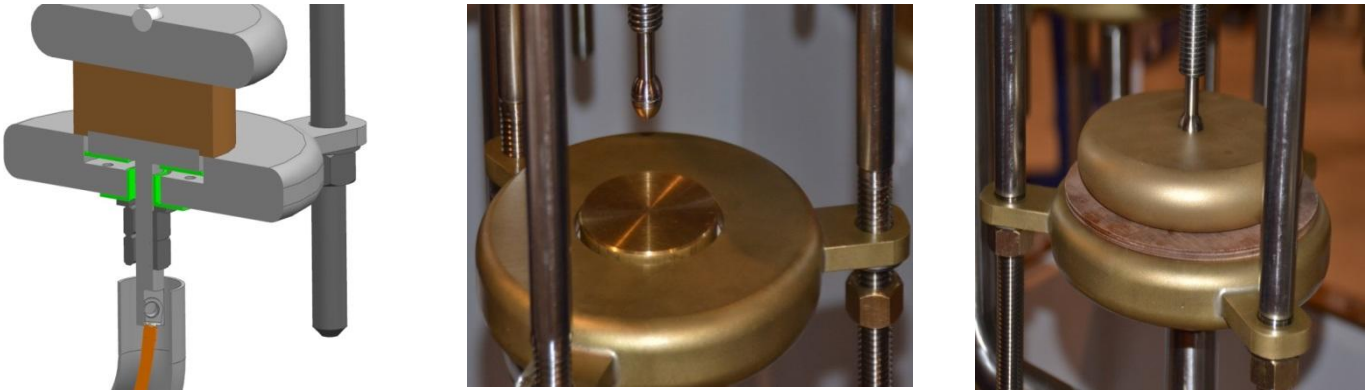


Figure 41: General view of the testing tank in- and outside

Inside the tank, a set of 5 electrodes configuration has been installed. Each electrode configuration consists of high- and low-voltage electrode connected to high- and low voltage bushing respectively installed on the top of the tank. In addition, the low voltage electrode is surrounded by guarding electrode. The last one is connected directly to the tank construction and is therefore earthed (see Figure 42). Such arrangement helps to eliminate stray capacitances between the electrodes but also prevents surface leakage currents along the sample surface. Moreover, separate bushings allow to measure the  $\tan\delta$  for each sample individually. In the tank, 3 temperature sensors are installed as well. This helps to monitor the temperature of the oil.



**Figure 42: HV and LV Electrode with a guard inside the testing tank**

The tank with test samples inside is assembled at SMIT transformers, vacuumed, and filled with oil at ambient temperature. Directly after impregnation of the samples, the tank is transported to High Voltage Laboratory in Delft. The total time between releasing the vacuum from the tank and the delivery to Delft is approximately 2 hours. In addition, approximately 1 hour is necessary for offloading the tank and the equipment connecting.

By arrival to the laboratory, the tank is connected to the test equipment. And the monitoring of the post impregnation process starts.

# 4. THE RESULTS OF PD AND TANΔ MEASUREMENTS

In this chapter, the results of PD and tanδ measurements performed on different samples made of KP and PSP materials during post impregnation process are presented. Section 4.1 includes the results of PD measurements and tanδ measurements of samples prepared and impregnated at high voltage laboratory. In section 4.2, the results of PD and tan δ measurements using SMIT testing tank.

## 4.1.SAMPLES IMPREGNATED AT HIGH VOLTAGE LABORATORY IN DELFT

In this section the results obtained for samples impregnated and tested for PD at high voltage laboratory in Delft, will be presented and analyzed.

### Test 1: PD test of Samples made from KP and PSP material

During electrical testing of the oil-filled transformer, the maximal stress that occurs between two electrodes is 4 kV/mm AC-50Hz. Between these electrodes several layers of oil and transformerboard can be found. This implies that stress in PSP and KP material during electrical testing is much lower.

- **Transformerboard - PSP material**

Two samples of 10 mm height are chosen. One sample is impregnated under vacuum and tested directly after vacuum release (the time between impregnation and testing is about 10 min). the other sample is tested without impregnation, the sample was simply immersed into oil. The results of the tests are summarized in Table 4.

Samples	Applied voltage	PD occurrence
Impregnated sample under vacuum (10 mm)	Up to 45 kV	PD free
Sample without impregnation (10mm)	Up to 45 kV	PD free

**Table 4: Summary of PD measurements performed on the PSP sample impregnated under vacuum at ambient temperature (~22°C)and the sample immersed in oil at ambient pressure and temperature**

- **Laminated wood - KP material**

Two dried sample with height of 10mm are tested. One sample is impregnated under vacuum at ambient temperature and then taken for testing. The sample was PD free. The second sample was simply immersed in oil at ambient pressure. When testing, PDs were observed. The discharges were probably originating in the bubbles of the gas which was escaping from the sample. A chain of bubbles travelling to the oil surface could be seen in the container. The results of the PD tests is summed up in Table 5.

Sample	applied voltage	PD occurrence
Impregnated sample under vacuum	Up to 45 kV	PD free
Sample without impregnation	12kV	PD occurrence due to air bubbles in oil coming from the sample. Sample was not vacuumed

**Table 5: Summary of PD measurements performed on the sample impregnated under vacuum and the sample immersed into oil at ambient pressure**

- **Discussion**

In the above experiments, no PD were observed. This is in agreement with the theoretical analysis using the Paschen curve. The air cavities are too small to fulfill the conditions to generate the internal discharges. But the question is still present: can PDs occur in the oil-filled transformer? If so, where do they originate from? Therefore another hypotheses is generated:

*Are the PD originated from the interfaces between materials inside the oil-filled transformer? Such as paper-wood, paper-board, wood-board?*

### Test 2: PD testing in interfaces and defined cavity

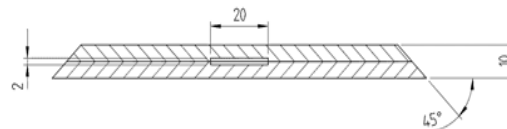
In order to investigate if the interfaces between different material can generate a PD and how the PD level and PD inception voltage change in the course of post impregnation standing time, several samples are created, impregnated and tested directly after impregnation. The first test object consists of two samples of laminated wood joined together with epoxy screws (see Figure 43 a). The second is made of two samples of transformerboard, which are glued together with a less dense material in between (see Figure 43 b). The last one is formed by two samples of transformerboard glued together with a defined cavity (diameter 10mm and a height of 2 mm)(see Figure 43 c).



(a)



(b)



(c)

**Figure 43: Test samples (a) Screwed KP samples (b) glued PSP Samples (c) Sample with defined cavity**

Directly after impregnation at ambient temperature, the three sample types a), b) and c) are tested.

Total thickness of sample type a) is 10 mm the maximum applied voltage is 42 kV what results in the stress level of 4.2 kV/mm. The noise level during testing was approximately 0.15pC. The PD inception voltage is 22 kV. At 42kV the PD level was between 1.36-2.85pC (see Figure 44).



Figure 44: PD activity observed during testing of sample type a)

The thickness of sample type b) is 10 mm. The noise level 0.338pC-0.6pC and the applied voltage is 40.2 kV. which means that the sample was stressed by approximately 4kV/mm. The sample is PD free (see Figure 45).

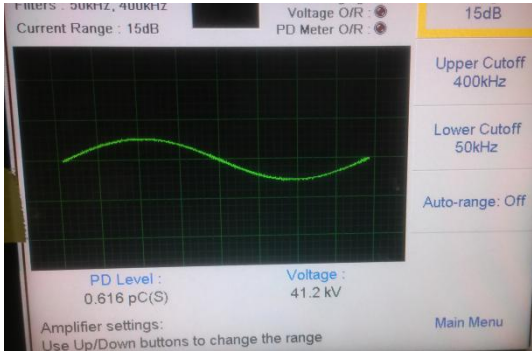


Figure 45: The measured PD level in sample type b)

For sample with defined cavity, the stress level 4.5kV/mm. the noise during testing was approximately 0.5pC. No PD has been observed.

An overview of the test results are shown in Table 6.

Sample type	PDIV	PD level
a)	22kV	1.36-2.85pC
b)	Up to 41.2kV	~0.338pC-0.6pC= Noise level
c)	Up to 45 kV	~ 0.5pC= Noise level

Table 6: PDIV and PD level of different samples

The partial discharge inception voltage for the sample type a) is 22kV. However the PD level is only 1 pC which is a very low. The PD acceptance level of a transformer is much higher than the measured value.

**Test 3: Tanδ measurements for PSP and KP**

a PSP sample of type S2 and a KP Sample of type C4 are prepared and impregnated at ambient temperature according to the same procedure. The results of  $\tan\delta$  measurements of both samples are presented hereunder:

- **PSP material**

After impregnation under vacuum, every 30 min the  $\tan\delta$  is measured. According to the method described in chapter 3 using TETTEX; for several voltage levels up to 28kV. The results of the test is depicted in Figure 46.

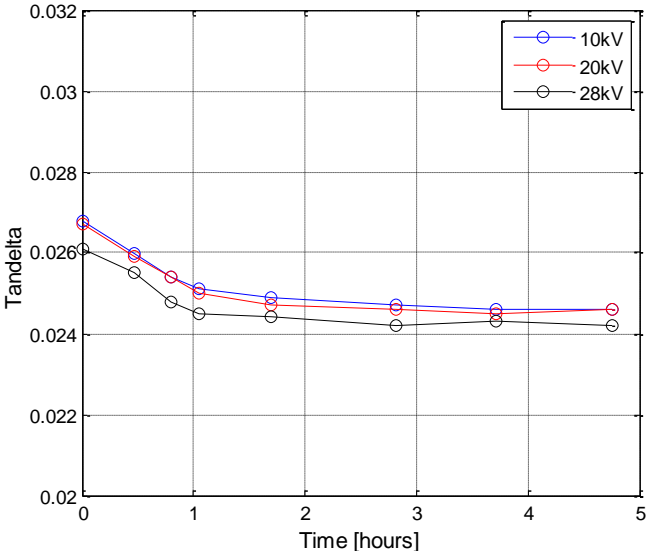


Figure 46:  $\tan\delta$  in function of time of PSP material at different voltage levels.

- **KP Material**

$\tan\delta$  measurements results for KP sample of type C4 are depicted in Figure 47.

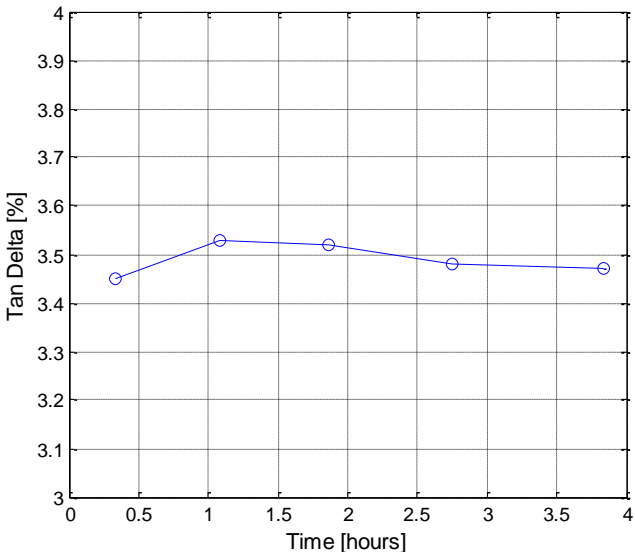
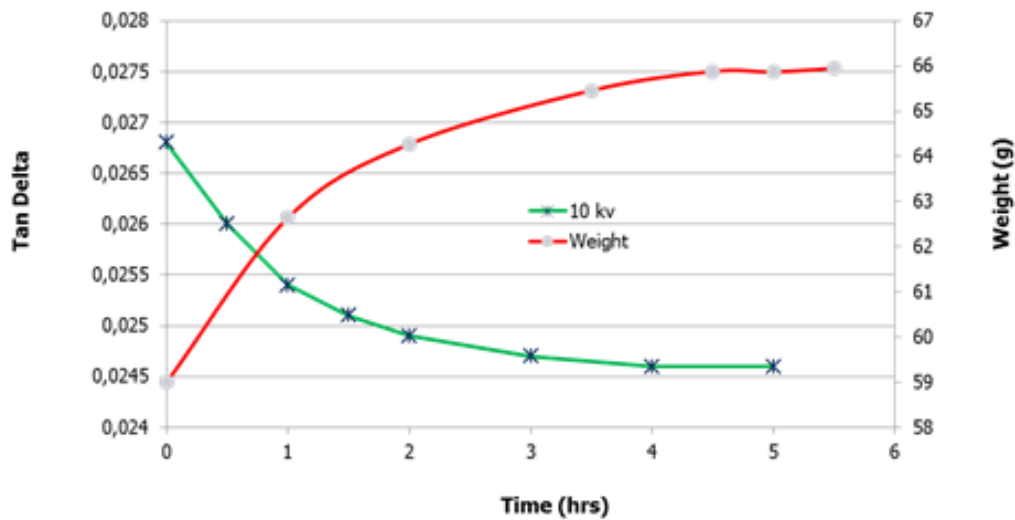


Figure 47:  $\tan\delta$  in function of time of impregnated KP material

- **Discussion**

1. For PSP material, the measured value of  $\tan\delta$  is higher when comparing to the known value of fully impregnated pressboard which is  $50 \cdot 10^{-4}$  [32]. However, it can be observed that the value of  $\tan\delta$  decreases slightly over time. This can be related to the continuing impregnation process and so the oil ingress into the cellulose material. Figure 48 correlates the weight increase (sample type S2) to  $\tan\delta$  decrease as a function of time for two identical samples.



**Figure 48: Weight and  $\tan\delta$  of PSP Sample( Type S2) versus time**

2. For KP material, the  $\tan\delta$  remain the same during the post impregnation time. This can be related to the fast oil ingress to the KP material (see Figure 47).

## 4.2. MEASUREMENTS USING SMIT TESTING TANK

This section includes a description of the samples used for  $\tan\delta$  and PD measurements using SMIT testing tank and the obtained results.

### 4.2.1. SAMPLES DESCRIPTION

In the first experiment, five samples were investigated – the details with respect to the sizes and shapes of the samples can be seen in Table 7 and Appendix B.

In order to slow down the impregnation process of sample E, it has been covered with epoxy and a small surface is left without epoxy. (see Figure 49) The epoxy free area is indicated with a red line.

Sample name	Size [mm] (Diameter*thickness)	Material	Remarks
A	110-120*5	PSP	The edges are inclined
B	100-120*5	PSP	The edges are inclined
C	180*5	PSP	
D	180*5	KP	
E	100/120*10	PSP	A defined cavity (10mm*2mm)is made inside the sample

**Table 7: The description of the samples used for the measurements**

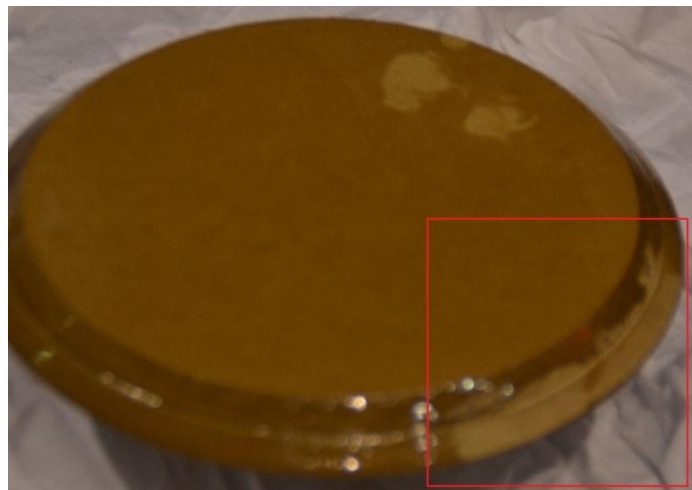


**Figure 49: General view of sample E- an area without epoxy is indicated**

The tank with test samples is assembled at SMIT transformers, vacuumed and filled with oil at ambient temperature. Directly after filling the tank, the tank is transported to High Voltage laboratory in Delft. The total time between releasing the vacuum from the tank and the delivery to Delft is approximately 2 hours. In addition, approximately 1 hour is necessary for offloading the tank and connecting the equipment.

On arrival to the lab, the tank is connected to the test equipment and the monitoring of the post impregnation process starts.

#### *4.2.2. TANA MEASUREMENTS RESULTS*

In this section the results of  $\tan\delta$  measurements using IDAX will be presented. The test is performed at ambient temperature (22 °C) on each of the 12 days after the tank delivery. The applied voltage is 1400 V RMS and the frequency range is from 5 mHz/0.5mHz up to 1000Hz.

$\tan\delta$  [%] in function of frequency [Hz] during 12 days for sample A are presented in Figure 50.  $\tan\delta$  [%] of samples B, C, D, and E are presented in Appendix D.

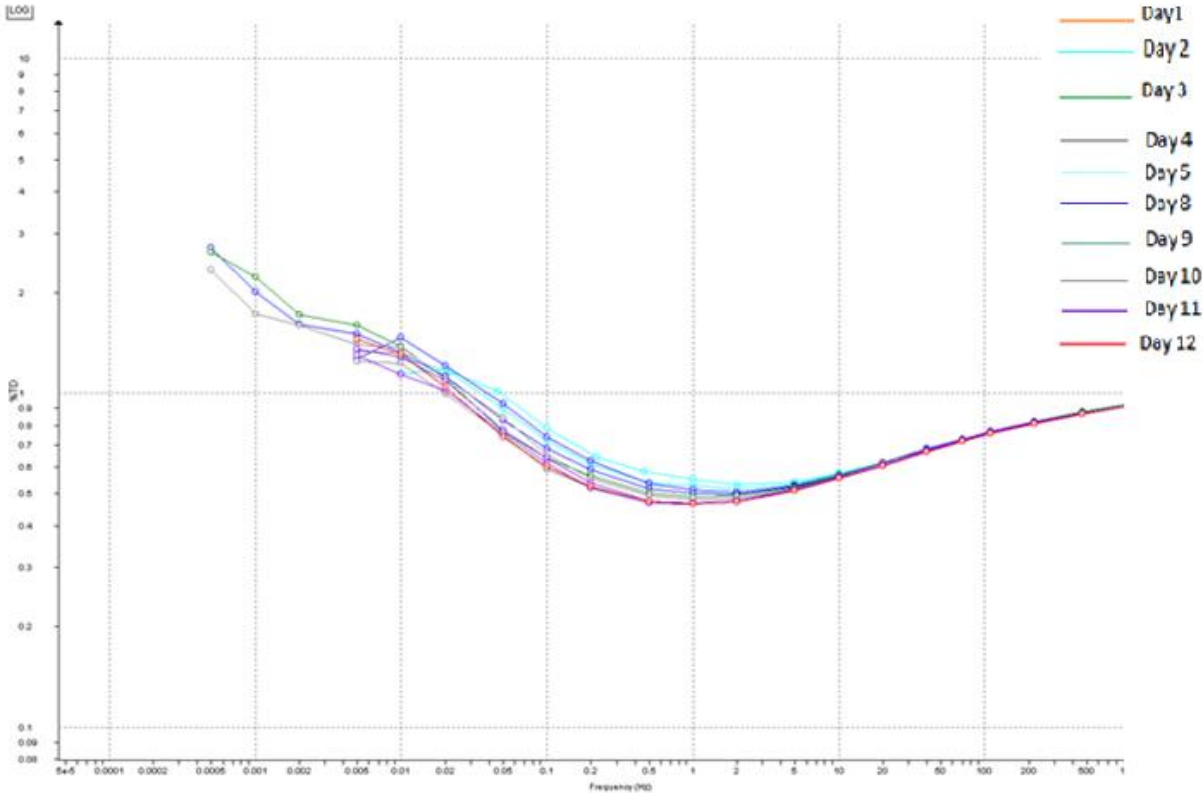


Figure 50:  $\tan\delta$  of sample A in function of frequency at ambient temperature.

No significant changes in  $\tan\delta$  are noticeable. At 50 Hz the  $\tan\delta$  is constant during 12 days of testing. However at low frequencies some slight changes occur. This small changes at low frequencies might be because of the interfacial polarization process due to the mismatch of permittivity of oil and cellulose material. For instance, when an electric field is applied, the positive and negative charges move and deposit on the interface of both dielectrics and then form dipoles as well. This process is very slow, therefore it can be noticeable only at frequencies below the power frequency range [36].

4.2.3. PD MEASUREMENTS RESULTS

The maximum voltage level of the high-voltage bushing installed on the tank is 70 kV. Using PD detector (DDX-9101), the results of the PD measurements performed on each sample at the day of tank arrival to Delft; are presented in Table 8. The results of PD test during 12 days after impregnation are extensively presented in Appendix C.

Sample	PDIV [kV]	PD level (pC)
A	27	2

B	46	0.6
C	12	0,7
D	4.5	2.5
E	31,3	4

**Table 8: Results of PD measurements (1<sup>st</sup> day of impregnation ) of samples A, B, C, D, E**

## Discussion

Based on the measurements results presented above when using SMIT testing tank, two main conclusions can be drawn:

1) The  $\tan\delta$  measured at 50 Hz during the post-impregnation standing time does not change visibly. For the lower frequencies (<1 Hz) the difference in the values measured in different periods of standing time appear. Unfortunately, there is no clear trend in the decrease or increase the value of  $\tan\delta$  at low frequencies. In this case, the impregnation process could not be monitored by  $\tan\delta$  measurement.

2) The measured values of PDIV also do not provide any conclusive information. In the case of samples A, B and C, the PDIV voltage remains fairly constant except for the value obtained in the first day of measurements. Sample D shows decreased PDIV only during the first two days, later on it becomes stable. For sample E, the measured value stayed approximately stable for the whole period of measurements.

### 4.3. TESTING THE TANK

In order to check whether the occurring PDs are generated in the sample or in the test setup itself. It is important to investigate if the test tank construction is PD free.

In this section the results of testing the tank are presented after a short description of the test circuit and used samples.

#### 4.3.1. TEST CIRCUIT AND DESCRIPTION

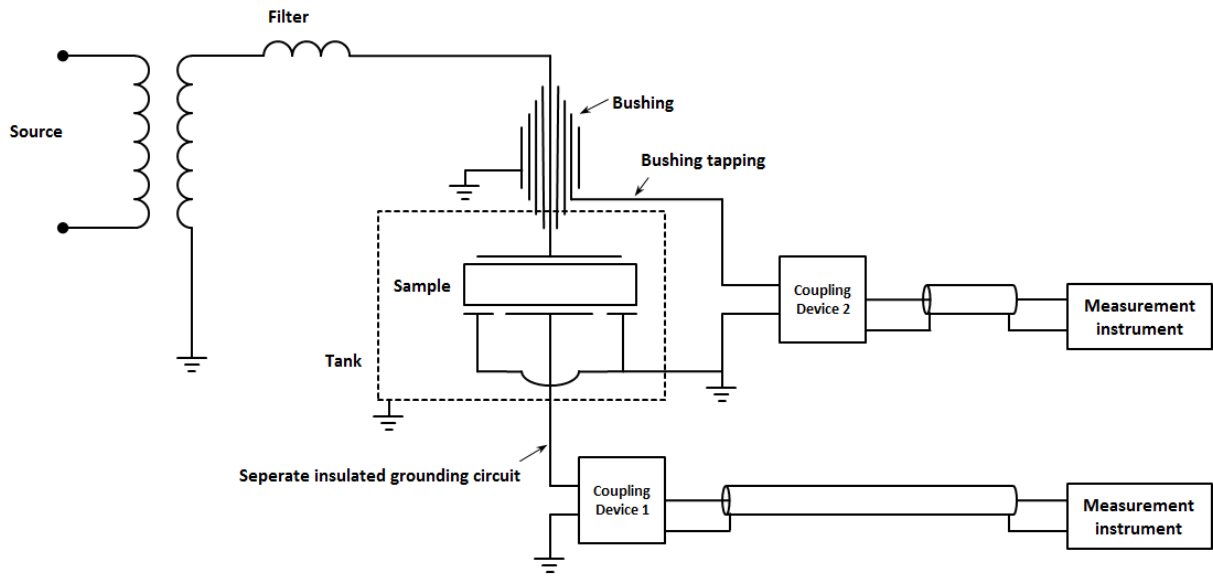
In order to test the tank configuration, thick sample (see Table 9) of PSP material of 50 mm height are chosen. In this way the electric field in the samples is decreased.

<b>Material</b>	<b>Diameter [mm]</b>	<b>Thickness [mm]</b>
PSP3052	180	50

**Table 9: Description of samples used for testing tank.**

The test circuit is shown in Figure 51. The filter is used to reduce the noise coming from the HV source. In this configuration two devices for simultaneous PD measurements are used.

In this test, two coupling modes are used e.g. coupling device in series with coupling capacitor and coupling device in series with the test object.



All grounding symbols are connected to tank grounding

Figure 51: Circuit configuration for testing tank

#### 4.3.2. RESULTS AND DISCUSSION

Table 10 and Table 11 show the PD level at different voltages when the CD in series with coupling capacitor and when CD in series with samples respectively.

V [kV]	A	B	C	D	E
5	1	0,2	4	1,5	0,2
10	1	0,5	5	1,7	0,28
25	2,5	0,3-6	11	6	0,6
30	3	4-6	9	6,2	0,6
45	4	6,5-7	7	4,5	12
Flashover voltage	~47	~50	~50	~55	~47

Table 10: PD level in function of applied voltage when CD in series with coupling capacitor

<b>V [kV]</b>	<b>A</b>	<b>B</b>	<b>C</b>	<b>D</b>	<b>E</b>
5	≤0,2	≤0,3	0,1	0,1	0,1
10	≤0,2	≤0,3	0,1	0,1	0,1
20	≤0,2	≤0,3	0,1	0,11	0,1
25	0,2	≤0,3	0,1	0,11	0,13
30	≤0,2	≤0,3	0,1	0,11	0,1
35	0,2	0,3	0,15	0,1	0,1

**Table 11: PD level in function of applied voltage when CD in series with Samples**

The source of measured PD is not in the samples but in the bushings installed on the tank. This might suggest that measured PD level measured in previous test is originated in the bushings as well.

## 5. ANALYSIS AND MODELLING OF IMPREGNATION TIME

Theoretical analysis of the impregnation process of high density cellulose material is very complicated. This is due to the complexity of the structure of the material and the non-uniform distribution of the capillaries inside the material. Moreover, the estimation of the internal pressure inside the cavities is not obvious as it is dependent on the residual gases inside the capillary.

Previous studies have been focused on the estimation of the impregnation depth for the case of mono-dimensional impregnation [2][4][22][23]. Assuming that the pressboard consists of parallel cylindrical capillaries that obeys the Poiseuille's law. By integrating the Poiseuille's equation the distance that the oil penetrates the capillary can be derived. However this is only valid in the case of cylindrical pores. This means that if the capillary radius varies along the length of the capillary and if the capillary contains a pocket the equation is not valid [41].

In this research, an empirical model will be developed to estimate the time needed to fully impregnate an arbitrary sample of high density cellulosic material. This model is based on the measurements of the weight increase of different samples of cellulosic materials (KP, PSP) along the post impregnation standing time.

In section 5.1, we will propose a model that describes the impregnation process. In particular, the effect of the side surface of the sample, its shape and the oil temperature on the impregnation time for PSP material and KP material will be presented in section 5.2 and 5.3 respectively. The model describing the time needed for a complete impregnation of a sample depending on a material type, sample shape and dimensions and impregnating medium temperature is presented in section 5.4.

### 5.1. IMPREGNATION PROCESS MODELLING

The empirical modelling of the impregnation process is based on the measured data. This data is collected from monitoring the weight increase during the impregnation process associated to different sample types (R, C, S) made of the two material types (PSP, KP). The used samples, the corresponding preparation and weight measurement method are described in chapter 3. In the following sections, the model proposed for the impregnation process is described.

#### 5.1.1 PROPOSED MODEL FOR IMPREGNATION PROCESS

Figure 52 a and Figure 52 c show the measured weight of a PSP sample of Type R1 and S1, respectively.

In order to combine and compare the results, a normalization of the measured data was made. Clearly, first we determine the weight increase of the sample during impregnation by subtracting the measured weight from the weight measured just after vacuum release. Then, this weight increase is further normalized to its maximum (saturation weight). This is done to fulfill the condition that the maximum weight of the sample is 100% saturated. As consequence the oil absorption during vacuum will be compensated as we are only interested in studying the post-impregnation period. This can be expressed as follows:

$$\frac{\Delta w}{\max\{\Delta w\}} = \frac{w - w_0}{\max\{\Delta w\}} \quad (28)$$

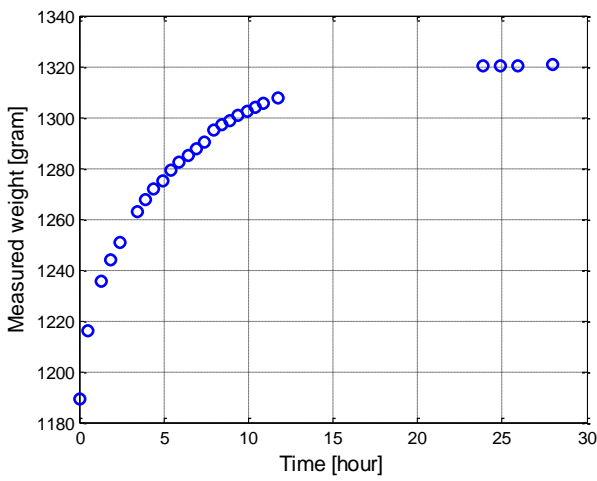
Where:

$w$  : is the measured weight of the sample.

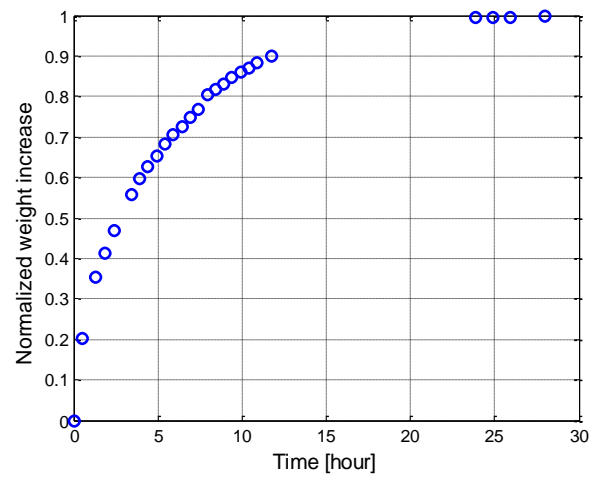
$w_0$  : is the initial weight of the sample; the measured weight just after releasing vacuum.

$\max\{\Delta w\}$  : is the maximal measured weight increase of the sample; weight at saturation.

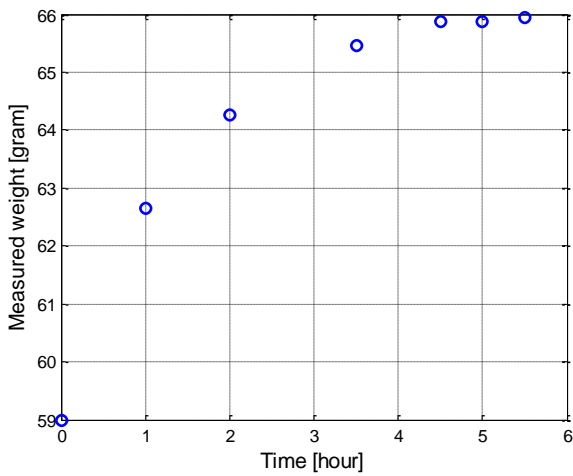
An example of the normalized weight versus the post impregnation standing time at ambient temperature of a PSP sample type R1 and S1, are depicted in Figure 52 b and Figure 52 d, respectively.



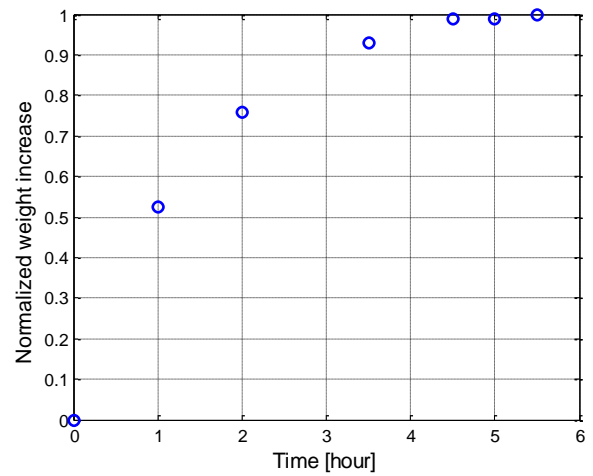
(a)



(b)



(c)



(d)

Figure 52: (a) Measured weight during post impregnation of sample type R1, (b) normalized weight of sample R1, (c) measured weight during post impregnation for sample S1, (d) fitting curve for sample S1.

By assessing the obtained data, it was observed that the weight versus time can be divided in two regions. In the first region the weight is exponentially increasing with time till the saturation is reached. In the second region the weight remains constant with time. For a given sample, to describe the normalized weight increase over time, the following empirical model is proposed:

$$\frac{\Delta w}{\max\{\Delta w\}} = \begin{cases} 1 - e^{-\frac{t}{\tau(T,V,S)}} & t < t_s \\ 1 & t \geq t_s \end{cases} \quad (29)$$

Where:

- $t$  : is the observation time
- $T$  : is the temperature of the oil
- $V$  : is the volume of the sample
- $S$  : is the side surface of the sample.
- $t_s$  : is the saturation time

The parameter  $\tau$  is determined by using the minimum least square estimation criterion.

Figure 2 shows the normalized weight increase of the sample R1 and its fitting curve using the model described above. The proposed model fits the measured data and it will be adopted as basic fitting model for our data analysis in order to estimate the rise time of the impregnation process.

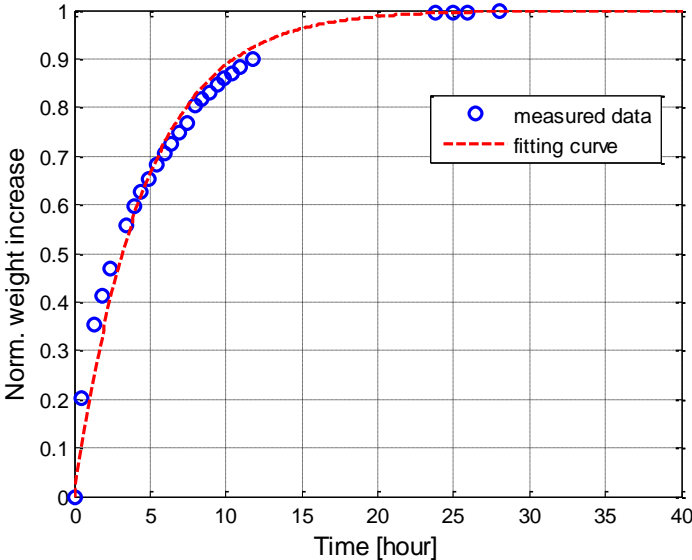


Figure 53: Normalized weight as function of post impregnation time for PSP sample Type R1: model versus data.

### 5.1.2 ESTIMATION OF SATURATION TIME

The main goal of this research thesis is to estimate the time needed for the total impregnation of the material. This means that our focus will be only on modelling the saturation time as function of material and oil properties.

The saturation time can be determined by the measured data. However, as it was not possible to monitor the weight increase during nights and weekend (especially for large samples), some large time gaps may occur. This will affect the estimation of the saturation time when this is based on the measured data. Therefore, the saturation time is estimated using the fitting curve instead of the measured data. As the proposed model with an exponential function will never saturate (in theory) then we assume that the saturation occurs at time equal to 5 times the rise time of the model:

$$t_s = 5 * \tau \quad (30)$$

Since the relation between the  $t_s$  and  $\tau$  is linear, we will focus on the modelling of  $\tau$ .

## 5.2. DATA ANALYSIS OF PSP MATERIAL

In this section, the obtained results of weight measurements PSP material will be studied. More specifically, the effect of the surface through which the oil will ingresses into a sample, the distance to the centre of a sample (shapes) and temperature will be discussed.

In laminated transformerboard, holes are drilled to accelerate the drying process. However these holes might also influence the impregnation process. The description of these holes and there effect on impregnation process will be also discussed in this section.

### 5.2.1 EFFECT OF SIDE SURFACE ON THE POST IMPREGNATION TIME OF PSP MATERIAL

The normalized weight increase versus impregnation time is depicted in Figure 54. Figure 55 shows the dependency of rise time of the impregnation process with respect to the sample side surface.

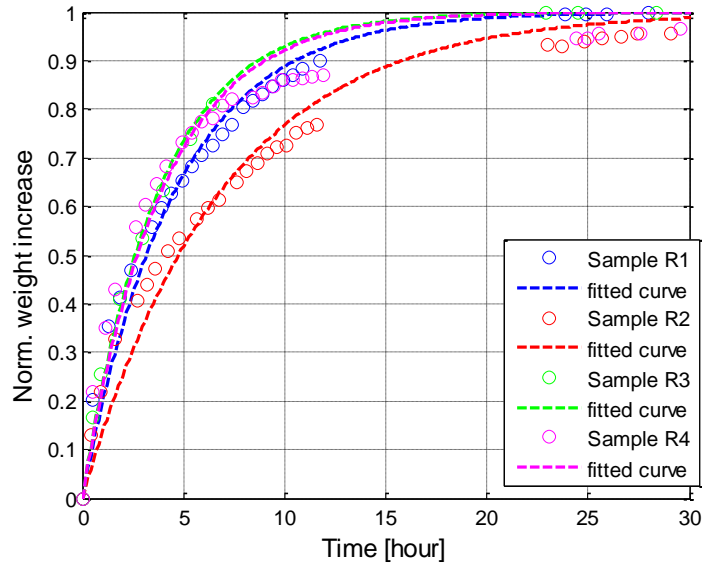


Figure 54: Normalized weight of sample types R1, R2, R3, and R4 versus impregnation time

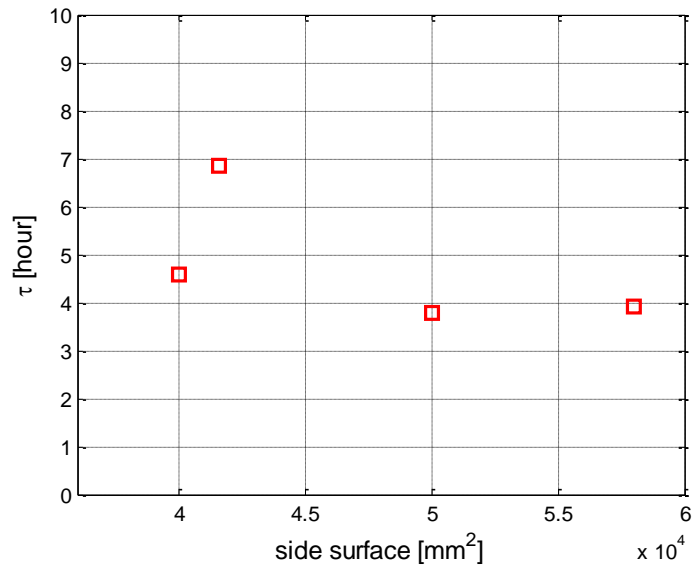
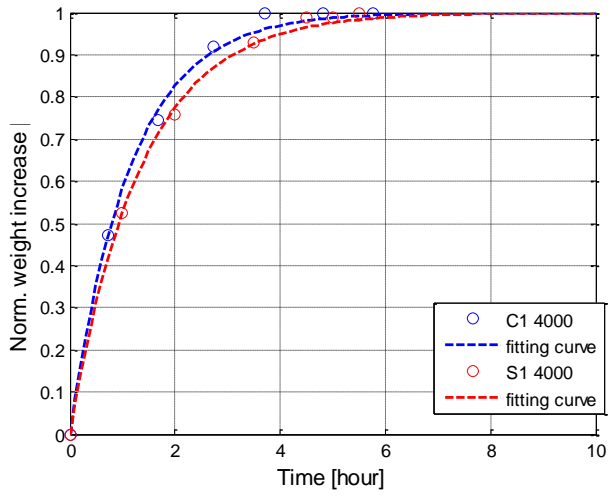


Figure 55:  $\tau$  versus side surface for sample types R1, R2, R3, and R4

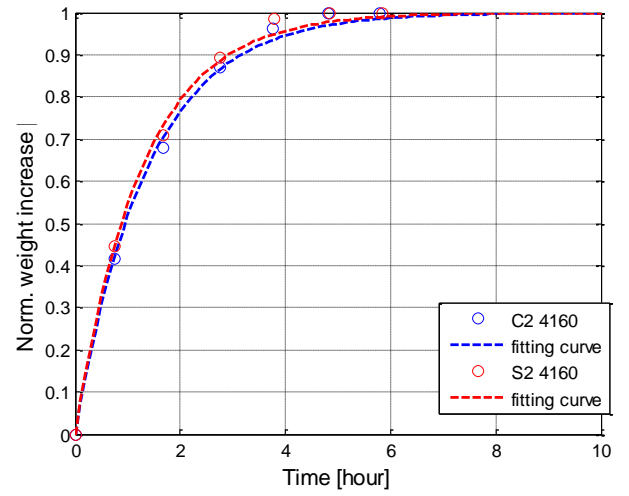
From this figure we see that the rise time of the impregnation process decreases with the side surface. Exception here is the rise time obtained for surface  $S=41.600 \text{ mm}^2$ . During the measurement it was observed that this sample was not impregnated through all the side surface. This might be related to the cutting procedure of this sample which may affect the opening of the capillaries.

### 5.2.2 EFFECT OF SHAPES (TRAVELING DISTANCE) ON THE POST IMPREGNATION TIME

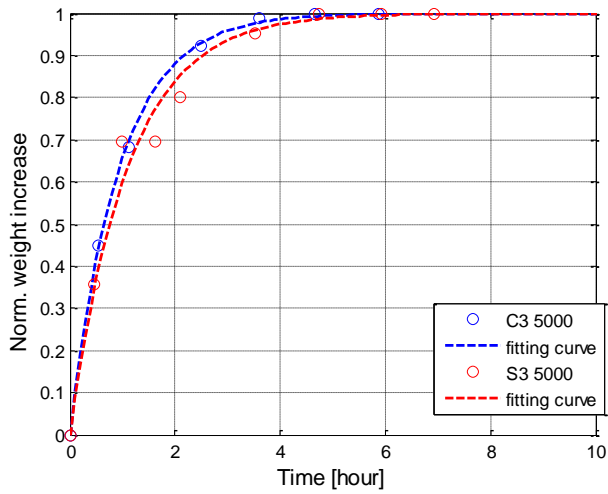
To study the shape effect of the sample (i.e. distance to the center that the oil has to travel during impregnation process), four cases are considered and for each case two samples types (C, S) are investigated. The normalized weight increase versus time is depicted in Figure 56.



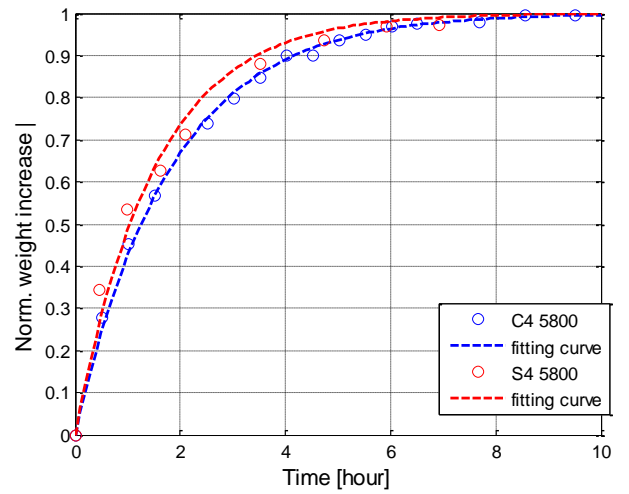
(a)



(b)



(c)



(d)

Figure 56: Normalized weight and a fitted curve versus time for samples types S1 and C1 ( $S=4000 \text{ mm}^2$ ) (b) for sample types S1 and C1 and cylinder with  $S=4160 \text{ mm}^2$  (c) square and cylinder with  $S=5000 \text{ mm}^2$  (d) square and cylinder with  $S=5800 \text{ mm}^2$

Case	Sample Type	Minimum distance to center (mm)	$\tau$ [h]
Case 1: $S=4000\text{mm}^2$	C1	31.75	1.14
	S1	25	1.34
Case 2: $S=4160\text{mm}^2$	C2	33	1.37
	S2	26	1.26
Case 3: $S=5000\text{mm}^2$	C3	40	0.94
	S3	31.25	1.09
Case 4: $S=5800\text{mm}^2$	C4	46.5	1.80
	S4	36.25	1.50

Table 12:  $\tau$  for samples with different distances (shapes) and same side surface

From Table 12, it can be concluded that the shape has no big effect on the saturation time. This might be due to the fact that the distance to the center of samples types C and S is almost the same. The rise time of impregnation process of all samples for both types are shown in Figure 57.

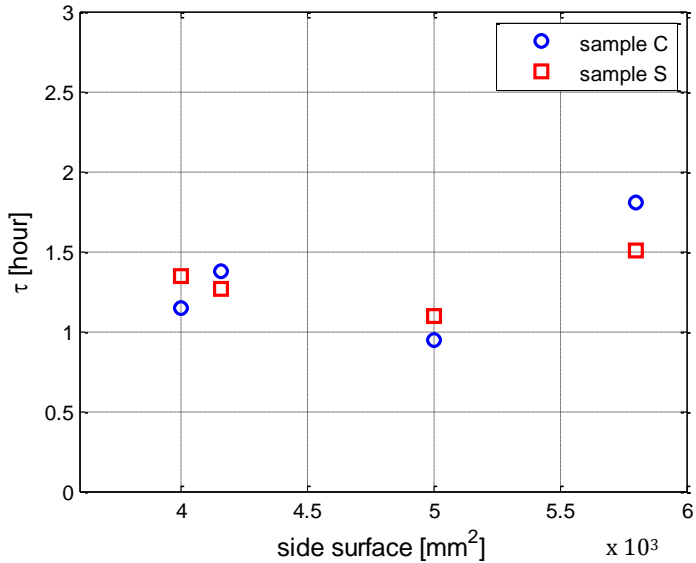


Figure 57:  $\tau$  vs surface of sample type S and type C

5.2.3 EFFECT OF TEMPERATURE ON THE POST IMPREGNATION TIME

The viscosity of the oil is highly dependent of the temperature. On the one hand, the oil viscosity will become lower by increased temperature which may speed up the impregnation process, on the other hand the residual gases inside the void may expand which may causes an increase in internal pressures and then work against the oil pressure. Therefore it is necessary to study the effect of the impregnation at different oil temperatures on the time necessary to impregnate a sample completely. Figure 58 shows the normalized weight as function of time for samples impregnated at ambient temperature (~22 °C), 50 °C, and 70 °C.

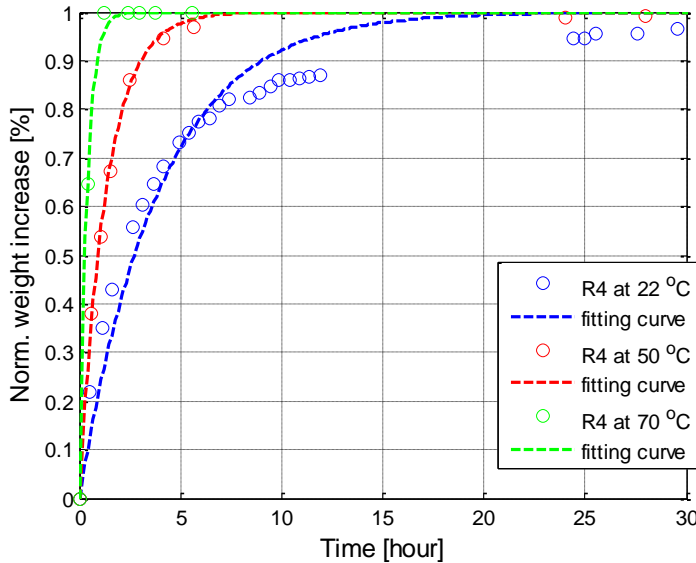


Figure 58: Normalized weight versus time for different temperature

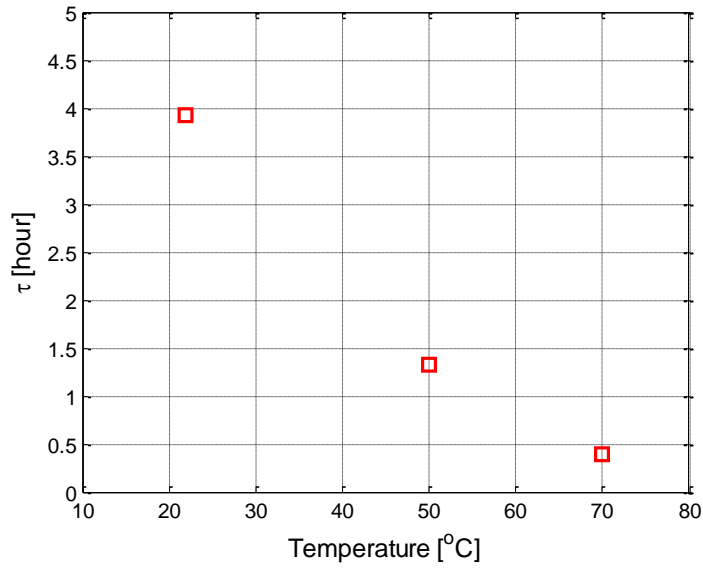


Figure 59:  $\tau$  as a function of impregnation temperature ( Sample type R4)

The time constant of the sample decreases linearly with increasing temperature. The obtained results confirm that increasing temperature (lower viscosity) speed up the impregnation process (see Figure 59).

Further study of the dependency of the oil absorption and the temperature is carried out. This is done by analyzing the results by normalizing the data to the initial weight of the sample before and after vacuum. The material absorbs less oil.

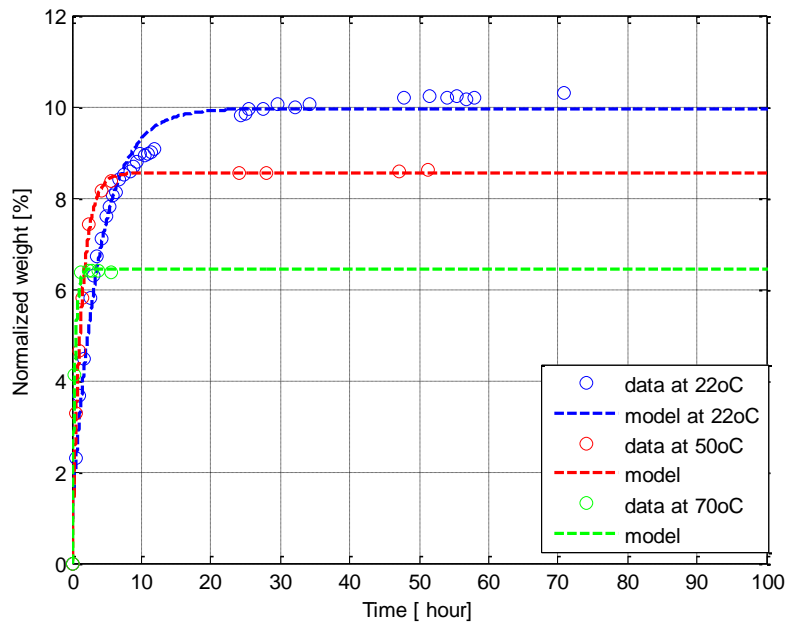


Figure 60: Weight increase as a function of time

In Figure 60, at 70 °C the weight increase of the sample is approximately 4 % less than the weight increase at ambient temperature. This difference in weight increase can be explained by two items:

1. Oil amount absorbed under vacuum:

The observation time starts when the vacuum is released. However during vacuum, certain amount of oil ingresses the sample as consequence of capillary action and also due to the pressure difference when the vacuum is released. The capillary effect is dependent on the dynamic viscosity of the oil (see chapter 2 equation (4)) which is a function of temperature T as described by

$$\eta = k * e^{b/(T-a)} \tag{31}$$

Where the constants k, b, and a are  $0.577 \cdot 10^{-4}$ , 676, and 177 respectively for Nynas oil used in the experiments.

At vacuum the sample absorbs more oil at 70° C compared to the case of impregnation at ambient temperature. And because the observation time starts at the moment of releasing vacuum, the absorbed oil during vacuum phase is not included.

Figure 61 shows an example of the weight increase of sample type A4 including the impregnation during vacuum. The weight increase at 70°C is 2.5% less.

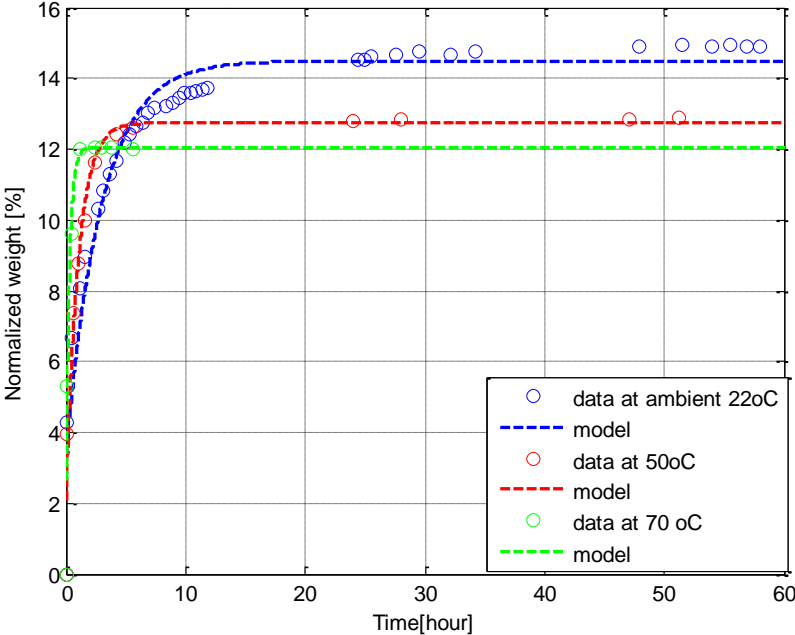


Figure 61: weight increase of sample type A4 versus impregnation time including impregnation in vacuum at different temperature (~22°C, 50 °C, 70 °C)

2. Oil expansion due to high temperature:

Another reason for the weight difference at higher temperature is the expansion of the oil at higher temperature

The volume of oil expands by:

$$\frac{\Delta V}{V} = \beta \Delta T \quad \text{and} \quad V = m/\rho \quad (32)$$

Where:

V: volume at ambient

$\Delta T$ : difference in temperature

$\Delta V$ : increase in volume (=volume at 70C – volume at ambient temperature)

$\beta$ : expansion coefficient of the oil  $\beta = -\frac{1}{\rho} \cdot \frac{d\rho}{dT} \cong \frac{1}{\rho}$ ; for Nynas oil is approximately  $0.787 \cdot 10^{-3}$  [1/K].

The density of the oil is a function of temperature T as described hereunder:

$$\rho = 889 - 0.7T \quad (33)$$

The density at ambient, 50°C and 70°C is 682.5 kg/m<sup>3</sup>, 662.9 kg/m<sup>3</sup> and 648.9 kg/m<sup>3</sup> respectively.

The weight of 1m<sup>3</sup> of oil at ambient is  $\rho * V = 682.5 \text{ kg}$ . Where the weight of 1m<sup>3</sup> of oil at 70°C is 648.9kg. Therefore the weight difference of 1m<sup>3</sup> between ambient temperature and 70°C is about 4% and the weight difference between 50 °C and ambient is 2%.

After saturation of the samples which were impregnated at 70 °C, the samples are cooled down and the weight is measured in order to investigate the amount of the oil absorbed. The measured weight increase is found to be about 0.5%. which is small and hence it can be neglected

#### 5.2.4. EFFECT OF DRILLED HOLE IN TRANSFORMERBOARD SAMPLE

Inside the transformer, holes with diameter of 10 mm are drilled in in PSP and KP materials to improve the drying process of the materials. However these holes can have a positive effect on the impregnation process as well.

To study the effect of this holes, samples of type I, II, III, IV are impregnated at different temperatures. The description of the samples is given in Table 13.

Sample type	Dimensions (diameter *height) in mm	Holes descriptions
Type I	140*20	Without hole
Type II	140*20	With hole of 10mm
Type III	280*20	Without hole
Type IV	280*20	With hole of 10mm

Table 13: Samples used for investigation of hole effects

The results of weight monitoring of sample type III and IV are depicted in Figure 62.

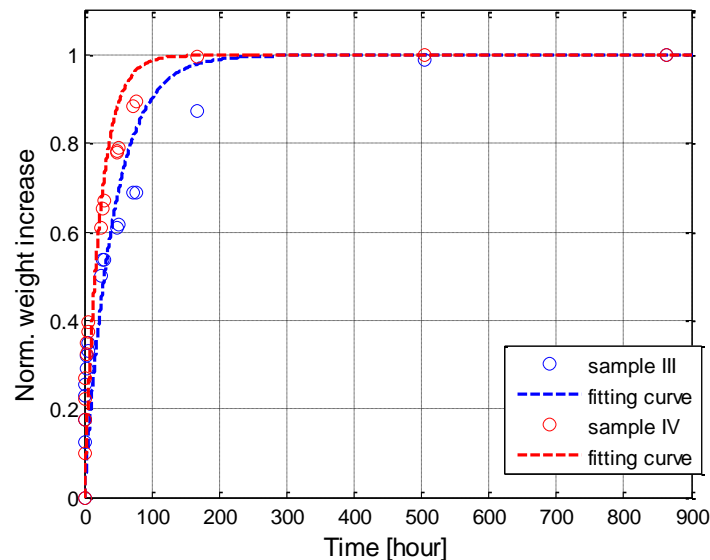


Figure 62: Normalized weight versus time of sample type III and type IV at ambient temperature

Table 14 includes time constants of impregnation process of the sample types I, II, III, IV at different impregnation temperature ( ambient, 50 °C , 70 °C)

Sample	$\tau$ at T=22 °C	$\tau$ at T=50 °C	T at T= 70 °C
Type I	7.55	5.13	1.76
Type II (+hole)	6.12	5.05	1.61
Type III	43.13	6.29	4.89
Type IV(+hole)	23.02	6.27	4.76

Table 14: time constant  $\tau$  for different samples types ( with/without hole) at different temperature

From the results, it can be concluded that adding a hole in the sample has an effect on the impregnation time. This effect depends on the temperature. The lower the temperature the higher the effect on the rise time of the impregnation process. For example, the impregnation time decreases with almost 18% for the case type I and II. And for temperature 50°C and 70°C is less than 2%.

During monitoring of the post impregnation of type III and type IV, it was observed that some area in the side surfaces was not permeable for oil as can be seen in Figure 63. This explains why

the time constant of the impregnation process for type III at ambient temperature has a high value.



Figure 63: Sample Type III with not permeable side area to oil

### 5.2.5 SUMMARY: DATA COLLECTION FOR PSP MATERIAL

Table 15 summarizes all saturation of the impregnation process for all investigated sample at different temperature ( ambient  $\sim 22^{\circ}\text{C}$ ,  $50^{\circ}\text{C}$ , and  $70^{\circ}\text{C}$ )

Sample type	dimensions [mm]	Sample Volume [mm <sup>3</sup> ]	Side surface [mm <sup>2</sup> ]	$\tau$ at ambient	$\tau$ at $50^{\circ}\text{C}$	$\tau$ at $70^{\circ}\text{C}$
R1	100*100*100	1,000,000	40,000	4.57	36.79	1.01
R2	133*75*100	1,000,000	41,600	6.85	2.60	1.00
R3	200*50*100	1,000,000	50,000	3.77	4.08	0.55
R4	250*40*100	1,000,000	58,000	3.92	1.32	0.38
S1	50*50*20	50,000	4000	1.34	0.54	0.66
S2	52*52*20	54,080	4160	1.26	0.64	0.78
S3	63.5*63.5*20	78,125	5000	1.09	0.49	0.30
S4	72.5*72.5*20	105,125	5800	1.50	0.62	0.47
C1	63*20	63,340	3989.8	1.14	0.59	0.17
C2	66*20	68,420	4146.9	1.37	0.54	0.51
C3	80*20	10,053	5016.5	0.94	0.66	0.25
C4	93*20	13,586	5843.4	1.80	0.95	0.36

Table 15:  $\tau$  time constants for PSP samples at ambient,  $50^{\circ}\text{C}$ ,  $70^{\circ}\text{C}$

From the above table, it can be seen that the obtained time constants show dispersion for different sample shapes. For example for the first sample type R1, the time constant at  $50^{\circ}\text{C}$  is 36.79 hours where at ambient is only 4.57 hours. This can be explained by several issues that were observed during drying and impregnation process:

1. Leaking glue:

After drying process of a sample, it was noticed that the used glue between the layers was leaking (see Figure 64).



**Figure 64: Sample with glue leaking on the side surface**

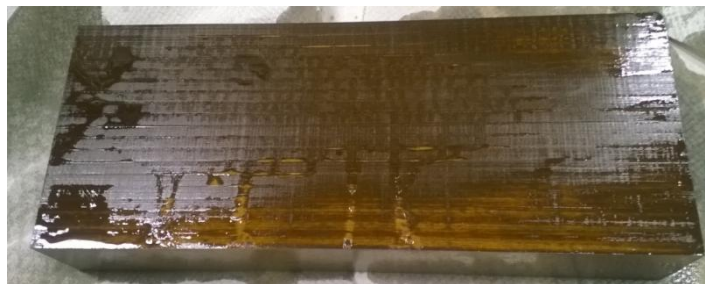


**Figure 65: Sample from figure 67 after the impregnation**

As it is already mentioned, the glue used between the layer is not permeable to oil. Thus the oil cannot enter the sample from the covered area by glue (see Figure 65). This phenomenon slows the impregnation process down.

2. Cracks:

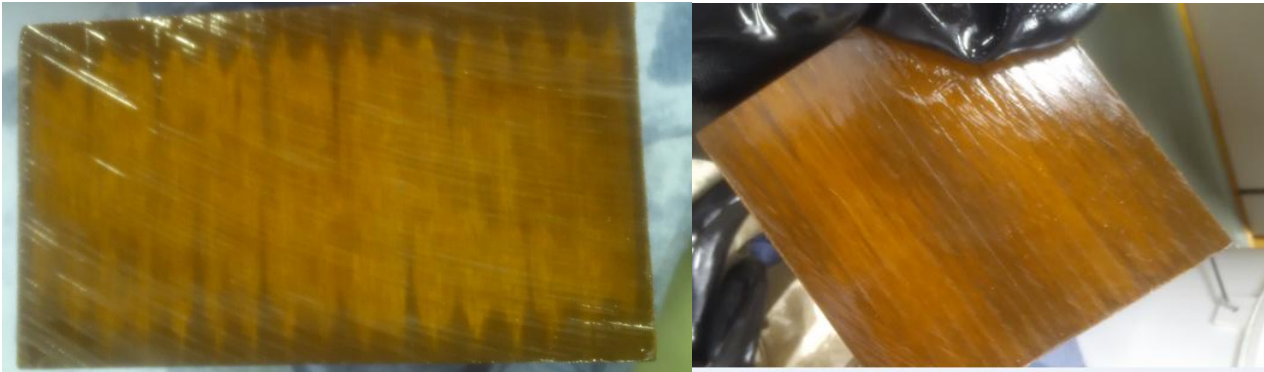
During drying process, some samples are cracked (see Figure 66). The oil can enter in this cracks and the impregnation process will speed-up



**Figure 66: Crack in a PSP Sample**

3. Not permeable area:

During impregnation process, it was noticed that some areas of the impregnated samples were not permeable for oil (see Figure 67). This proves that more attention is to be given to the cutting methods in order not damage the opening of the capillary.



(a)

(b)

**Figure 67: Not permeable area for oil in a PSP sample**

4. During impregnation at high temperature, keeping the temperature at desired value is difficult. The samples are taken out of the oil and measured at ambient temperature and they cool down. These can affect the accuracy of the measurements.

### 5.3. DATA ANALYSIS OF KP MATERIAL

This section presents the obtained data that represent the impregnation process of samples made of KP material. In particular, the effect of side surface size, sample shape, and temperature on the impregnation time.

#### 5.3.1 EFFECT OF SURFACE

To investigate the effect of the surface, four KP samples of the same volume and different side surfaces are dried and impregnated at ambient temperature under vacuum. After the vacuum has been released, the weight increase is monitored until saturation of the samples. Figure 68 (a) shows the normalized measured weight increase of the samples and its related model in function of post-impregnation standing time. The modelling procedure is the same as described in section 5.1.

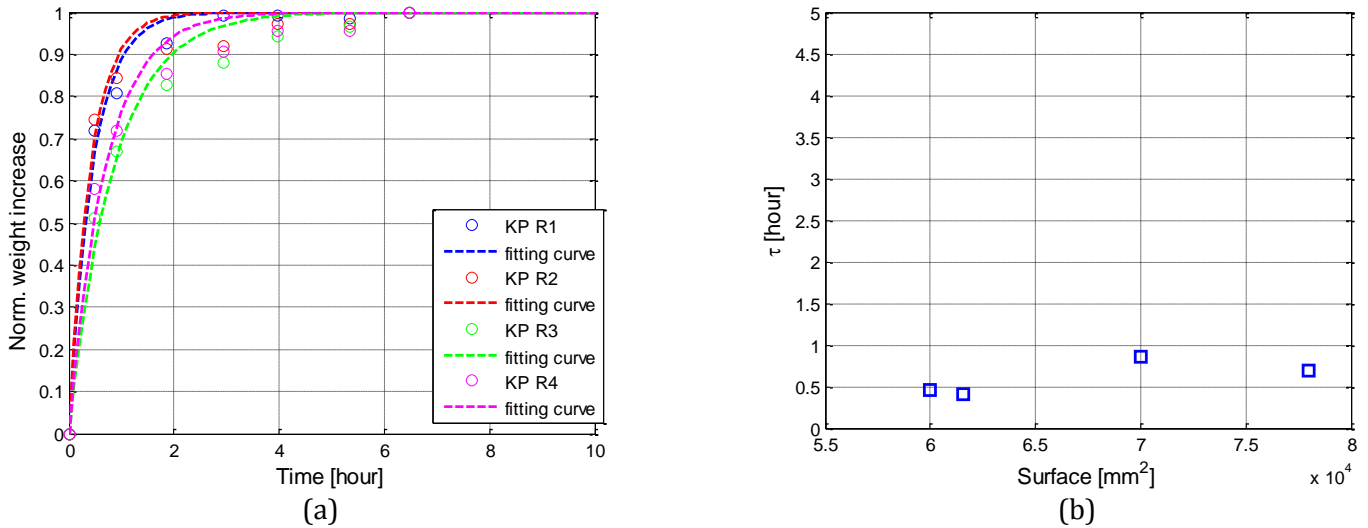


Figure 68: (a) Normalized Weight versus Impregnation time for samples types R1, R2, R3, R4 (b) Time constants versus total surface

### 5.3.2 EFFECT OF SHAPE

To investigate the distance from the edges of the sample to its center on the impregnation process cylindrical (type C) and cubical (type S) samples with same side surface are chosen. Figure 69 shows the time constants  $\tau$  of impregnation process for four cases: samples types S1 and C1 with  $S=4000\text{mm}^2$ , sample types S2 and C2 with  $S=4160\text{mm}^2$ , samples types S3 and C3 with  $S=5000\text{mm}^2$ , and samples types S4 and C4 with  $S=5800\text{mm}^2$ .

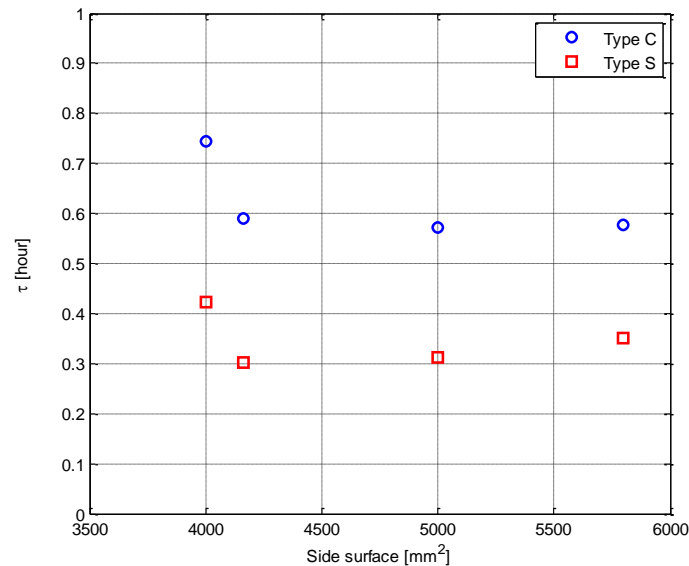


Figure 69: Time constants  $\tau$  of impregnation process of samples with cylindrical and cubic shape for four cases:  $S=4000\text{mm}^2$ ,  $S=4160\text{mm}^2$ ,  $S=5000\text{mm}^2$ ,  $S=5800\text{mm}^2$

### 5.3.3 EFFECT OF TEMPERATURE

The effect of temperature is studied by impregnating the same sample type at different temperatures (ambient (~22 °, 50 °C, 70 °C). The obtained results for one sample of type A1 (L=100mm, W=100mm, h=100mm) are depicted in Figure 70.

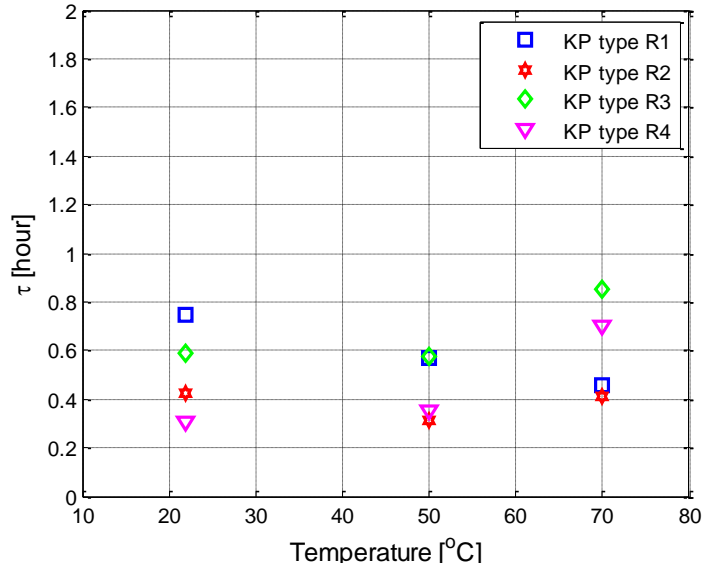


Figure 70: Effect of Impregnation temperature of KP Sample Type R1 , type R2, type R3, and type R4

Based on the results obtained, it can be noticed that the impregnation process of KP material is faster than for PSP. The Time constants of the impregnation process decreases as the temperature increases. However the material absorbs less oil compared when the sample is impregnated at ambient temperature.

After saturation of the samples when impregnating at 70 °C, the samples are cooled down and the weight is measured. The samples absorbs more oil. The average oil absorption during cooling down is 0.5%

### 5.3.4 SUMMARY: DATA COLLECTION FOR KP MATERIAL

Table 16 presents the descriptions of all studied samples made of KP material. This includes shape, dimensions, impregnation temperature and the determined time constants of the impregnation process at different temperatures (ambient~22°C, 50 °C, 70 °C)

Sample Type	Sample Volume [mm <sup>3</sup> ]	Sample total surface [mm <sup>2</sup> ]	Sample Side surface [mm <sup>2</sup> ]	$\tau$ [hrs] at ambient	T [hrs] at 50 °C	T [hrs] at 70 °C
R1	1,000,000	60,000	40,000	0.45	0.46	0.59
R2	1,000,000	61,550	41,600	0.41	0.46	0.51
R3	1,000,000	70,000	50,000	0.58	1.52	0.45
R4	1,000,000	78,000	58,000	0.69	0.82	0.51
S1	50,000	9,000	4000	0.42	0.31	0.05
S2	54,080	9,568	4160	0.30	0.37	0.19
S3	78,125	12,813	5000	0.31	0.53	0.24
S4	105,125	16,313	5800	0.35	0.47	0.17
C1	63,340	4616.5	3989.8	0.74	0.35	0.06
C2	68,420	4798.3	4146.9	0.59	0.21	0.08
C3	10,053	5816.1	5016.5	0.57	0.17	0.06
C4	13,586	6761.2	5843.4	0.57	0.33	0.34

**Table 16: Time constants for KP samples**

From the obtained data, it can be seen clearly that KP material can be impregnated faster comparing with PSP. For comparison see Table 15 and Table 16.

It must be mentioned that it was difficult to maintain a constant temperature during the post impregnation standing time. In addition, the sample was periodically taken for measurements what was also affecting the oil temperature. Therefore, for some samples the effect of temperature could not have been seen.

#### 5.4 MODELLING OF THE IMPREGNATION TIME

In this section, a model describing the impregnation time with respect to the sample size, shape and oil temperature is introduced. The model is based on the weight increase measurements, in particular, the rise time is observed for the samples as described in previous sections.

The sample characteristics that influence the impregnation time are: material type, distance that has the oil to travel to the center and the volume and the side surface of the sample. According to the obtained results, the KP material impregnates faster when comparing to PSP material. For

instance the time rise for sample made from KP material is 5 times shorter. For this reason, our modeling approach will be focused only on PSP material.

The model that has to be developed relates the sample shape, its dimensions and temperature to the time constants  $\tau$  of the impregnation process as explained in section 5.1. Since the volume (V) and the side surface (S) are correlated to the distance to the center of the sample, the ratio V/S is chosen to describe the sample dimensions. This ratio is dependent on the dimension of the layer of a PSP sample. In this section two models will be proposed for cylindrical and cuboidal shape separately.

#### 5.4.1 DATA MODELING OF RISE TIME CONSTANT

For each temperature (T=22, T=50 and T=70 °C), the rise time of impregnation process of cylindrical samples (type C, II, and III) and cuboidal samples (R, S) are modeled separately as a function of V/S as described below:

$$\begin{aligned} T = 22 & \rightarrow \tau = f_1\left(\frac{V}{S}\right) \\ T = 50 & \rightarrow \tau = f_2\left(\frac{V}{S}\right) \\ T = 70 & \rightarrow \tau = f_3\left(\frac{V}{S}\right) \end{aligned} \quad (34)$$

Where :

$f_i$  is a function to be determined by fitting techniques.

The  $\tau$  is dependent also on the temperature T. B The ratio V/S is independent on temperature, only the coefficients of the function  $f_i$  are dependent on T. This relation can be determined by modeling these coefficients as function of T.

#### **Models of $\tau$ as function of V/S at different impregnation temperature:**

The data has been analyzed in term of  $\tau$  versus V/S for different temperature. Figure 71 shows an example of rise time of cylindrical samples at ambient temperature. Looking at the data, the rise time increases with increasing V/S. Both exponential and polynomial models were used to fit the data. The polynomial model gives a better fit when compared to the exponential model. This is due to the fact that the rise time for small samples is almost constant (i.e. small variation in rise time over all small samples) and when using the exponential model to fit the hole data (small and big samples), a high rise time error is obtained between the exponential model and measured data. This is not the case for the polynomial model where the obtained error is very small when compared to the exponential model.

Therefore, we used a polynomial function to model the rise time versus V/S. Analysis of the data shows that a second order of the polynomial function is sufficient to model the rise time as the associated error is small.

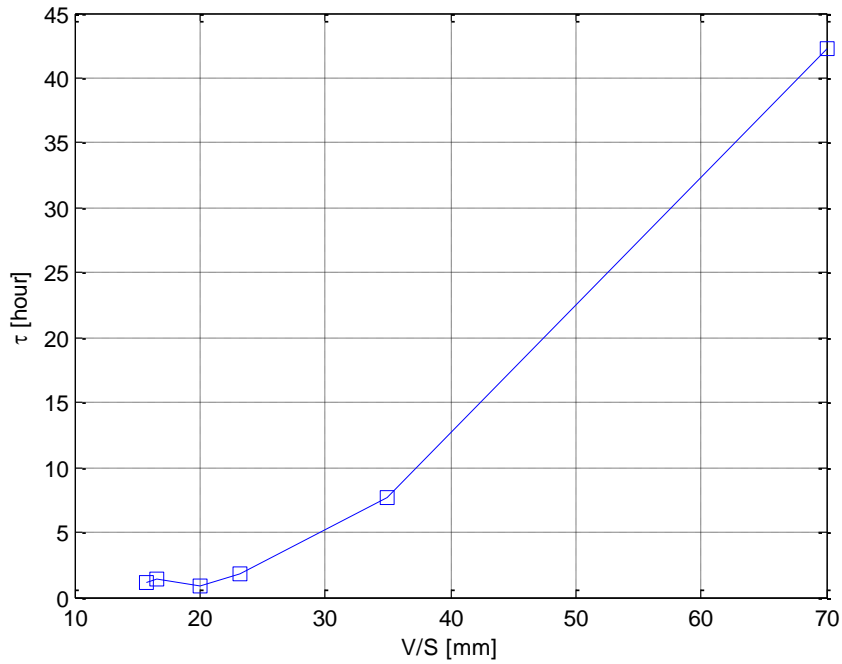


Figure 71: Time constant of cylindrical samples versus V/S ratio

The model can be expressed as:

$$\tau_{220c} = a_1 * (V/S)^2 + b_1 * V/S + c_1 \quad (35)$$

$$\tau_{500c} = a_2 * (V/S)^2 + b_2 * V/S + c_2 \quad (36)$$

$$\tau_{700c} = a_3 * (V/S)^2 + b_3 * V/S + c_3 \quad (37)$$

Where the coefficients of each model of each temperature has to be determined for each shape.

### Model ling of $\tau$ as a function of V/S and T

The obtained parameters  $a_i$ ,  $b_i$  and  $c_i$  are in turn dependent on the impregnation temperature (T). These parameters are modeled as a function of T. The model of  $\tau$  as function of V/S and T can be described as follow:

$$\tau = a_i(T) * (V/S)^2 + b_i(T) * V/S + c_i(T) \quad (38)$$

The obtained coefficients a, b, and c are fitted to a polynomial function of order two of T. These functions are described hereunder:

$$a_i(T) = \alpha_1 * T^2 + \beta_1 * T + \theta_1 \quad (39)$$

$$b_i(T) = \alpha_2 * T^2 + \beta_2 * T + \theta_2 \quad (40)$$

$$c_i(T) = \alpha_3 * T^2 + \beta_3 * T + \theta_3 \quad (41)$$

#### 5.4.2. MODEL PARAMETERS FOR CYLINDRICAL SHAPE

The coefficients of the models of  $\tau$  as function of  $V/S$  (see equation (35), (36), (37)) for the cylindrical shape are given in Table 17.

Impregnation temperature[°C]	$a_i$	$b_i$	$c_i$
22	12.37 $10^{-3}$	-298.63 $10^{-3}$	2.51
50	1.29 $10^{-3}$	-4.08 $10^{-3}$	0.28
70	0.26 $10^{-3}$	67.49 $10^{-3}$	-1.067

**Table 17: Model parameters for cylindrical shape at different temperature (ambient, 50°C, and 70°C)**

the parameters  $\alpha_i$ ,  $\beta$ , and  $\theta_i$  of the model of  $\tau$  as function of  $V/S$  and  $T$  (equation (38)) are given in Table 18

Temperature	$\alpha_i * 10^{-3}$	$\beta_i * 10^{-3}$	$\theta_i * 10^{-3}$
$a_i$	0.007165	-0.91156	28.961
$b_i$	-0.14459	20.93	-689.11
$c_i$	0.25062	-97.678	4542.1

**Table 18: Model parameters for cylindrical shape at different temperature (ambient, 50°C, and 70°C)**

Figure 72(a), 72(b), and 71(c) show how the model fits the data at different temperatures.

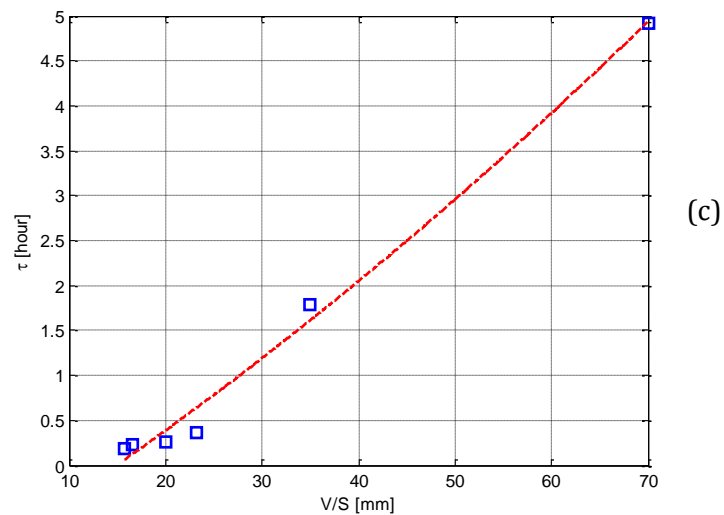
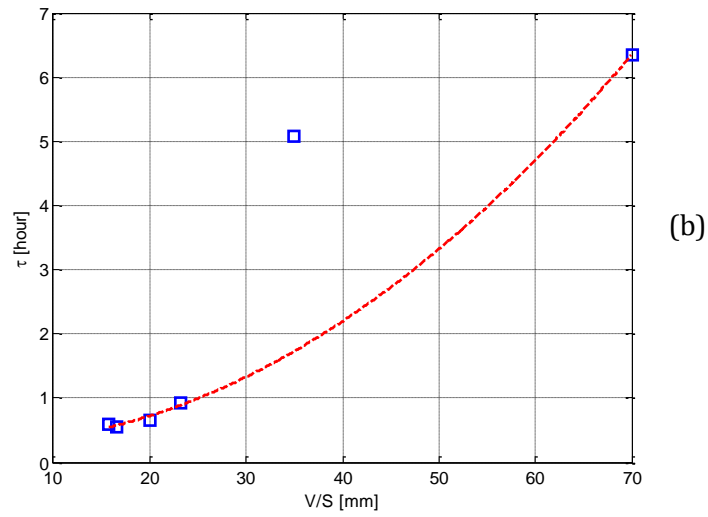
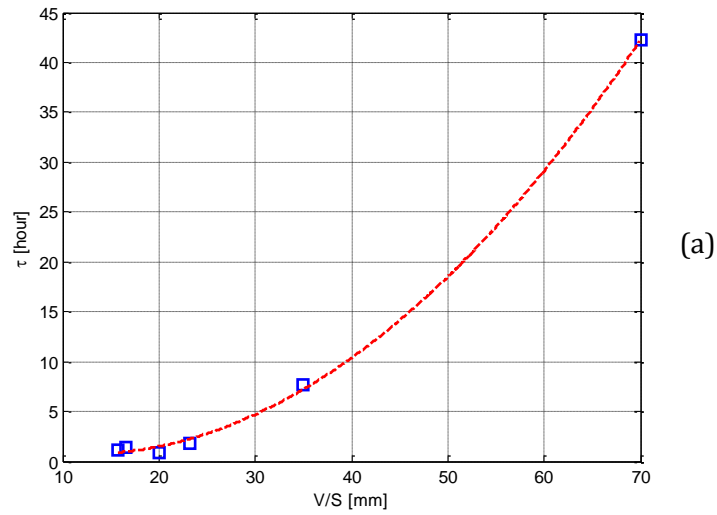


Figure 72: Model of  $\tau$  as function of V/S : (a) ambient temperature (b) 50 °C (c) 70 °C

To investigate the goodness of the model the statistical parameter (i.e. mean and variance) of the error between the real and estimated  $\tau$  are computed. For all temperature the mean of the error is zero and the variance is 0.20, 1.86, and 0.03 for 22, 50 and 70 °C respectively.

The variance at 50 °C is higher because of the sample of V/S=35 was not used in the estimation of the model because this sample has some measurement error as mentioned before. However it was used to calculate the variance.

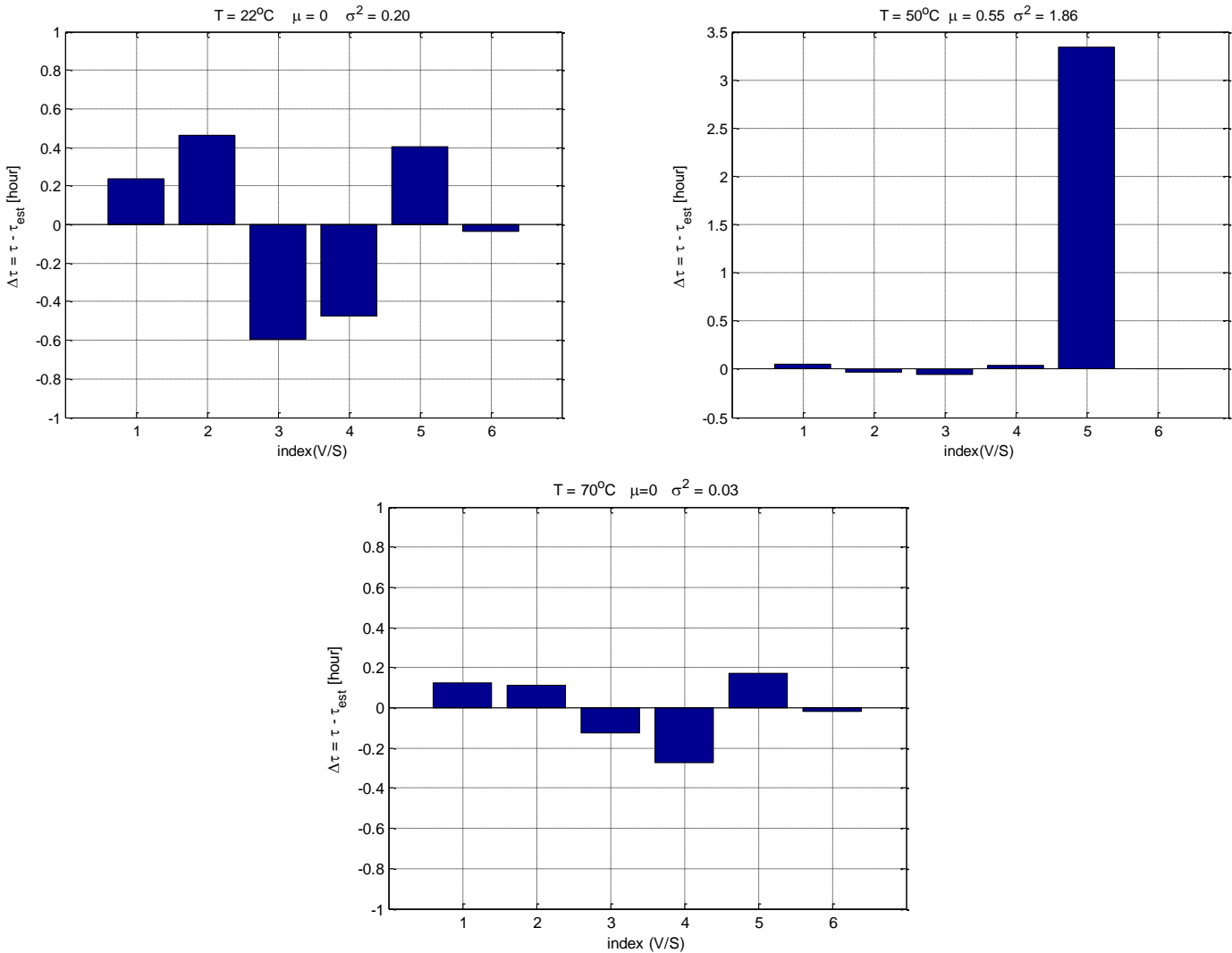


Figure 73: Error between the data and estimated  $\tau$  using the model

Figures 74, 75, and 76 show the modelling of the coefficient  $a_i$ ,  $b_i$  and  $c_i$  of the models described by equations 35, 36, and 37 as function of Temperature (T). These figures show also the errors of this fitting. As it can be seen, the models (equation (39), (40), and (41)) fits the coefficients a, b, and c well as the error is negligible.

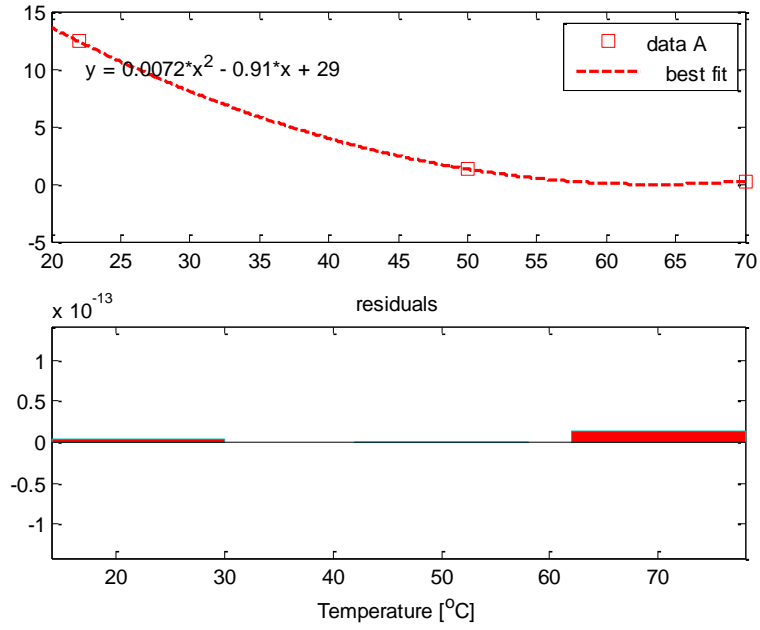


Figure 74: The model of coefficient  $a$  as function of  $T$  and the

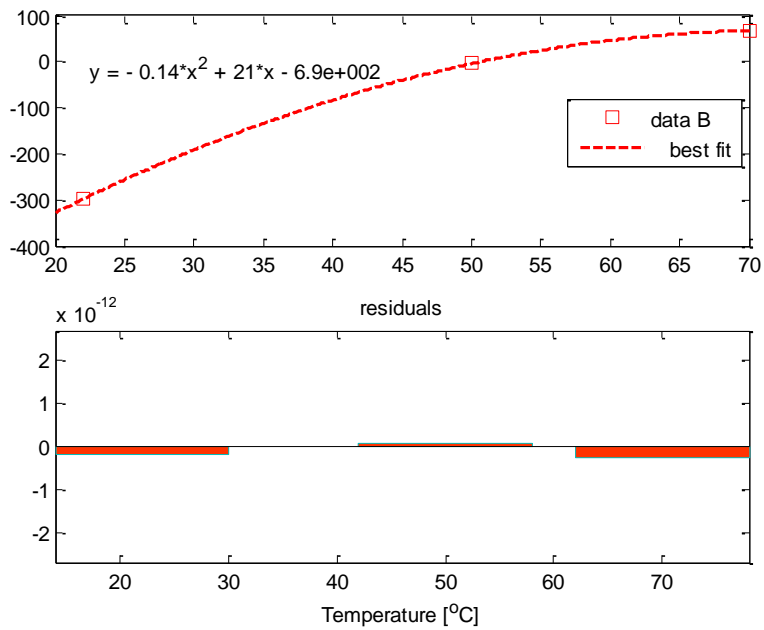
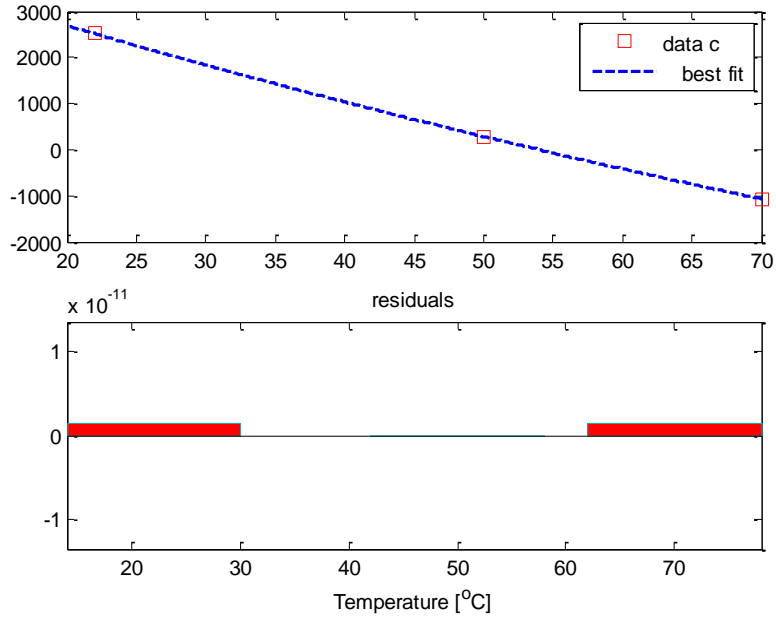


Figure 75: The model of coefficient  $b$  as function of  $T$  and the error



**Figure 76: The model of coefficient c as function of T and the error**

#### 5.4.3. MODEL PARAMTERS FOR CUBOIDAL SHAPE

The same modelling procedure as described above will be used for the cuboidal samples (Type R and S). The coefficients of the model for cuboidal shape are given in Table 19 and Table 20. The Figure 77, Figure 78, Figure 78, and Figure 79 shows the model of rise time as a function of V/S for temperature 22 °C, 50 °C and 70 °C respectively. The figures show also the error in terms of its mean and variance. The error variance is 1.22 hour, 0.27 hour and 0.01 hour for ambient temperature, 50°C, and 70 °C respectively.

Impregnation temperature[°C]	$a_i$	$b_i$	$c_i$
22	$9.36 \cdot 10^{-3}$	0.0286	0.746
50	$134.32 \cdot 10^{-3}$	-3.964	29.33
70	$11.93 \cdot 10^{-3}$	-0.416	4.046

**Table 19: Coefficients of model of  $\tau$  as function of V/S for each temperature (ambient, 50°C, 70°C)**

Temperature	$\alpha_i \cdot 10^{-3}$	$\beta_i \cdot 10^{-3}$	$\theta_i$
$a_i$	-0.2205	6.667	-0.0487
$b_i$	20.337	-662.64	4.582
$c_i$	-331.35	10499.80	-77.976

**Table 20: Parameters of the model of the coefficients (a, b, c) as function of T**

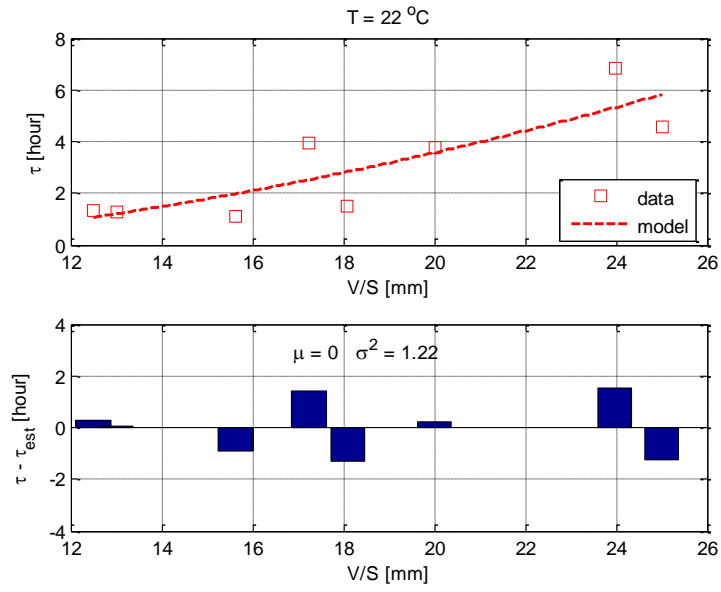


Figure 77: Model of  $\tau$  as function of  $V/S$  at ambient temperature and error

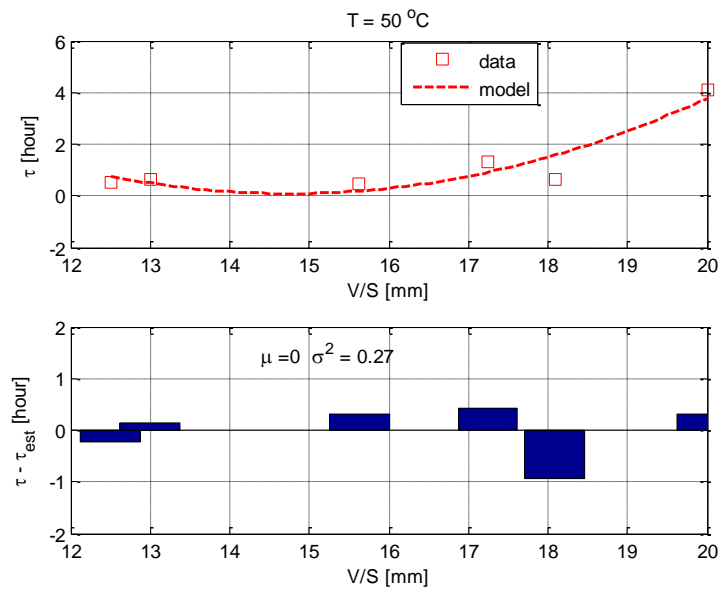
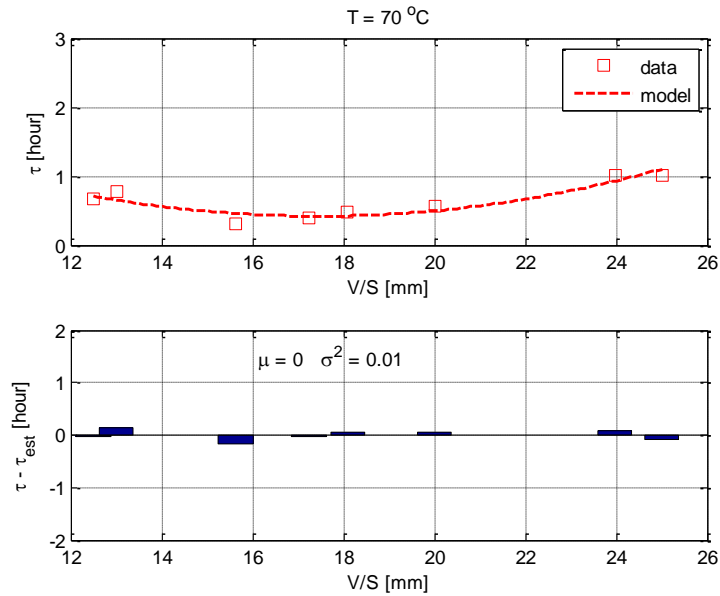
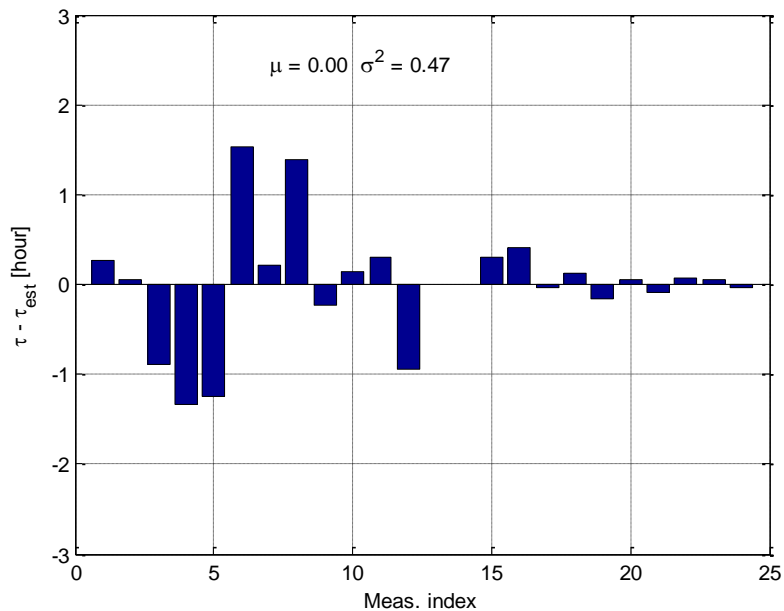


Figure 78: Model of  $\tau$  as function of  $V/S$  at 50 °C



**Figure 79: Model of  $\tau$  as function of  $V/S$  at 70°C**

Figure 80 shows the error of the model of  $\tau$  as a function of  $V/S$  and  $T$ . The variance of the error is 0.47 hour. It can be seen that the error is higher at ambient temperatures. This can be explained by the fact that impregnation process at ambient is slower than higher temperature which may lead to high data dispersion. Clearly, at high temperature the impregnation is faster and the variance of  $\tau$  tends to decrease.



**Figure 80: The errors of estimated and obtained  $\tau$  from the data of cuboidal samples**

#### 5.4.4 MODEL VALIDATION

In order to validate the proposed model, we compared the computed rise time  $\tau$  from the measurement data to the estimated  $\tau$  obtained from the proposed model. The comparison procedure is illustrated in the flowchart given in Figure 81. For the evaluation of the results, we defined the error between the model and the measured data as:

$$error = \tau - \tau_{est}$$

Where  $\tau$  is the rise time as obtained from the measured data and  $\tau_{est}$  is the estimated rise time using the proposed model. Figure 82 gives the rise time error for the studied sample. The x-axis presents the index of the measurements which corresponds to the V/S as depicted in Table 21. The mean and variance of the error are 0 and 0.07, respectively. The variance of the error is low and hence it can be concluded that the proposed model matches the measurements. Please note again that the sample with V/S 35 (Sample type III) is excluded from the analysis (as this sample has a measurements error related to impenetrable area at side surface). It can also be seen that the error is higher at the ambient temperature when compare to other temperatures.

Figure 83 shows the cumulative distribution function (CDF) of the absolute value of the error. It can be read that with a probability of 90% the error in the estimated rise time will be less than 0.5 hours. Figure 84 gives examples of the normalized weight increase based on the measurement and the proposed model. This confirms the validity of the proposed model.

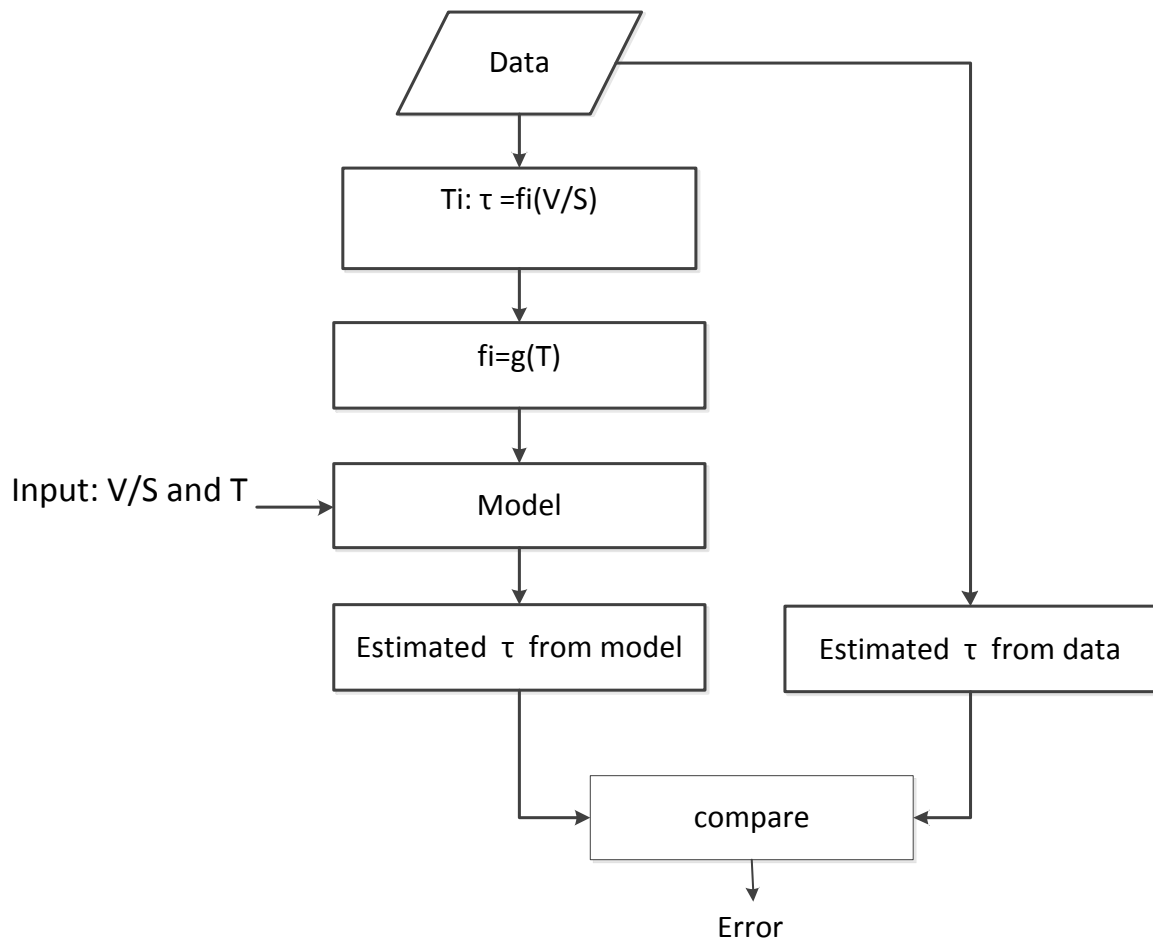


**Figure 81: The flowchart for calculating the error between the estimated  $\tau$  and obtained from data.**

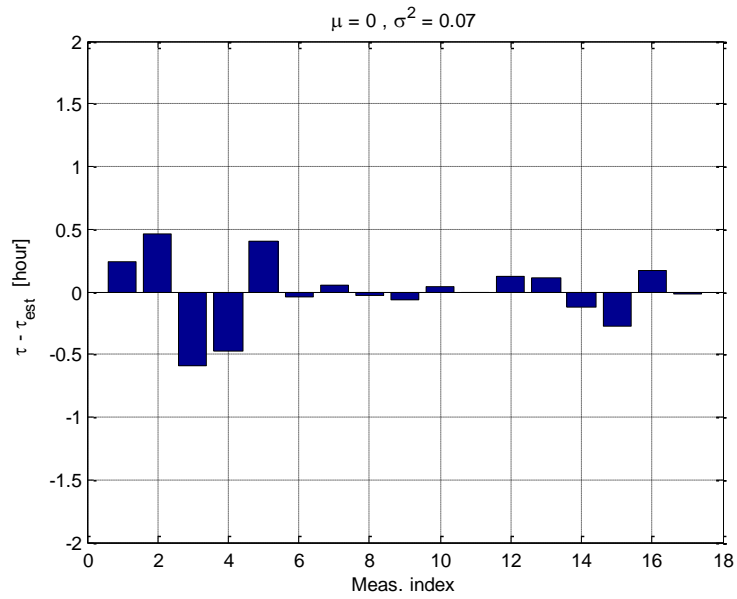


**Figure 82: The error between estimated**

index	1	2	3	4	5	6	7	8	9	10	11	12	13	14	15	16	17	18
V/S	15.7	16.5	20	23.2	35	70	15.7	16.5	20	23.2	35	70	15.7	16.5	20	23.2	35	70
T	22	22	22	22	22	22	50	50	50	50	50	50	70	70	70	70	70	70

**Table 21: Corresponding V/S to Index.**

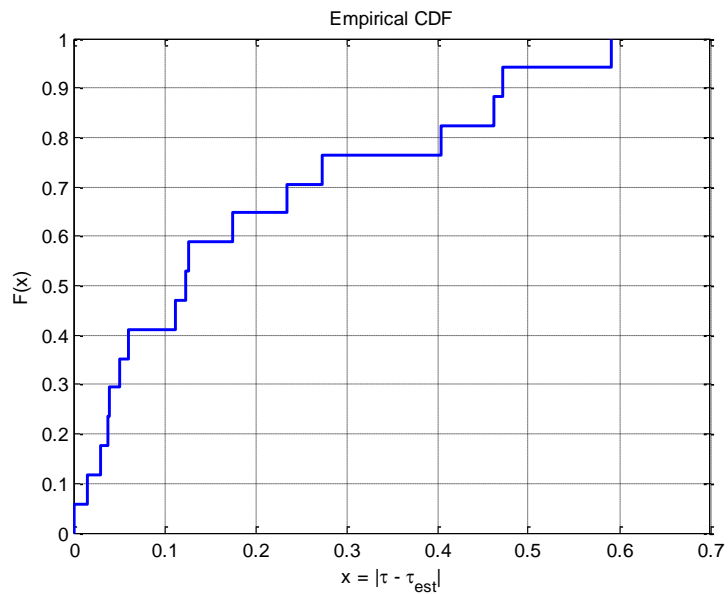
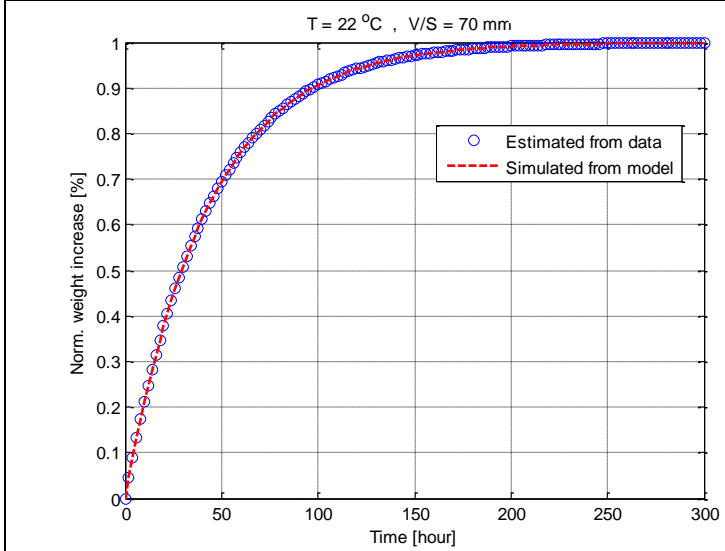
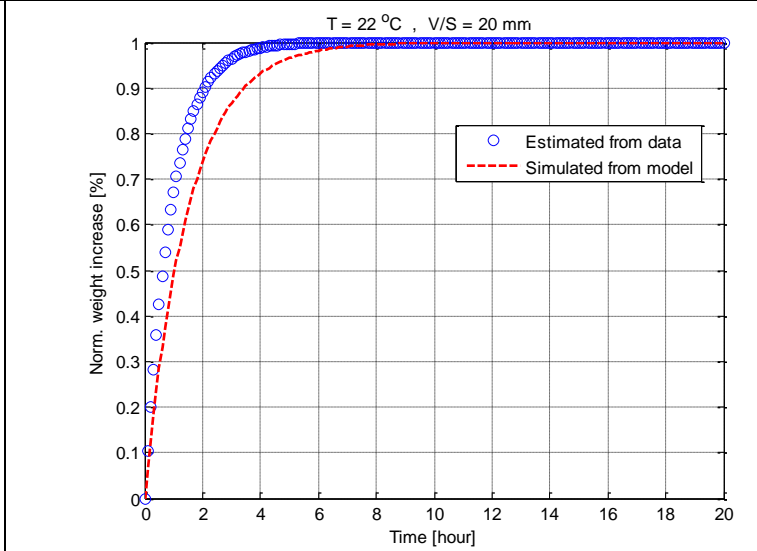


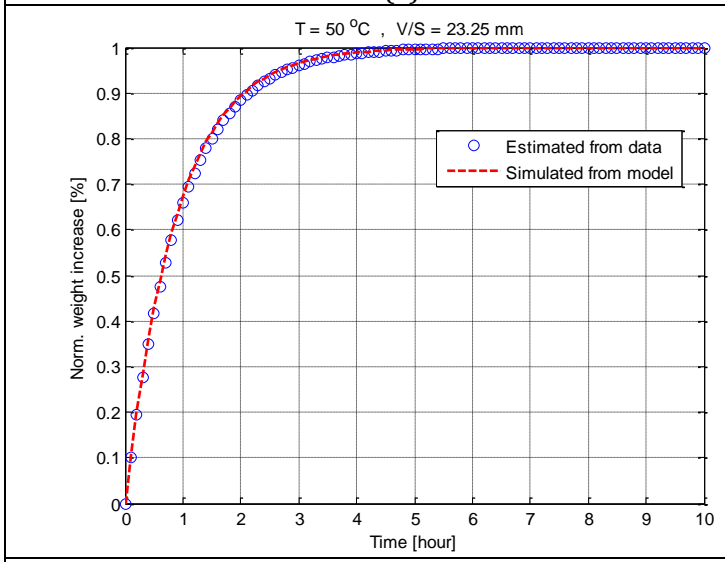
**Figure 83: CDF of the absolute value of the error**



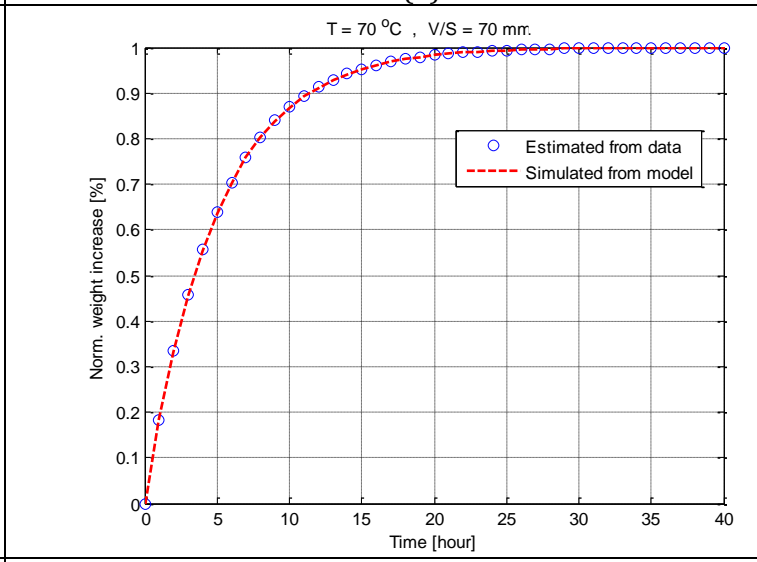
(a)



(b)



(c)



(d)

Figure 84: A comparison of normalized weight increase determine by estimated  $\tau$  and  $\tau$  from data for different samples

## 5.5.DISCUSSION

In previous section, a model for estimation the rise time of the impregnation process is proposed for two sample shapes: cuboidal and cylindrical. The proposed model shows a good agreement with the measurements for both cylindrical and cuboidal sample shapes. The proposed model is valid for temperatures between 22 and 70 , and for V/S between 15.35- 70 mm for cylindrical and 13 – 25 mm for cuboidal shape. It should be noted that the error variance of the cylindrical is much lower than for cuboidal shape (i.e. 0.04, 0.47 hour). This difference is mainly due to the fact in the cylindrical case the V/S changes linearly with radius of the sample which is not the case for the cuboidal sample. Clearly for cuboidal sample, when increasing the V/S does not mean necessarily that the minimum distance is increasing. This is can be illustrated by the following:

The V/S for cylindrical shape is determined as:

$$\frac{V}{S} = \frac{\pi r^2 h}{2\pi r h} = \frac{r}{2} \quad (42)$$

Whereas for the cuboidal shape is :

$$\frac{V}{S} = \frac{l.w.h}{2(l+w)h} = \frac{l.w}{2(l+w)} \quad (43)$$

Based on this, for the cuboidal shape V/S is non-linear with the width w which is related to the distance ( $d_{\min}=w/2$ ). For example if L becomes higher w has to be smaller which theoretically means that the sample can be impregnated faster as the distance becomes lower. Therefore, an appropriate approach to model the cuboidal shape is to change L and W with the same factor.

$$\frac{V}{S} = \frac{(\alpha.l).(\alpha.w)}{2(\alpha.l + \alpha.w)} = \alpha \cdot \frac{l.w}{2(l+w)} \quad (44)$$

This means that changing L and W with a constant factor  $\alpha$ , the V/S and the minimum distance to the center will also change with the same factor. For the cylindrical shape, this is always the case (changing V/S and r changes with the same factor).

Moreover, the structure of the material is non-homogenous (non-uniform distribution of the capillaries inside the material) which makes it difficult to model the impregnation process using deterministic models. Therefore it will be better and easy to use a statistical approach to model the impregnation process based on real measurements. This means that sufficient number of samples for each type has to be measured.

In this study, we adopt the simple exponential model  $1-\exp(-t/\tau)$  to model the weight increase of the samples and hence estimate the rise time of the impregnation process. However, when assessing the data, this model did not show a good fitting of the data just before the saturation.

Clearly, it was observed that the rise time of the exponential function in the beginning of the impregnation process is higher. However at certain time (before saturation) the rise time is slower than the function  $1-\exp(-t/\tau)$ . This means that one single exponential model is not always sufficient to model the data and hence it may produce errors in the estimation of the saturation time. This phenomena may be due to the internal pressure (residual gases) which stands in way of the penetration of the oil. This mainly occurs at ambient temperature for large samples where the vacuum may not be equally distributed. Therefore, an extra term has to be added to the exponential function to take this effect in the modelling of the saturation time. To this end, the previous exponential model (see equation 29) can be refined by the following:

$$\frac{\Delta w}{\max\{\Delta w\}} = \begin{cases} 1 - p_1 e^{-\frac{t}{\tau_1}} + p_2 e^{-\frac{t}{\tau_2}} & t < t_s \\ 1 & t \geq t_s \end{cases}$$

Figure 85 shows a comparison between the two models, the refined model gives a better fitting.

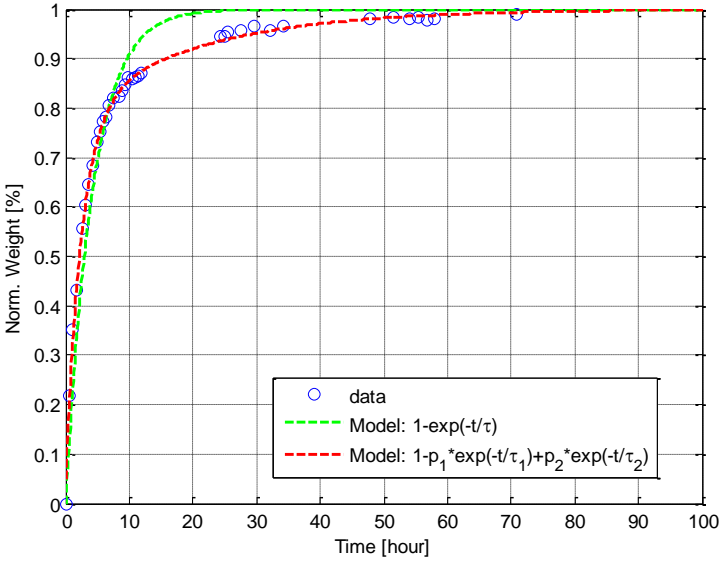


Figure 85: Normalized weight vs. time (sample type R1) at ambient temperature

## 6. CONCLUSIONS AND RECOMMENDATIONS

The aim of this thesis was to investigate the possibility of shortening the standing time (post-impregnation period) in order to optimize the production process of high voltage transformers. In particular, optimize the impregnation time of high density materials of cellulosic origin.

To reach this fundamental goal, a research into the velocity of the impregnation process of this type of materials was made. Finally, an empirical model that predicts the time needed to fully impregnate a cellulosic material sample with material, sample dimensions, impregnation temperature and time, was built. Besides, a number of partial discharges measurements on different samples were also performed to check if the standing time is related to occurrence of partial discharges in high density materials. Further on,  $\tan\delta$  measurements were performed to different samples in the course of impregnation process.

The conclusions drawn from this research are discussed in section 6.1, followed by recommendations regarding further research into the possibility of shortening the standing time in section 6.2

### 6.1 SUMMARY AND CONCLUSIONS

- PD measurements were performed according to IEC standard. The not fully impregnated, moisture free high density cellulose material is PD free. This has been observed when a sample of dry material was impregnated with dry oil. No internal partial discharges could be detected. This is confirmed by X-ray scanning showing cavity dimensions and Paschen law.
- In order to find the origin of the PD, several samples configurations were tested. These samples were with defined cavity and samples with different interfaces. In all cases, no PDs were observed.
- PD measurements were performed using testing tank for different samples. These samples were impregnated at Smit transformers. The samples were PD free.
- $\tan\delta$  measurements were performed on impregnated sample at HV voltage laboratory using Schering bridge setup. The results show that  $\tan\delta$  decreases slowly over time. It was also observed that a strong correlation exists between the decrease of  $\tan\delta$  and the weight increase of the sample during post impregnation.
- Additional  $\tan\delta$  measurements in the course of post-impregnation standing time were performed for different samples which have been impregnated at SMIT transformers. In this case,  $\tan\delta$  does not show any improvement during the post impregnation standing period.
- Weight measurements were performed to monitor the impregnation process. Two measuring methods were tested: continuous weight measurement and periodical weight measurements. The first one was not accurate because of the influence of the

force of Archimedes exerted on the sample by the oil and hence the second method has been selected.

- Different samples with different material, shape, dimensions were impregnated at different temperature. The data obtained from monitoring the weight of the samples during the impregnation process have been assessed. To extract the saturation time, the model  $1 - \exp(-t/\tau)$  has been used to determine the rise time  $\tau$  and hence the saturation time ( $t_s = 5 * \tau$ )
- The KP material impregnates faster than PSP material. The average rise time of KP material is faster 5 times than PSP material.
- The oil temperature has a high influence on the impregnation time. The higher the temperature the lower the rise time of the process ( approximately 5times less for PSP material).
- The side surface of the samples affects the impregnation time. For the same volume, when the side surface increases the impregnation decreases.
- It was hardly to draw a conclusion on the effect of the shape (cuboidal vs. cylindrical) when keeping the side surface fixed. This is because the dimensions of the used samples were comparable to each other.
- Drilling holes in the PSP samples shortens the impregnation time. This is because the side surface becomes higher from where the oil can penetrates.
- Based on the data, an empirical model for the rise time of the impregnation process has been developed. This model includes the shape, dimensions of the sample, and oil temperature. the model shows a good agreement with measurements.

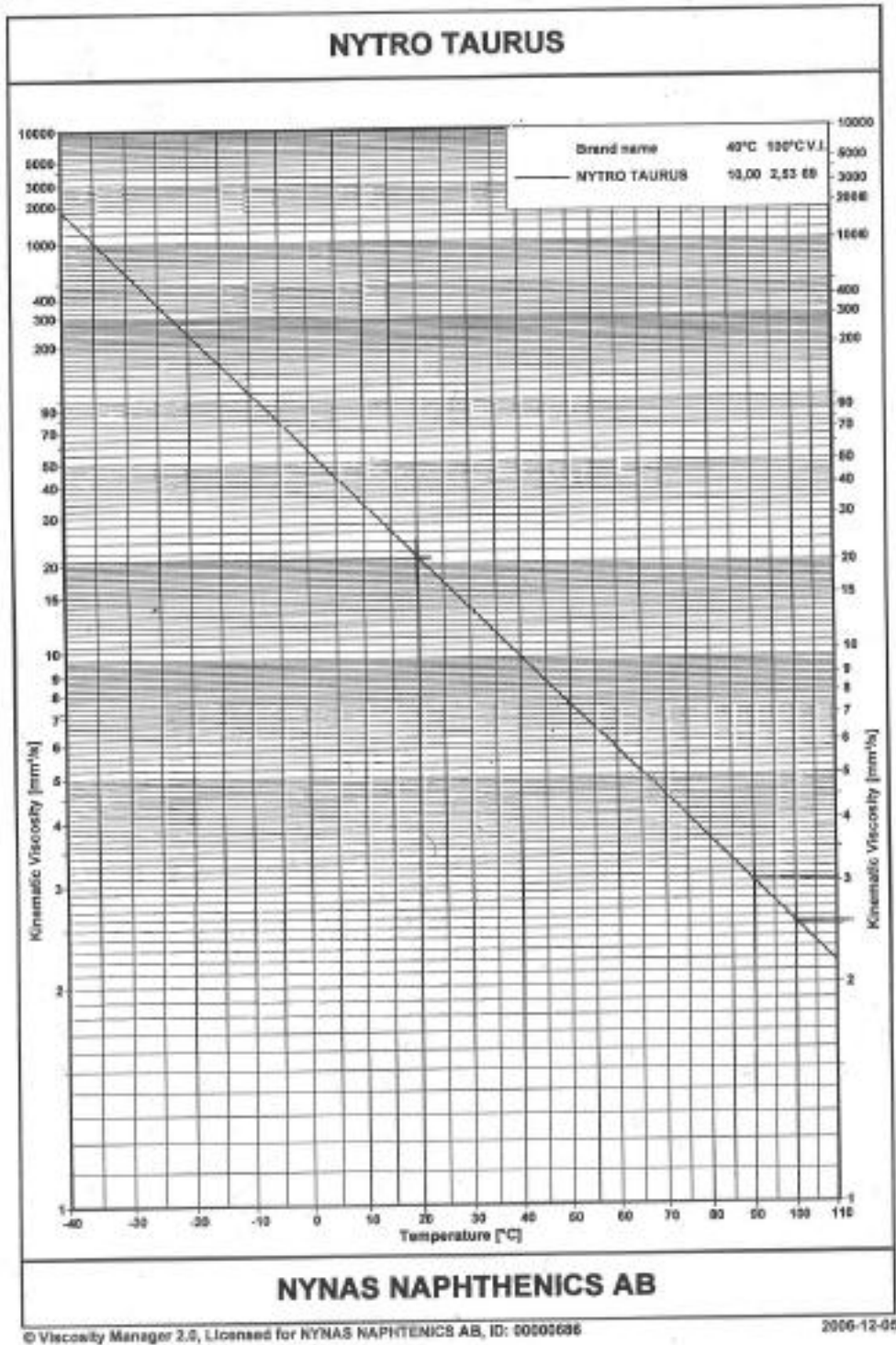
## 6.2.RECOMMENDATIONS FOR FUTURE WORK

- This research project is a part of SMIT Transformers B.V. project for investigating the possibility of shortening the standing time of transformers and optimize the production process. Based on the research on fully dried samples it can be stated that the standing time is not related to the occurrence of PD in the incompletely impregnated material. Therefore it is recommended to pay more attention to the effect of the moisture at the interface between the high density material and the oil, but also in the bulk material. Hence investigate the effect of the residual moisture on the PDIV in the course of standing time.
- Since the dimensions of the transformer reach several meters, the vacuum might not be uniformly distributed in all parts of the transformer. This may lead to residual air

and hence a source for PD especially at the interface between KP and PSP material. Further research could be focused on the effect of the impregnation pressure.

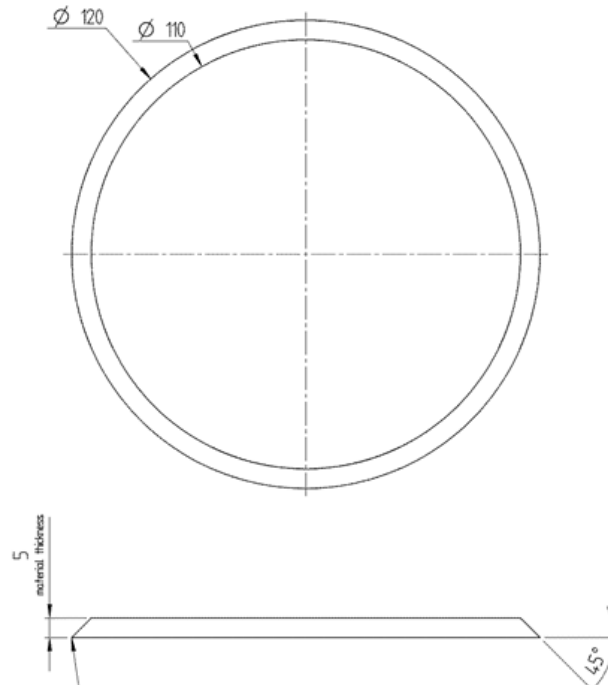
- Not only the PD are harmful during electrical testing of transformers but also flashovers that might occur along the insulating material (barriers). Therefore it is necessary to investigate this effect with respect to the standing time.
- In this study an empirical approach was used to model the impregnation time of PSP material. During the data analysis, discrepancies were observed for some samples. And it was difficult to relate this to the sample itself or to the measurement error. One way to eliminate this, it is recommended to use a statistical approach instead of empirical approach to model the impregnation process for PSP material.
- For the cuboidal shape, the measurements were performed by assuming a fixed volume while changing the side surface which is related to the minimum distance to the center. However the ratio of changing the side surface is not the same as the ratio of changing the minimum distance. In this case the effect of the width and length of the cuboidal shape cannot be separated. Therefore in order to develop an accurate model for the cuboidal shape it is recommended to select samples in such a way that the change in ratio of  $V/S$  of the samples has to be the same as the change of the minimum distance to the centre.
- The weight increase of the impregnation process is modelled by a single exponential function given as:  $1 - \exp(-t/\tau)$  which shows a good fitting to the measured data. However for a portion of large samples investigated, the model does not provide a good fitting to the data just before saturation. This may be due to the residual gases inside the sample. Therefore, it is recommended to investigate and use the following model:  $1 - p_1 \exp(-t/\tau_1) + p_2 \exp(-t/\tau_2)$ . Clearly, investigate the second exponential term with respect to the impregnation pressure.

# APPENDIX A: MINERAL OIL NYNAS VISCOSITY VERSUS TEMPERATURE

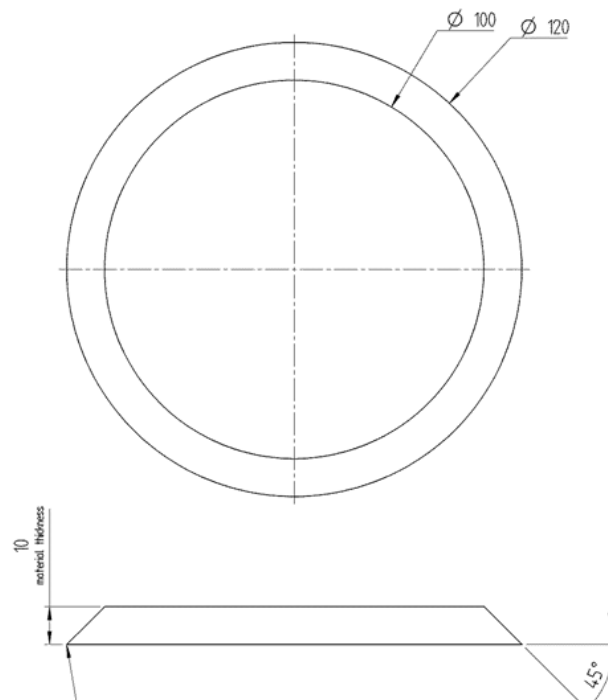


# APPENDIX B: A SCHEMATIC FOR SAMPLES USED FOR PD/TAN $\Delta$ MEASUREMENTS USING SMIT TANK

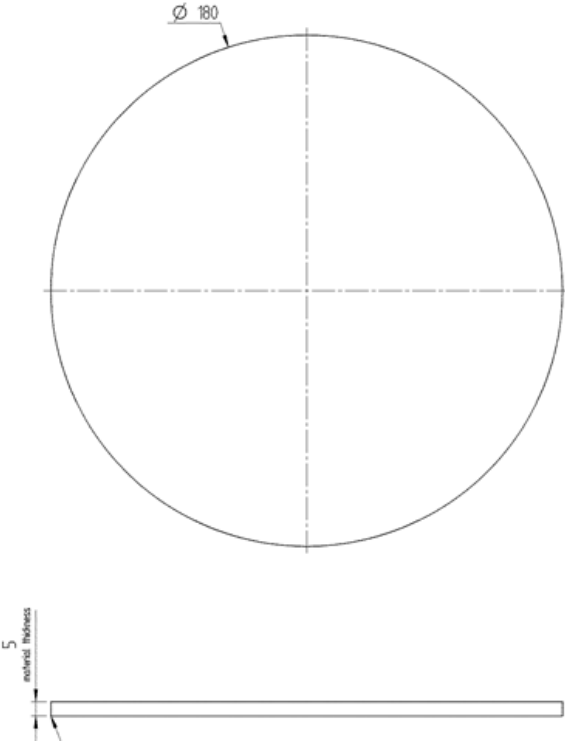
**Sample A:** Made from PSP material



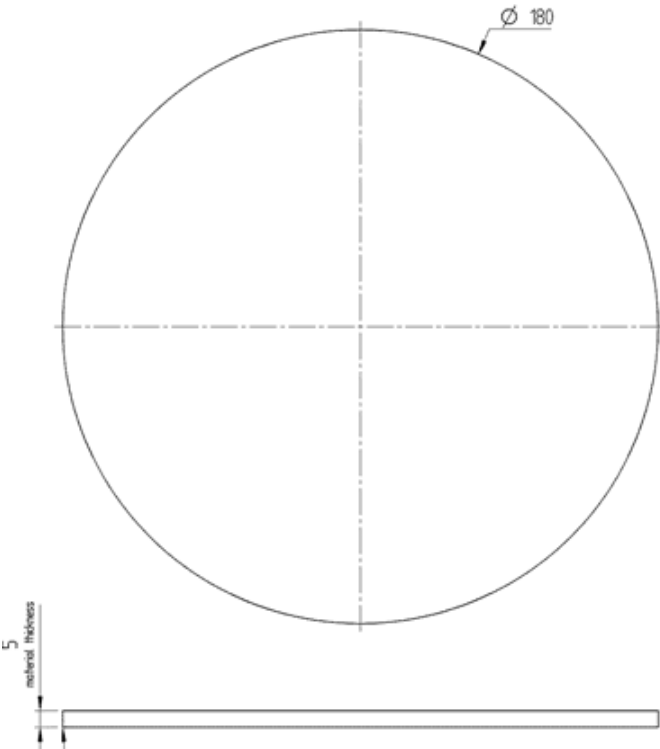
**Sample B:** Made from PSP material



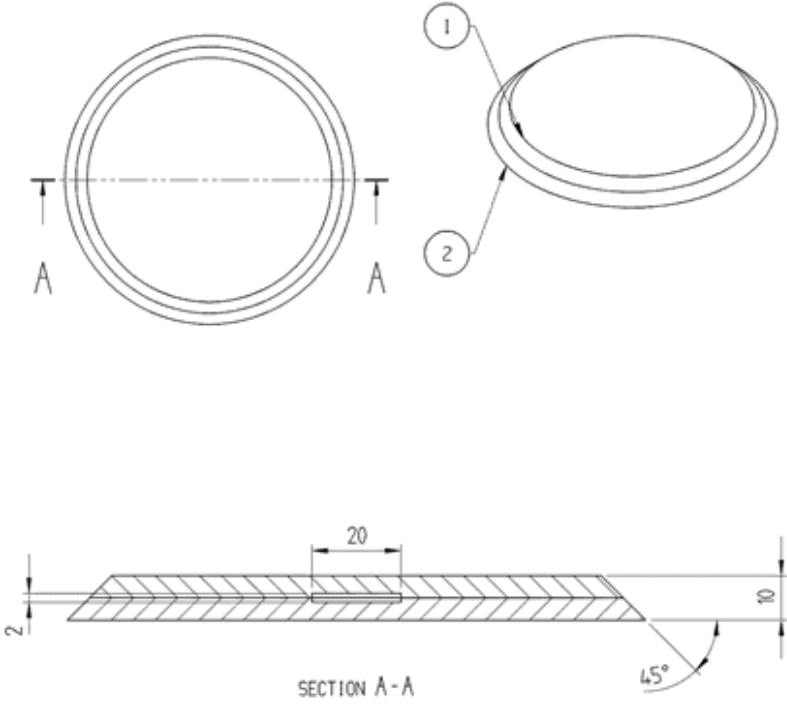
**Sample C:** Made from PSP material



**Sample D:** Made from KP material



**Sample E:** Made from PSP material with defined cavity



## APPENDIX C: PD TEST RESULTS USING SMIT TANK

Results of PD measurements of sample impregnated at Smit transformers during 12 days. The noise level is about 0.215pCa 0.3pC

### Sample A

The measured PD's in sample A during 12 days, are almost the same. No significant changes can be seen.

Date	PD inception Voltage [kV]	PD level [pC]
1 <sup>st</sup> day	27	2
2 <sup>nd</sup> day	11	1,2
3 <sup>rd</sup> day	10.6	0.7-1.9
4 <sup>th</sup> day	8.89	1.5
5 <sup>th</sup> day	11	1,5
8 <sup>th</sup> day	11	0.7-2
9 <sup>th</sup> day	11,6	0.7-1,,2
10 <sup>th</sup> day	5	0.5-0.6
11 <sup>th</sup> day	11.62	1.6
12 <sup>th</sup> day	7.96	0.6-0.7

Table A1: PDIV and measured discharges during 12 days after impregnation for sample A

### Sample B

During the test in the first day, flashover occurred. In second day of testing, the inception voltage is almost the halve and discharges is 0.7pC. from Day 3, No PD's occurred.

Date	PD inception Voltage [kV]	PD level [pC]
1 <sup>st</sup> day	46	0.6
2 <sup>nd</sup> day	21	0.7
3 <sup>rd</sup> day	Up to 25	Noise level
4 <sup>th</sup> day	19.75	<1pC
5 <sup>th</sup> day	Up to 19.75	0.3-0.6 ~ noise level
8 <sup>th</sup> day	Up to 22kV	0.2 noise
9 <sup>th</sup> day	Up to 22	0.2 noise level
10 <sup>th</sup> day	Up to 22	0.2
11 <sup>th</sup> day	Up to 22.45	0.22
12 <sup>th</sup> day	Up to 22.19	0.2

TableA2: PDIV and measured discharges during 12 days after impregnation for sample B

### Sample C

For sample C, No significant changes in PD inception voltage and the PD level

Date	PD inception Voltage [kV]	PD level [pC]
1 <sup>st</sup> day	12	0,7
2 <sup>nd</sup> day	Up to 20	
3 <sup>rd</sup> day	20.3	1.7
4 <sup>th</sup> day	20	0.7-1.15
5 <sup>th</sup> day	18.8	0.6
8 <sup>th</sup> day	Till 10kV	0.2-0.4
9 <sup>th</sup> day	12kv	0.4-0.6
10 <sup>th</sup> day	12.7kv	0.4-0.5
11 <sup>th</sup> day	15kV	0.6
12 <sup>th</sup> day	15kV	0.3-0.6

Table A3: PDIV and measured discharges during 12 days after impregnation for sample C

### Sample D

In the first day of impregnation, Some Partial discharges of 2.5pC occurred at voltage level of 4.5 kV. From 2<sup>nd</sup> day No PDs are measured.

Date	PD inception Voltage [kV]	PD level [pC]
1 <sup>st</sup> day	4.5	2.5
2 <sup>nd</sup> day	4,5	0,5
3 <sup>rd</sup> day	Up to 10 kV	Noise level
4 <sup>th</sup> day	10	0.3-1.5
5 <sup>th</sup> day	9.99kv	0.3
8 <sup>th</sup> day	10	0.2
9 <sup>th</sup> day	10.29	0.2
10 <sup>th</sup> day	Up to 10.22	0.2
11 <sup>th</sup> day	Up tp 10	0,2
12 <sup>th</sup> day	Up to 10	0.2-0.5

Table A4: PDIV and measured discharges during 12 days after impregnation for sample D

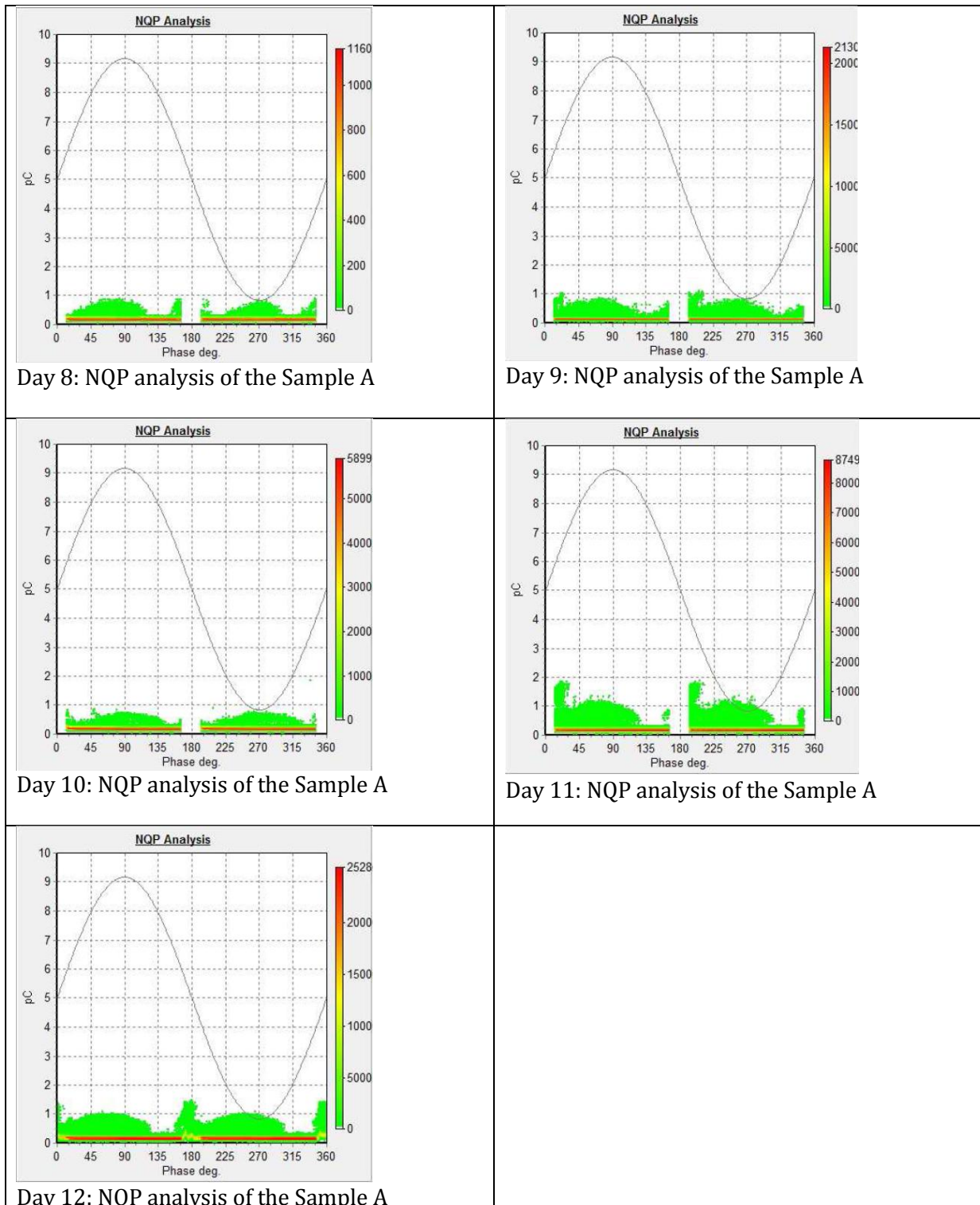
### Sample E

Date	PD inception Voltage [kV]	PD level [pC]
1 <sup>st</sup> day	31,3	4
2 <sup>nd</sup> day	30	1.3
3 <sup>rd</sup> day	28	3pC
4 <sup>th</sup> day	32.2	3-6
5 <sup>th</sup> day	28.7kV	4pC
8 <sup>th</sup> day	32.2	0.7-5pC
9 <sup>th</sup> day	32,2	0.4-2
10 <sup>th</sup> day	32.3	0.8-1.2pC
11 <sup>th</sup> day	30,6	6-8
12 <sup>th</sup> day	10	2pC

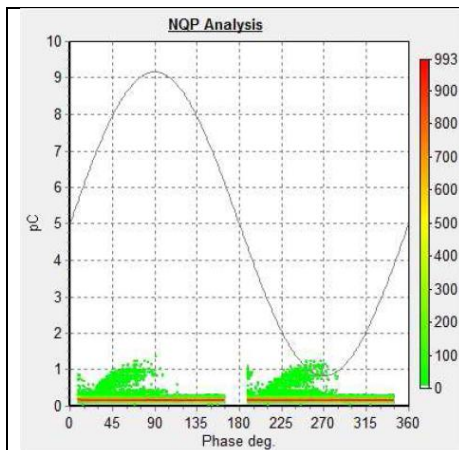
Table A5: PDIV and measured discharges during 12 days after impregnation for sample E

# NQP Analysis of the samples A, B, C, D and E

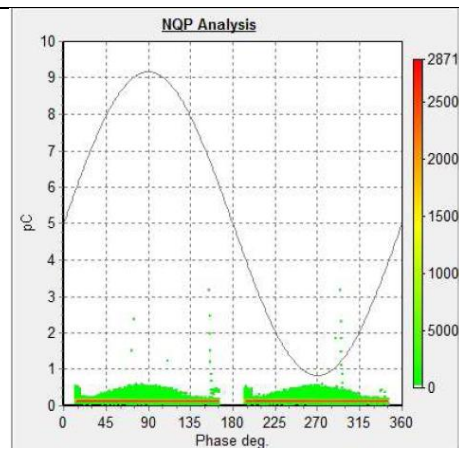
## Sample A



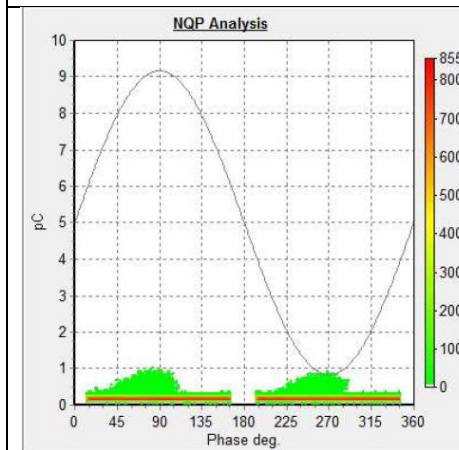
# Sample C



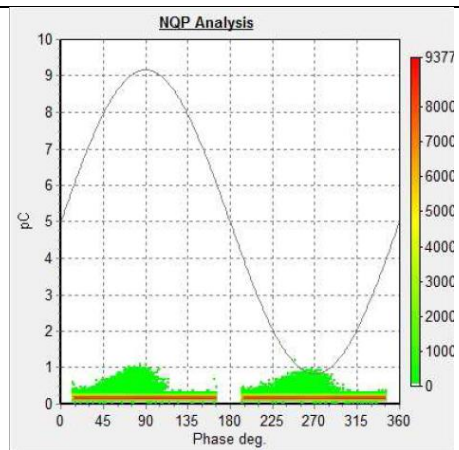
Day 8: NQP analysis of the Sample C



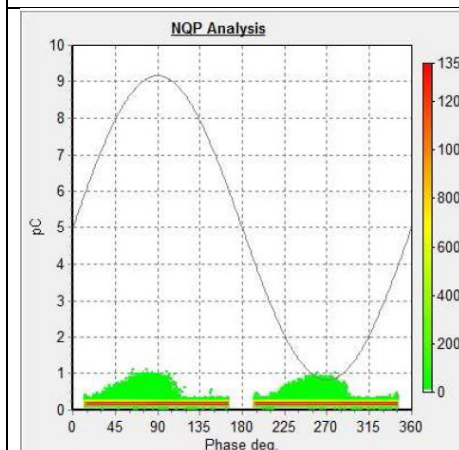
Day 9: NQP analysis of the Sample C



Day 10: NQP analysis of the Sample C

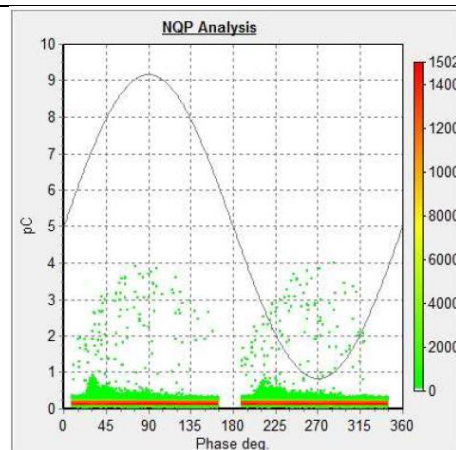


Day 11: NQP analysis of the Sample C

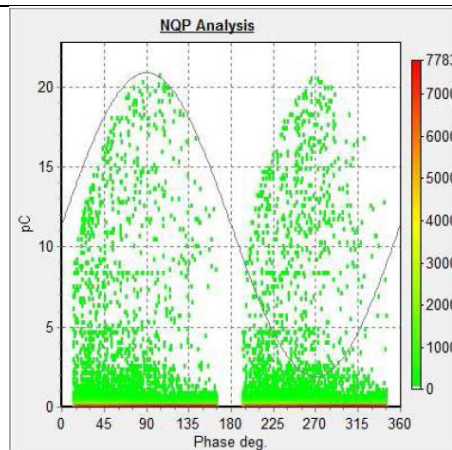


Day 12: NQP analysis of the Sample C

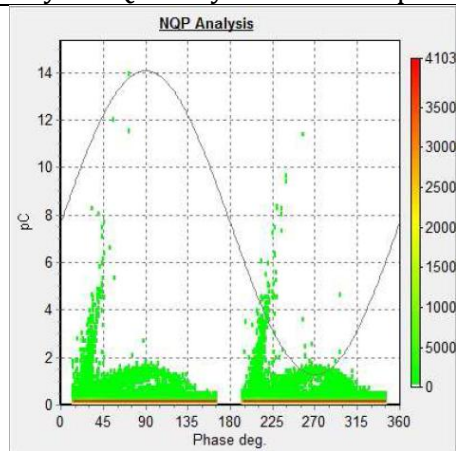
# Sample E



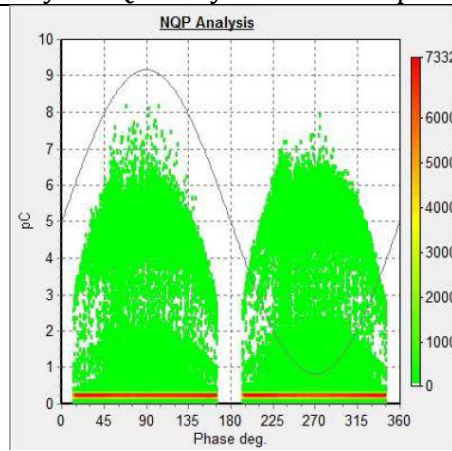
Day 8: NQP analysis of the Sample E



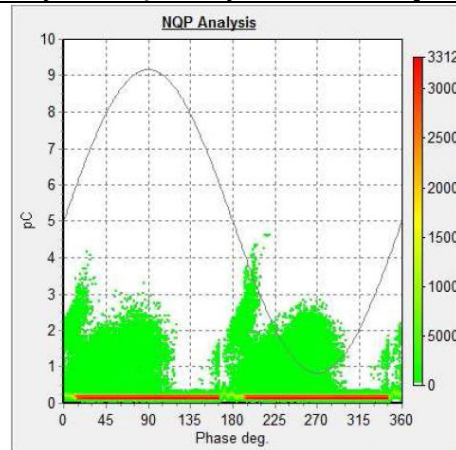
Day 9: NQP analysis of the Sample E



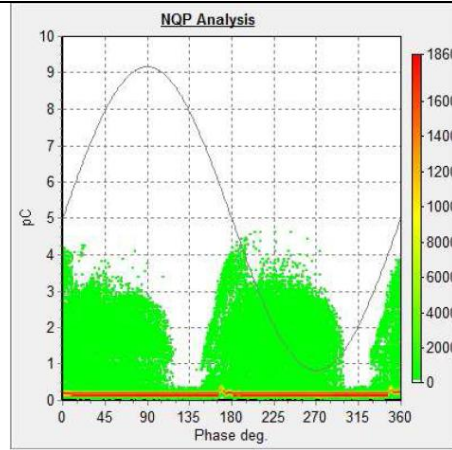
Day 10: NQP analysis of the Sample E



Day 11: NQP analysis of the Sample E



Day 12: NQP analysis of sample E at voltage 13kV



Day 12: NQP analysis of sample E at voltage 30-32kV

# APPENDIX D: TANA RESULTS USING TESTING SMIT TANK

## Sample B

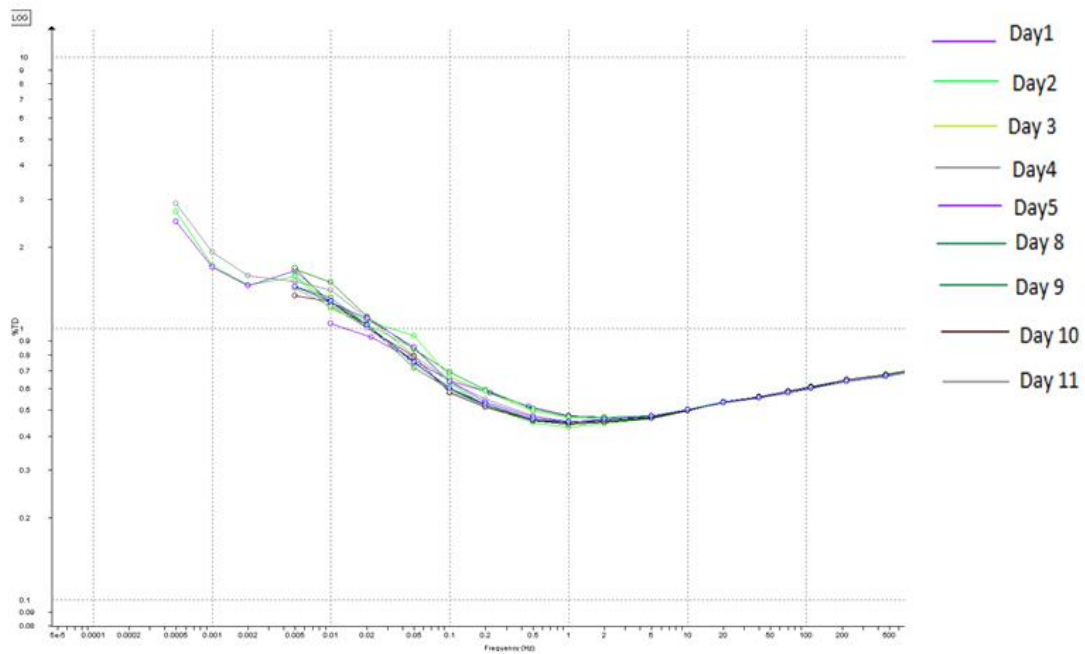


Figure D1:  $\tan \delta$  of sample B in function of frequency at ambient temperature

## Sample C

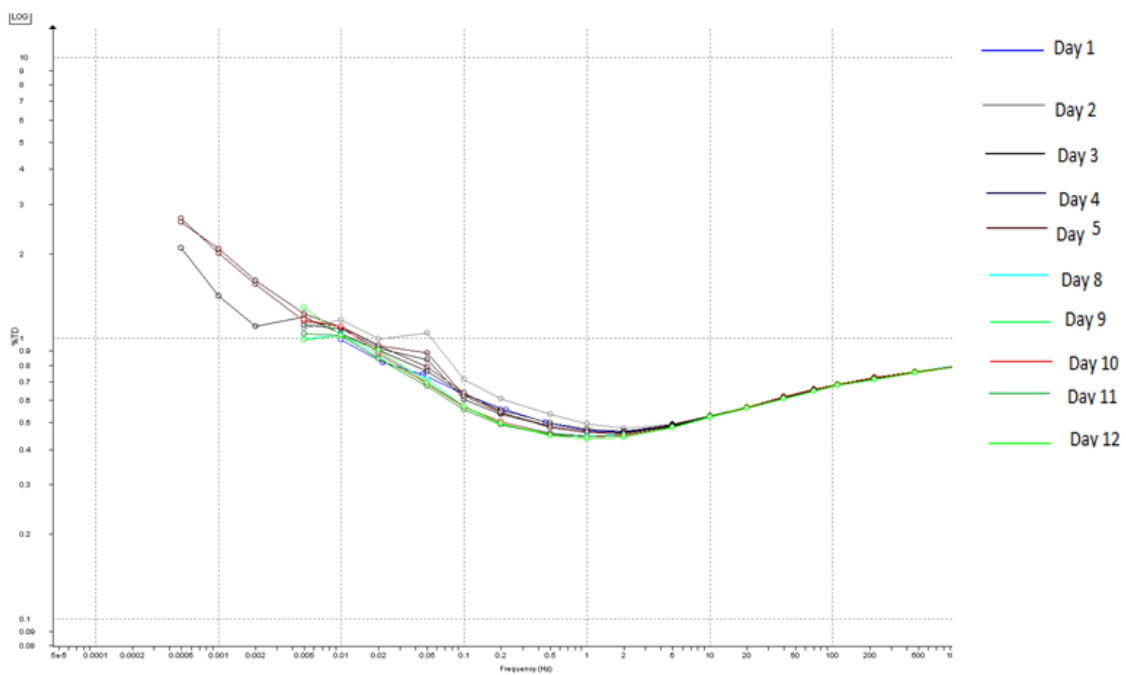


Figure D2:  $\tan \delta$  of sample C in function of frequency at ambient temperature

Sample D

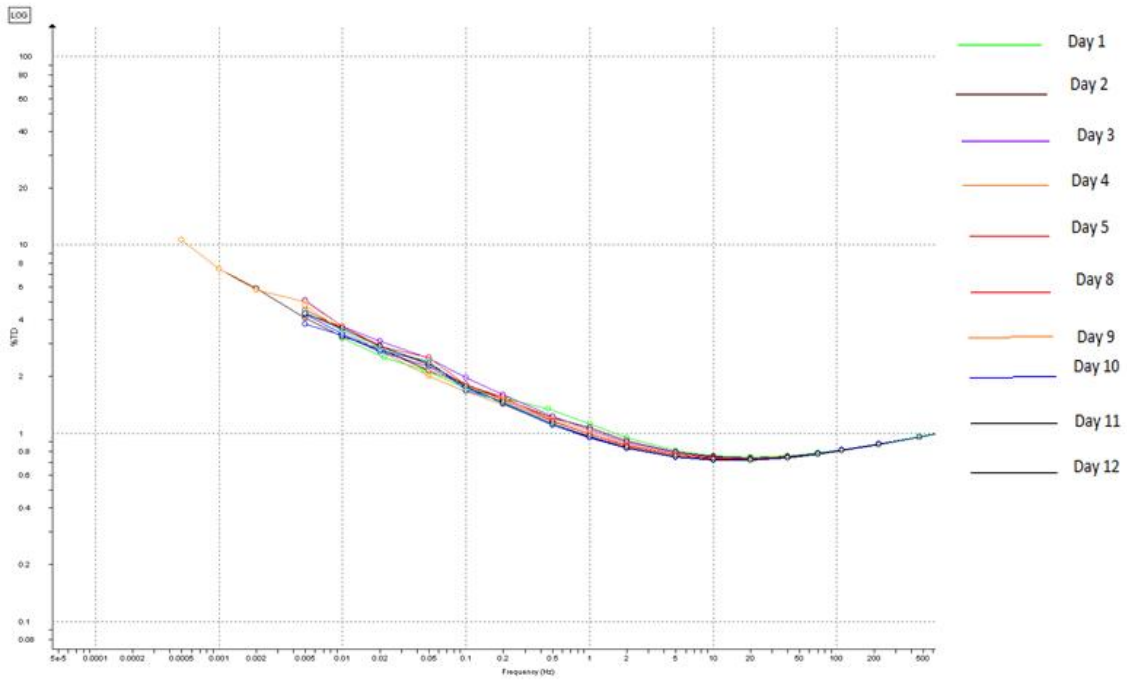


Figure D3: Tanδ of sample D in function of frequency at ambient temperature

Sample E

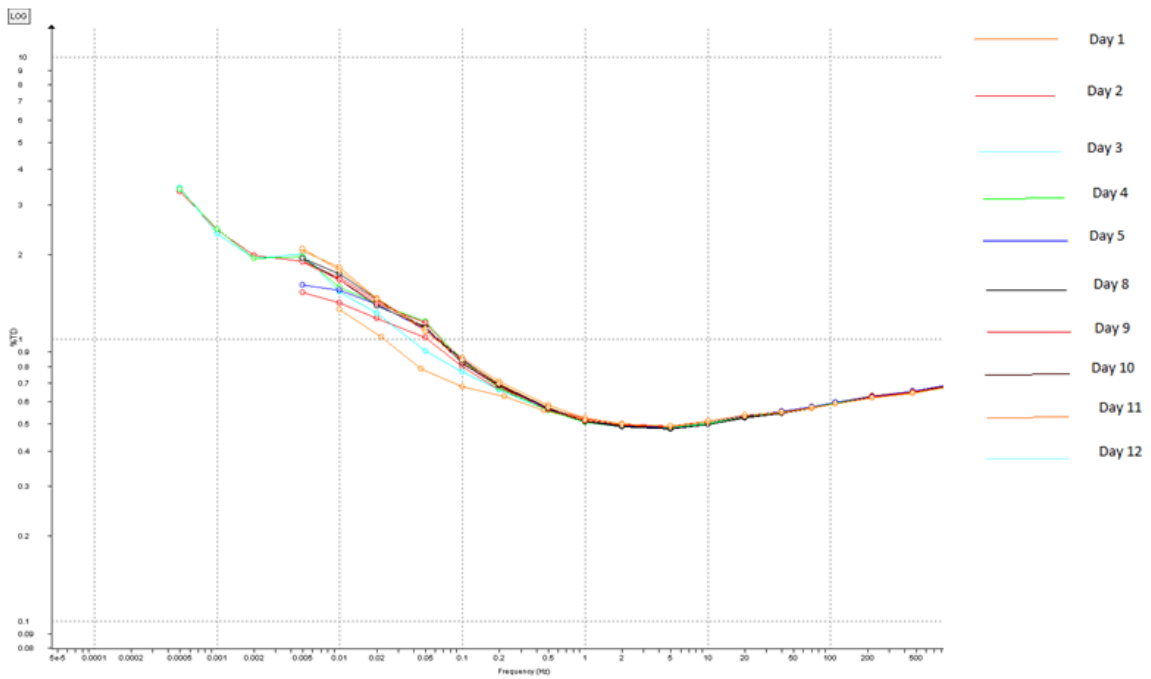


Figure D4: Tanδ of sample E in function of frequency at ambient temperature

## ACKNOWLEDGMENTS

I am indebted to a number of people who directly or indirectly contributed to the completion of this thesis. First of all, I would like to thank my supervisor dr. ir. P. Morshuis for giving me the opportunity to pursue this thesis at DC system and Storage group within the electrical sustainable energy department and for his advices and discussions.

An enormous amount of gratitude to my daily supervisor Dr. L. Chmura for his guidance and support during my research work and for being always available to help me through this whole project.

A special thanks to Royal Smit Transformers company in particular Mr. Kees Spoorenberg and Mr. Maarten Deutekom for explaining the construction process of power transformers, providing me with all necessary literature and materials.

Also I would like to owe my gratitude to Anna Peksa from Civil Engineering faculty for explaining me the fluid dynamics and providing me with the necessary literature.

The experiments presented in this thesis were conducted with the support from several people of TU Delft and Smit Transformers company. In particular, I would like to thank Ing. Paul van Nes who gave me the assistance for performing the measurements. I also want to thank Mr. Wim Termorshuizen for always being helpful.

I am, of course, particularly indebted to my parents, my sisters and my brothers for their monumental, unwavering support and encouragement on all fronts.

## 7. BIBLIOGRAPHY

- [1] K. Griese- "Electrical strength of pressboard componenets for transformer insulations" *IEEE Electrical Insulation Magazine*. Jan/Feb 1966, Vol. 12.
- [2] J. Dai, Z.D. Wang, P. Dyer, A. Darwin , I. James - "Investigation of the Impregnation Cellulosic Insulations by Esters Fluids", Annual Report Conference on Electrical Insulation and Dielectric Phenomena, 2007.
- [3] V. Dahinden, Weidmann Limited - "Insulation treatment of power transformer and methods of status surveillance" Rapperswil-Switzerland 1989
- [4] V. Wasserberg, M. Krins, H. Borsi, E. Gockenbach - "Investigation on Cavities inside Liquid-immersed paper and pressboard insulation materials and their influence on the electrical behavior", IEEE International symposium on electrical insulation, Anaheim, USA, April 2000
- [5] J. Erbrink, "On-Load Tap Changer Disagnosis on High-Voltage Power Transformers using Dynamic Resistance Measurements", Delft 2011.
- [6] Diagnostics for high voltage assets and lab course, first lecture : Insulation coordination, 2014"
- [7] H. william and P. Bartly , "Analysis of transformer Failures," International Association of engineering Insures , 2003.
- [8] S. Tenbohlen, "Transformer Reliability Survey: Interim Report," Electra, April 2014
- [9] M.J. Heathcote, "J&P Transformer Book", 12<sup>th</sup> ed., Newnes, Oxford, 2007, ISBN 07506-1158-8.
- [10] IEC 60071-4 Standard, " Insulation co-ordination-Part 4: Computational guide to insulation co-ordination and modelling of electrical networks," 2004.
- [11] H. Zainuddin - " Study of Surface Discharge Behaviour at the oil-pressboard Interface", Doctoral thesis, University of Southampton, 2013.
- [12] J. Winders, "Power Transformers: Principles and Applications," New York 2002, ISBN 0-8247-0766-4
- [13] David, L. Harris, P.E., - "Transformer winding design-The design and performance of circular disc, Helical and layer windings for power transformer applications," Minnesota Power Systems Conference, Minneapolis, 2009.
- [14] J. Harlow, "Electric Power Transformer Engineering," USA 2004, ISBN 0-8493-1704-5
- [15] Y. Wang, S. Gong , S. Grzybowski, "Reliability Evaluation Method for Oil-Paper Insulation in Power Transformers," *Energies*, 9 September 2011
- [16] J. A. M. Veens "Transformer insulation Design Based on the Analysis of impulse Voltage Distribution," *Electromagnetic transients in Transfomer and Rotating Machine Windings IGI Global*, 2013. 438-455. Doi 10.4018/978-1-4666-1921-0. Ch11 2013.
- [17] W. Ziomek, "High Voltage Power Transformer Insulation Design," *Electrical insulation Conference (EIC)*, Annapolis 2011.
- [18] H.P. Moser, " Transformerboard", Vermont, 1979.
- [19] K. Griese - " The effect of Cellulose insulation Quality on Electrical Intrinsic Strength", *IEEE Electrical Insulation Magazine*, 1994, Vol 10.5

- [20] J. Rouger, P. Mutje, "Correlation between the cellulose fibers beating and Fixation of a Soluble Cationic Polymer," *British Polymer Journal*, vol. 16, pp. 83-86, 1984
- [21] "www.transformer-supplies.nl/producten/de-producten.aspx," Transformer Supplies BV, 2011. [Online]. [Accessed 23 januari 2015].
- [22] M. G. Dufour A., "A Study of Pressboard Monodimensional Impregnation with Transformer Oil and Its Influence on Dielectric Strength," *IEEE Translations on Electrical Insulation*, Vol E1-10, December 1975.
- [23] M. Takagi, T. Suzuki, "Oil impregnation in Transformer Boards (2)," *IEEE Transactions on Electrical Insulation* 1984, vol. 19.
- [24] "CT scan of wood sample," [Online]. [Accessed 5 2014]
- [25] S. Malkov, P. Tikka, J. Gullichsen, "Towards complete impregnation of wood chips with aqueous solutions," Finland 2002.
- [26] L. F. Hawley, "Wood-liquid Relations," Technical bulletin number 248, United States, Dept. of agriculture, 1931.
- [27] O. H. Anders W. Kjellow, "Supercritical wood impregnation," *The journal of Supercritical Fluids*, vol. 50, pp. 297-304, 2009.
- [28] J. B. Flynn "Impregnation study of porous elements of high voltage components" *IEEE translations on Electrical insulation* vol. EI-20 No.3, June 1985.
- [29] M. Steurer and K. Frohlich, "The Impact of Inrush Currents on the Mechanical Stress of High Voltage Power Transformer Coils," *IEEE Transactions on power delivery*, Vol. 17, January 2002.
- [30] M. Balasubramanian, G. Ravi, V. Dharmalingam, "Interdependence of Thermal and Electrical Stresses on Initiating Degradation of Transformer Insulation Performances," *IEEE-International Conference on advances in Engineering, Science and management (ICAESM)* 2012.
- [31] IEC 60270 Standard, "High voltage test techniques. Partial discharge measurements" 2000.
- [32] F. Kreuger, *Industrial High voltage*, Delft universty Press, Delft 1991.
- [33] *High Voltage Construction "lecture 5: Gas at Low Pressure"*.
- [34] E. Perscke R von olshausen 1999, *Cable systems for high amd extra high voltage*. Berlin: Publicis MCD verlag. Elang and Munich, ISBN 3895781185, 9783895781186
- [35] W. Yugoung, X. Zhao, F. LI and Z. Fan" evaluation of mixing rules for dielectric constants of composite Dielectircs by MC-FEM Calculation on 3D Cubic lattice" *Journal of electroceramics* 2004
- [36] W.S. Zaengl, "Dielectric Spectroscopy in Time and Frequency Domain for HV Power Equipement, Part I: Theoretical considerations". *IEEE Electrical Insulation Magazine*, Sep/Oct, 2003, Vol 19.
- [37] IEC 60 247,"Insulating liquids- Measurments of relative permittivity, dielectric dissipation factor and dc resistivity". 2004
- [38] F. Kreuger. *Industrial High- voltage*. Delft University Press, Delft 1992, ISBN 90-6275562-3
- [39] Weidmann manufactured product data sheets
- [40] Rochling Engineering, *Transformerwood data sheets*.
- [41] E. Washburn, Edward. *The dynamics of capillary flow*, physical review vol. 17, 1921



